

**Mechanism and Regulation of Dynamin Related  
Protein 6 (Drp6) nuclear recruitment in  
*Tetrahymena thermophila***

*By*

**HIMANI DEY**

**Enrollment No. LIFE11201404005**

**National Institute of Science Education and Research (NISER)**

**Bhubaneswar**

*A thesis submitted to the  
Board of studies in Life Sciences*

*In partial fulfilment of requirements*

*for the Degree of*

**DOCTOR OF PHILOSOPHY**

*Of*

**HOMI BHABHA NATIONAL INSTITUTE**

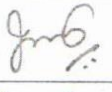
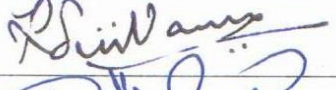
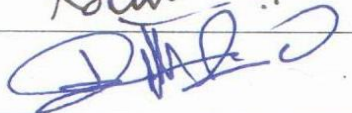
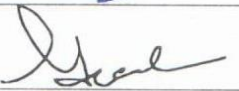


**January, 2022**

# Homi Bhabha National Institute<sup>1</sup>

## Recommendations of the Viva Voce Committee

As members of the Viva Voce Committee, we certify that we have read the dissertation prepared by Himani Dey entitled "Mechanism and regulation of Dynamin Related Protein 6 (Drp6) nuclear recruitment in *Tetrahymena thermophila*" and recommend that it may be accepted as fulfilling the thesis requirement for the award of Degree of Doctor of Philosophy.

Chairman – Dr. Moloy Sarkar		18/01/2022
Guide / Convener – Dr. Abdur Rahaman		18/01/2022
Co-guide - Name & Signature with date (if any)		
Examiner – Dr. Jomon Joseph		18/01/2022
Member 1- Dr. Ramanujam Srinivasan		18/01/2022
Member 2- Dr. Renjith Mathew		18/01/2022
Member 3- Dr. Chinmay Pradhan		18/01/2022

Final approval and acceptance of this thesis is contingent upon the candidate's submission of the final copies of the thesis to HBNI.

I/We hereby certify that I/we have read this thesis prepared under my/our direction and recommend that it may be accepted as fulfilling the thesis requirement.

Date: 18.01.2022

Place: Jatni, NISER. Signature

Co-guide (if any)



Signature

Guide

## **STATEMENT BY AUTHOR**

This dissertation has been submitted in partial fulfillment of requirements for an advanced degree at Homi Bhabha National Institute (HBNI) and is deposited in the Library to be made available to borrowers under rules of the HBNI.

Brief quotations from this dissertation are allowable without special permission, provided that accurate acknowledgment of source is made. Requests for permission for extended quotation from or reproduction of this manuscript in whole or in part may be granted by the Competent Authority of HBNI when in his or her judgment the proposed use of the material is in the interests of scholarship. In all other instances, however, permission must be obtained from the author.



Himani Dey

## DECLARATION

I, hereby declare that the investigation presented in the thesis has been carried out by me. The work is original and has not been submitted earlier as a whole or in part for a degree/diploma at this or any other Institution/University.

A handwritten signature in blue ink that reads "Himani Dey". The signature is written in a cursive style with a horizontal line underneath the name.

Himani Dey

## **List of Publications arising from this thesis**

### **Journal**

#### **Published**

- Kar UP\*, **Dey H\***, Rahaman A. (2021). Cardiolipin targets a dynamin-related protein to the nuclear membrane. *eLife*, doi: 10.7554/eLife.64416 (pertaining to thesis).  
\*Equal contribution.

#### **To be communicated**

- **Dey H**, Kar UP and Rahaman A. Dynamin Related Protein 6 self-assembly is middle domain and G-domain independent but is not sufficient for nuclear recruitment. (to be communicated, pertaining to thesis)
- **Dey H**, Kar UP, Rahaman A. Enhanced cardiolipin interaction upon phosphorylation changes DRp6 localization upon GTPase activity inhibition. (to be communicated , pertaining to thesis)

#### **Other publications**

- Kar UP, **Dey H**, Rahaman A. (2017) Regulation of dynamin family proteins by post-translational modifications. *J Biosci.* 2017 Jun; 42(2):333-344. doi: 10.1007/s12038-017-9680-y
- Kar UP, **Dey H**, Rahaman A. (2018). Tetrahymena dynamin-related protein 6 self-assembles independent of membrane association. *J Biosci* 43:139–148. DOI: doi.org/10.1007/s12038-017-9726-1
- Preeyanka N, **Dey H**, Seth S, Rahaman A, Sarkar M. (2020) Highly efficient energy transfer from a water soluble zinc silver indium sulphide quantum dot to organic J-aggregates. *Phys. Chem. Chem. Phys.* 22(22) DOI: 10.1039/D0CP01845G

## **Conference Presentations**

### **International**

- Regulation of Dynamin Related Protein 6, a nuclear remodeling dynamin in *Tetrahymena* by post-translational modifications. Dey H, Kar UP, Rahman A. **International Conference of Cell Biology 2018-The Dynamic Cell: Molecules and networks to form and function. 27th Jan-31st Jan, 2018, Leonia Holistic Destination, Hyderabad.**
- Nuclear recruitment of Dynamin Related Protein 6 in *Tetrahymena thermophila* is mediated by cardiolipin and regulated by post translational modification. Dey H, Kar UP, Rahaman A. **Quantitative aspects of Membrane fusion and Fission. May 6-10, Padova , Italy**
- Phosphorylation regulates cellular localization and membrane fusion function of Dynamin Related Protein 6 by affecting GTPase activity, self-assembled structure and cardiolipin affinity. Dey H, Rahaman A. **Junior Investigator Ciliate Molecular Biology Meeting (Virtual ) July 20-24 2020**

### **National**

- Regulation of Dynamin Related Protein 6, a nuclear remodeling dynamin in *Tetrahymena* by post-translational modifications. Dey H, Kar UP, Rahman A. **XLII All India Cell Biology Conference The Cell in Action: Trends in Cell and Molecular Biology December 21-23, 2018**

**Dedicated to My Family**

## **Acknowledgments**

I would like to express my deepest gratefulness to my project supervisor Dr. Abdur Rahaman for his valuable guidance, constant support, motivation and constructive criticism, which has helped me in the completion of this project. I will forever be indebted to him for his support not only as a guide but also like a guardian. I am very grateful to my doctoral committee members Dr. Ramanujam Srinivasan, Dr. Renjith Mathew, Dr. Moloy Sarkar and Dr. Chinmay Pradhan, for their critical evaluation and valuable suggestions during the course of my Ph.D. I am thankful to Dr. Mohammed Saleem, Dr. Tirumal Kumar Chowdhary for their help related to certain experiments for this project. I am thankful to my seniors, Dr. Anoop N. Pillai, Dr. Sushmita Shukla and especially to Dr. Usha Pallabi Kar, for their guidance during most of my Ph.D tenure, and my other lab members Sakti Ranjan Rout, Soham Mukhopadhyay, for their support in carrying out my experiments and beyond. All of them made my lab stay a pleasant and memorable experience. I am especially thankful to Dr. Usha Pallabi Kar for being a constant unconditional support as a friend, family and senior. I would also like to thank my friends Md. Khurshidul Hassan, Bushra Hayat, Somdatta Saha, Pragyesh Dixit, Durga Prasad Biswal, Satyamurthy, Dipika Mishra, Rojalin Pradhan for always being there unconditionally when I needed help. I will be forever indebted to all of them. I am grateful to the academic and non-academic staff of NISER, for their help, blessings and encouragement. I would like to thank all my teachers and friends, who have always helped me, and accepted me with my faults.

I am highly indebted to my family, for their unconditional love, patience and support. They have stood beside me at every phase of my life, and words alone would not suffice my gratitude towards them. I would like to apologize to anyone for omissions in this brief acknowledgment, it doesn't mean in anyway my lack of gratitude towards them.

## CONTENTS

S.No.	Title	Page No.
	<b>Summary</b>	1-2
	<b>List of abbreviations</b>	3-5
	<b>List of figures</b>	6-10
	<b>List of tables</b>	10
1	<b>Chapter 1: Review of literature</b>	11
1.1	Membrane Remodeling	12
1.2	Membrane curvature	12
1.2.1	Mechanisms of membrane curvature generation	13
1.3	Dynamain family of mechanozymes	14
1.3.1	Domain architecture of dynamain family proteins	16
1.3.1.1	The GTPase domain (GD)	17
1.3.1.2	The middle domain (MD)	17
1.3.1.3	Pleckstrin homology (PH) domain	18
1.3.1.4	The GTPase effector domain (GED)	18
1.3.1.5	The Proline rich domain (PRD)	18
1.4	Biochemical properties of dynamain family of proteins	19
1.4.1	Self-assembly	19
1.4.2	GTP binding and hydrolysis	20
1.4.3	Membrane binding and remodelling	21
1.5	Function of the dynamins and dynamain related proteins	22
1.5.1	Vesicle Scission	22
1.5.2	Mitochondrial maintenance	24
1.5.3	Antiviral activity	25
1.5.4	Endoplasmic reticulum fusion	26
1.5.5	Cytokinesis	27
1.6	Regulation of dynamins by post-translational modifications	27
1.6.1	Phosphorylation	28
1.6.2	Ubiquitination	29
1.6.3	SUMOylation	30
1.6.4	S-Nitrosylation	30
1.6.5	Acetylation	31
1.7	Nuclear envelope remodelling	33
1.8	Nuclear expansion in <i>Tetrahymena</i>	34
2	<b>Chapter 2: Mechanism of Drp6 function and regulation by post-translational modifications</b>	38
2.1	Introduction	39
2.2	Materials and Methods	41
2.3	Results	49
2.3.1	Drp6 is a fusion dynamain	49
2.3.2	Effect of phosphorylation on self-assembly of Drp6	53
2.3.3	Effect of phosphorylation on GTPase activity of Drp6	55
2.3.4	Inhibition in GTPase activity is not due to reduced GTP binding	57
2.3.5	Effect of phosphorylation on localization of Drp6	58

2.3.6	Phosphorylation at S248 enhances cardiolipin binding affinity	61
2.3.7	Phosphorylation at S248 enhances membrane fusion activity of Drp6	64
2.3.8	Phosphorylation at S248 stabilizes the self-assembled ring structures	68
2.3.9	Phosphorylation of S248 enhances membrane tubulation and tubular network formation	70
2.4	Discussion	72
3	<b>Chapter 3: Mechanism of cardiolipin interaction specificity and nuclear envelope recruitment of Drp6</b>	74
3.1	Introduction	75
3.2	Material and methods	77
3.3	Results	82
3.3.1	Drp Targeting Determinant (DTD) of Drp6 is the membrane binding domain	82
3.3.2	Identification of a hydrophobic patch in the DTD.	83
3.3.3	An isoleucine residue at 553rd position is essential for nuclear recruitment and cardiolipin binding of Drp6	85
3.3.4	Mutations at I553 does not affect GTPase activity and self-assembly property	88
3.3.5	Mutation at I553 does not alter the protein conformation	90
3.3.6	Nuclear recruitment of Drp6-I553M mutant is restored by co-expression of wildtype protein.	94
3.3.7	Residues in the vicinity of I553 are not essential for nuclear envelope recruitment and cardiolipin binding specificity of Drp6	96
3.4	Discussion	100
4	<b>Chapter 4: The role of G domain and middle domain in the self-assembly and nuclear envelope recruitment of Drp6</b>	102
4.1	Introduction	103
4.2	Material and methods	106
4.3	Result	108
4.3.1	GD and MD are not essential for oligomerization	105
4.3.2	Drp6 $\Delta$ GD-MD self-assembles into helical rods	111
4.3.3	GD and MD are important for nuclear recruitment of Drp6	111
4.3.4	Loss of nuclear envelope recruitment of Drp6 $\Delta$ GD-MD is not due to loss of cardiolipin interaction	113
4.4	Discussion	115
5	<b>Chapter 5: Mechanism of nuclear expansion by Drp6 and role of microtubule structure</b>	118
5.1	Introduction	119
5.2	Materials and methods	121
5.3	Results	124
5.3.1	Drp6 interacts with microtubule and dynein	124
5.3.2	Interaction with microtubule and dynein is important for nuclear envelope localization of Drp6	126
5.3.3	Interaction with microtubule and dynein is required for macronuclear development	128

5.3.4	Perinuclear ER network depends on Drp6 function and microtubule structure	130
5.4	Discussion	133
6	<b>Chapter 6: Summary and Conclusion</b>	135
6.1	Summary	136
6.2	Conclusion	141
7	<b>Bibliography</b>	144

## Summary

Dynamain family of proteins are a group of large GTPases which remodel their target membranes to cause membrane fission, fusion or tubulation. These proteins which are categorized as classical dynamain and dynamain related proteins, perform vital cellular processes e.g. endocytosis, mitochondrial fission and fusion, endoplasmic reticulum tubulation, cell plate formation and antiviral activity, by localizing at their site of action. This recruitment requires target membrane binding and self-assembly into helical spirals and/or rings. Self-assembly of dynamains occurs via interfaces which involve GTPase domain (G-domain/GD), middle domain (MD) and GTPase effector domain (GED). Classical dynamains bind target membrane via their PH domain. Dynamain related proteins(Drps)which lack PH domain interact with target membrane via a transmembrane domain or membrane binding loop of positively charged residues. These properties of self-assembly and membrane binding together determine the localization of these proteins and are regulated by various post-translational modifications.

*Tetrahymena thermophila* has eight DRPs, of which Drp6 has evolved a novel function in nuclear remodelling. During macronuclear development stage of conjugation, 2 out of 4 identical post-zygotic micronuclei expand to form new macronuclei. Drp6 exerts its functions during this macronuclear expansion stage. It localizes on the nuclear envelope and ER derived cytoplasmic puncta. It interacts with membrane by specifically interacting with three phospholipids namely, cardiolipin(CL), phosphatidic acid (PA) and phosphatidyl serine (PS), and interaction with CL determines its nuclear recruitment. This study aimed to understand the mechanism and regulation of Drp6 mediated nuclear expansion. The study also elucidates the molecular basis of how a single isoleucine residue in the membrane binding domain of Drp6 determines cardiolipin binding specificity and thereby its nuclear recruitment.

Mechanism and regulation of stage specific localization and function of Drp6 by post-translational modification are also addressed in this study where we found that phosphorylation at a particular serine residue regulated membrane fusion function.

## LIST OF ABBREVIATIONS

BAR	Bin-Amphiphysin-Rvs
COP	Coat protein
Arf	ADP-ribosylation factor
PE	Phosphatidylethanolamine
PtdIns	Phosphatidyl inositol
CL	Cardiolipin
PC	Phosphatidylcholine
PS	Phosphatidylethanolamine
GD	GTPase domain
PH	Pleckstrin Homology
GED	GTPase Effector Domain
PRD	Proline Rich Domain
Drp1	Dynamin Related Protein 1
MxA	Myxovirus resistance A
MxB	Myxovirus resistance B
Opa1	Optic Atrophy 1
Vps1	Vacuolar Protein Sorting 1
hGBP1	Human Guanylate Binding Protein 1
BSE	Bundle signalling element
VL	Variable loop
GAP	GTPase Activator Protein
SH3	SRC-Homology 3 domain

Grb2	Growth Factor Receptor Bound Protein-2
PLC	Phospholipase C
Mgm1	Mitochondrial Genome Maintenance 1
GTP	Guanosine triphosphate
GDP	Guanosine diphosphate
PIP2	Phosphatidylinositol 4,5 Biphosphate
ROS	Reactive Oxygen Species
vRNP	Viral ribonuclear protein
ATL	Atlastin
PTM	Post-translational modification
MARCH-V	Membrane-associated RING-CH protein V
HDAC6	Histone Deacetylase 6
Fzo1	Fuzzy Onion like protein1
Ubp	Ubiquitin Binding Protein
Mdm-30	Mitochondrial distribution and morphology protein 30
SUMO	Small Ubiquitin-like Modifier
SEN3	SUMO Specific Peptidase 3
SIRT	Sirtuin 3
NE	Nuclear Envelope
MAC	Macronucleus
MIC	Micronucleus
TtDrp1	<i>Tetrahymena</i> specific Dynamin related protein1
Drp6	Dynamin Related Protein 6
GUV	Giant Unilamellar Vesicles

MST	Microscale Thermophoresis
GMPPNP	Guanosine 5'-[ $\beta,\gamma$ -imido]triphosphate
Fe-EDTA	Ethylenediaminetetraacetic acid iron(III)
TEM	Transmission Electron Microscopy
PCR	Polymerase Chain Reaction
LB	Luria Beratni
NaCl	Sodium Chloride
MgCl <sub>2</sub>	Magnesium Chloride
PMSF	Phenylmethylsulfonyl fluoride
SDS	Sodium Dodecyl Sulphate
PAGE	Polyacrylamide Gel Electrophoresis
DLS	Dynamic Light Scattering
DMC	Dryl's minimal composition media
SPP	Super Proteose Peptone
PMS	Paromomycin Sulphate
DAPI	4',6-diamidino-2-phenylindole
DTD	Drp Targeting Determinant
GFP	Green Fluorescence Protein
HDyn1	Human Dynamin 1

## LIST OF FIGURES

S.No.	Description	Page No.
Figure 1.1.1	Effect of shape of lipids and proteins on membrane curvature.	13
Figure 1.3.1	An overview of functions of members of dynamin superfamily	15
Figure 1.3.1.1	Domain organization of classical dyanmins and dynamin related proteins.	16
Figure 1.4.1.1	Self-assembly of dynamins.	20
Figure 1.4.3.1	Constriction of vesicles by dynamin.	23
Figure 1.7.1	Eukaryotes undergo division of nucleus by closed, semi-open or open mitosis.	33
Figure 1.8.1	Stages of nuclear division during conjugation in <i>Tetrahymena thermophila</i> .	35
Figure 1.8.2	<i>Tetrahymena</i> contains 8 Dynamin Related Proteins. Phylogenetic tree showing different members of dynamin family of proteins	36
Figure 2.3.1.1	Schematic representation of R18 dye dequenching during <i>in-vitro</i> membrane fusion assay.	50
Figure 2.3.1.2	Membrane fusion by Drp6	49
Figure 2.3.1.3(A)	Image showing fusion states during <i>in-vitro</i> membrane fusion	52
Figure 2.3.2.1(A)	Schematic representation showing residues of Drp6 which undergo phosphorylation and ubiquitination as identified	54

	by MS	
Figure 2.3.1.3 (B)	Coomassie stained SDS-PAGE gel showing Drp6 and the phosphomimic variants	54
Figure 2.3.2.2	Size-exclusion chromatography of phosphomimic variants	55
Figure 2.3.3.1	GTPase activity of Drp6 and phosphomimic variants	56
Figure 2.3.3.2	TAP-tagged Drp6-S248D purified from <i>Tetrahymena</i> shows reduced GTPase activity	57
Figure 2.3.4.1	Phosphomimic Drp-S248D binding to GTP $\gamma$ S is similar to Drp6	58
Figure 2.3.5.1	Schematic representation of strategy used for mCherry tagging of endogenous Drp6.	59
Figure 2.3.5.2	Confirmation of endogenous replacement of Drp6 with mCherry tagged Drp6 or Drp6-S248A or Drp6-S248D by semi-quantitative PCR	59
Figure 2.3.5.3	Localization of Drp6 in presence or absence of phosphorylation at S248	61
Figure 2.3.6.1	GTP enhances Drp6 binding with CL	62
Figure 2.3.6.2	Drp6- S248D shows enhanced binding specifically with cardiolipin	63
Figure 2.3.6.3	Liposome co-floatation assay of Drp6-S86D, Drp6-S701D and Drp6-S705D	64
Figure 2.3.7.1	Phosphorylation at S248 (Drp6-S248D) enhances fusion activity	66
Figure2.3.8.1	Drp6-S248D stabilizes self-assembled ring structures	67

Figure 2.3.8.2	Electron micrograph of Drp6 and Drp6-S248D either in absence of nucleotide or in presence of GDP or in presence of GMP-PNP	69
Figure 2.3.9.1 (A)	Electron micrographs of CL containing liposomes in absence of any protein	71
Figure 2.3.9.1 (B)	Electron micrographs of CL containing liposomes in presence of Drp6	71
Figure 2.3.9.1 (C)	Electron micrographs of CL containing liposomes in presence of Drp6-S248D	71
Figure 3.3.1.1(A)	Domain organization of Drp6 and HDyn1	82
Figure 3.3.1.1 (B)	Sub-cellular fractionation of GFP-Drp6 and GFP-Drp6-DTD	82
Figure 3.3.2.1(A)	Drp6 contains a hydrophobic patch	84
Figure 3.3.2.1(B)	3-D structure of Drp6 generated using I-TASSER	84
Figure 3.3.3.1	Liposome co-floatation assay of Drp6 (A) and Drp6-I553M (B)	86
Figure 3.3.3.2	Drp6-I553A doesnot localize on the nuclear envelope	87
Figure 3.3.3.3	Liposome co-floatation assay of I553A-Drp6	88
Figure 3.3.4.1	GTP hydrolysis activity of Drp6 (WT), I553M-Drp6 (I553M) and Drp6-I553A (I553A)	89
Figure 3.3.4.2	Size exclusion chromatography profile of Drp6, I553M-Drp6 and I553A	90
Figure 3.3.5.1	Far UV-CD spectra of His-Drp6, His-Drp6-I553M and His-Drp6-I553A	91

Figure 3.3.5.2	Intrinsic tryptophan fluorescence spectra of His-Drp6, His-Drp6-I553M and His-Drp6-I553A	92
Figure 3.3.5.3	Effect of acrylamide quenching on tryptophan fluorescence spectra of Drp6 (A), Drp6-I553M (B) and Drp6-I553A (C)	93
Figure 3.3.5.4	<i>Stern-Volmer</i> plot for acrylamide quenching of His-Drp6 (Drp6), His-Drp6-I553M (Drp6-I553M) and His-Drp6-I553A (Drp6-I553A)	94
Figure 3.3.6.1	Co-expression of GFP-Drp6-I553M and mCherry-Drp6 restores nuclear envelope localization of Drp6-I553M	96
Figure 3.3.7.1 A	Scheme indicating the residues in the vicinity of I553	97
Figure 3.3.7.1 B	Liposome co-floatation assay of Drp6-M554L and Drp6-E552D	97
Figure 3.3.7.2	GFP-Drp6-E552D and GFP-Drp6-M554L localize on the nuclear envelope.	98
Figure 3.3.1	Drp6 localizes on nuclear envelope, plasma membrane and ER	99
Figure 4.3.1.1	Drp6 oligomerizes in absence of GD-MD	109
Figure 4.3.2.1	Drp6 $\Delta$ GD-MD self-assembles to form helical rod like structures	112
Figure 4.3.3.1	GFP-Drp6 $\Delta$ GD-MD fails to localize to the nuclear envelope	114
Figure 4.3.4.1	Liposome co-floatation assay of MBP-Drp6 $\Delta$ GD-MD	115
Figure 5.3.1.1	Confocal images of a live Tetrahymena cell expressing GFP-Drp6. Drp6 shows distribution that resembles	124

	microtubule network	
Figure 5.3.1.2	Drp6 interacts with tubulin	125
Figure 5.3.2.1	Nuclear envelope localization of Drp6 depends on microtubule structure and dynein function	127
Figure 5.3.3.1	MAC development depends on microtubule structure and dynein function	129
Figure 5.3.4.1	Inhibition of Drp6 function inhibits perinuclear ER network formation	130
Figure 5.3.4.2	Perturbation of microtubule structure inhibits perinuclear ER network	132
Figure 6.2.1	Proposed model of mechanism by which Drp6 performs nuclear expansion	141

### LIST OF TABLES

S.No.	Description	Page No.
Table 1.4.1	Overview of post-translational regulation of Dynamins. <i>Adapted from Kar UP et al. 2017</i>	31
Table 2.2.1.1.1	PCR reaction mix and program	41
Table:3.2.1	List of primers used for point mutations	75

*CHAPTER 1*

*REVIEW OF LITERATURE*

## **1.1 Membrane Remodeling**

Cellular membrane systems play vital roles in compartmentalization of contents of the cell. These compartments are dynamic and constantly undergo membrane remodeling to maintain their structures and perform their functions such as cell-division, endocytosis, inter-cell-cross talk, intra-cellular trafficking, and organelle maintenance. Membranes undergo constant turn over by formation of vesicles or tubules. These processes require generation of membrane curvatures and are essential for cell survival. Lipid bilayers among the eukaryotes have elastic properties that make them resistant to spontaneous bending. This necessitates active mechanisms to generate these changes in shapes. Specialised proteins like BAR proteins and clathrins harbour domains or motifs that are specialized in performing sensing, generating or stabilizing membrane curvature (1, 2). Additionally, some proteins act directly by changing lipid compositions, or providing scaffold or imposing tension on membranes. Membrane remodeling is carried out broadly in five ways: a) lipid asymmetry and composition variation, b) transmembrane domain partitioning and protein crowding (3) c) Insertion of hydrophobic protein motifs (4) d) scaffolding by oligomerizing hydrophilic protein domains and e) cytoskeleton mediated membrane scaffolding (5) (Fig 1.1.1).

## **1.2 Membrane curvature**

Membrane curvature is defined as the bending of membranes to mediate changes in shapes to generate tubules and vesicles. The process of bending the otherwise resistant membranes is an energy-dependent process that involves specialized proteins such as COPI, COPII, caveolin, and flotillin, Arf proteins (4, 6) and BAR domain containing proteins like dynamins (7).

## 1.2.1 Mechanisms of membrane curvature generation

### A) Effect of lipid shape, distribution

Properties like the head-group and acyl chain length confer specific shapes to the lipids. Change in their distribution across the membrane is essential for changes in membrane curvature (8). Lipids like phosphatidylethanolamine (PE) due to their smaller head group to acyl chain ratio attain a conical shape. As the head groups of PE lipid clusters come closer together, the broader acyl bases impose a negative curvature (membrane curved outward of the luminal side) on the membrane. On contrary, lipids like phosphatidylinositol phosphates (PtdIns) have a large head group to acyl chain ratio, have an inverted conical shape and hence impart positive curvature (membrane curved towards of the luminal side, inwards) to the membrane upon association (Fig. 1.1.1). Cardiolipin (CL) is a negatively charged lipid present in the inner mitochondrial membrane (9) and in the bacterial plasma membrane (10).

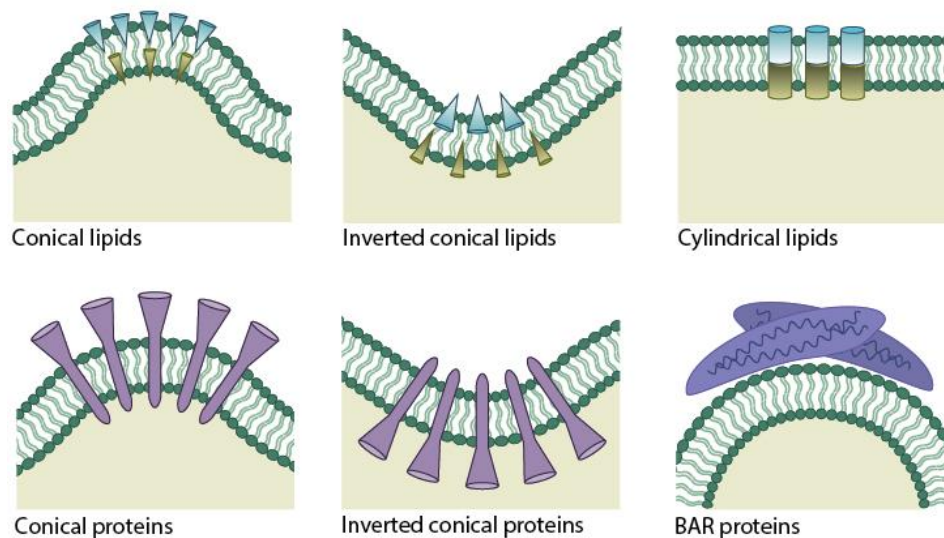


**Figure 1.1.1: Effect of shape of lipids and proteins on membrane curvature.** Conical shaped lipids like phosphatidylethanolamine (PE) provide a positive curvature to the membranes (bulging inward) while inverted-conical shaped lipids like phosphatidylinositol phosphates (PtdIn) provide a negative curvature (bulging outward) to the membranes. Cylindrical lipids like

phosphatidylcholine (PC) are cylindrical in shape and maintain lamellar membranes. **Image source:** <https://creativecommons.org/licenses/by-nc/4.0/legalcode>

The CL molecule is composed of two phosphatidic acids linked together by a short glycerol bridge which gives it a conical shape that contributes to negative curvature (10, 11). Phosphatidyl choline (PC) and phosphatidyl serine (PS) have a cylindrical shape which do not determine membrane curvature (Israelachvili J, 1991 Intermolecular & Surface Forces (Academic, London), 2nd Edition)

## **B) Effect of proteins on membrane curvature**

Membrane bending is carried out by integral membrane proteins which generate curvature by oligomerization (5,12). Examples of such proteins include Arf-proteins endophilin, synaptogamin. Certain group of proteins such as the coat proteins and BAR domain proteins can induce membrane curvature by binding to the membranes peripherally (13). Coat proteins like clathrin organise into multimeric forms to provide a scaffold to induce membrane curvature during vesicle scission (14). Dynamins and dynamin related proteins belong to a group of proteins that act on pre-existing curvatures to oligomerize into rings and helical spirals and cause fission, fusion or tubulation of the underlying membrane (15-17).

### **1.3 Dynamin family of mechanozymes**

This class of proteins called the “Dynamin superfamily” gets its name from the representative member, dynamin, a large GTPase which performs vesicle scission during endocytosis (2, 18, 19). This protein was initially discovered in a temperature-sensitive mutant in *Drosophila melanogaster*. The gene locus associated with this mutation was called the *Shibire* which gave temperature-sensitive paralysis phenotype due to mutation (20). The protein coded by

this locus was named “dynamin” (21,22). Dynamin was later found as a microtubule associating protein which dissociates from the microtubule bundles

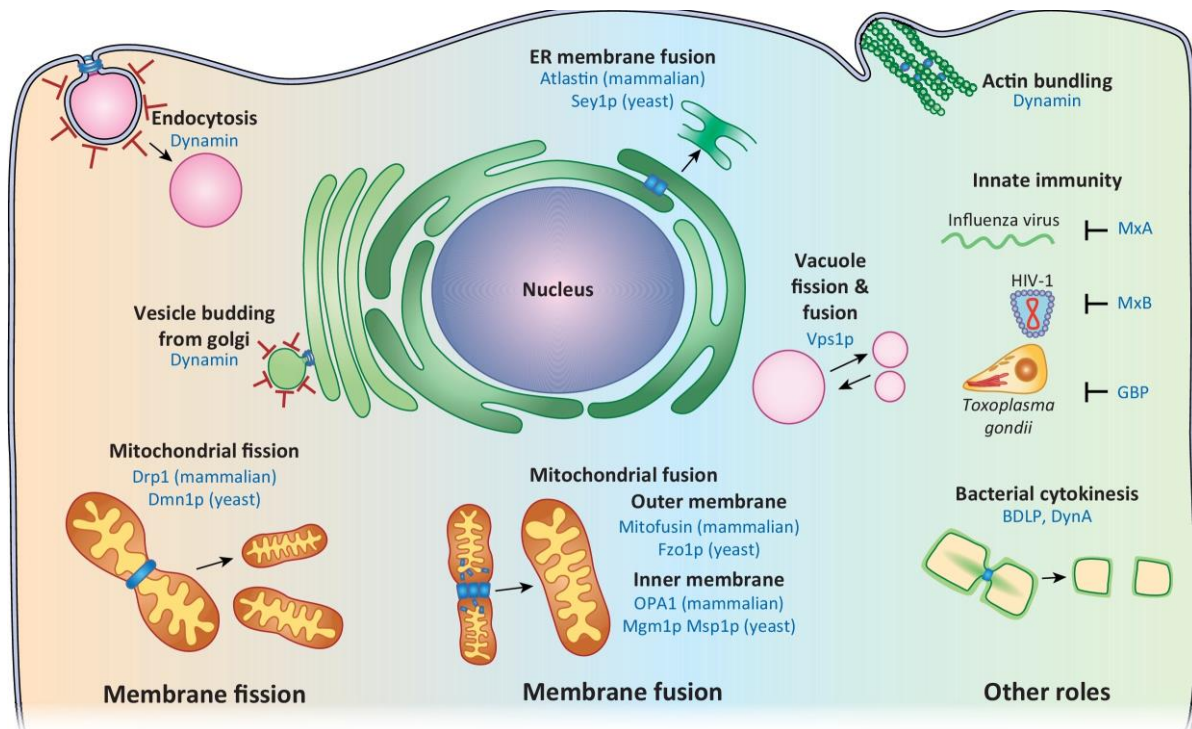


**Figure 1.3.1: An overview of functions of members of dynamin superfamily.** The image shows various cellular processes which require membrane remodeling by dynamin superfamily of proteins (**Image source:** Jimah JR *et al.*, 2019).

upon addition of nucleotides (23, 24). Further studies revealed that mutation in this protein inhibits neuronal endocytosis (25) and hence causes paralysis. Since then, a number of studies have been carried out to understand various aspects of this protein including its role, mechanism, cellular distribution and regulation of its functions. The ‘Dynamin superfamily’ is an umbrella term for mechanozymes that can be categorized based on their function (Fig. 1.3.1) and domain organization. All the members of this group of proteins perform membrane remodeling, and can be grouped as fission, fusion or tubulation proteins (26). A more distinct

classification based on their domain architectures are classical dynamins or dynamin related proteins. Classical dynamin term is used for the founder members, mammalian dynamin 1, dynamin 2 and dynamin 3 proteins which contain a GTPase domain (GD), a middle domain, a pleckstrin homology (PH) domain, a GTPase effector domain (GED) and a proline-rich domain (PRD) (27) (28). Function of each domain has been discussed later. Dynamin 1 is enriched in pre-synapse of brain whereas dynamin 2 is ubiquitously present. Dynamin 3 is mainly present in testis but also is enriched in brain post-synaptic regions (29,30-32). These isoforms have many splice variants which function at distinct locations within the cell. Invertebrates such as *Caenorhabditis elegans* and *Drosophila melanogaster* possess only a single dynamin gene (20, 33). On the other hand, dynamin related proteins are those group of proteins which lack a distinct PH domain and PRD while retaining the other three domains (26). This group of proteins include the dynamin relate protein-1 (Drp1), atlastin, MxA, MxB, Opa1, Mitofusin, Vps1, hGBP1, ARC5 etc. to name a few.

### 1.3.1 Domain architecture of dynamin family proteins:

Classical dynamins have a five domain structure while dynamin related proteins have a three domain structure. While the classical dynamins have GTPase domain, middle domain, pleckstrin homology (PH) domain, GTPase effector domain (GED) and Proline rich domain (PRD), the dynamin related proteins lack the PH domain and PRD domain but retain the other three domains. (Fig.1.3.1.1)

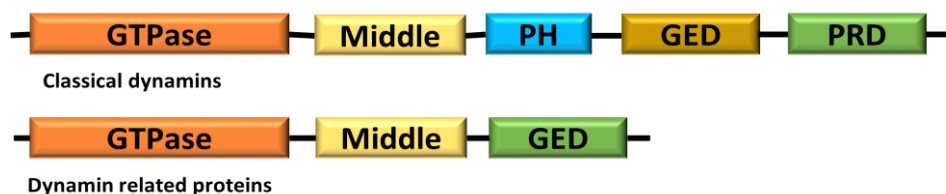


**Figure 1.3.1.1: Domain organization of classical dynamins and dynamin related proteins.** Classical dynamins have five domains, GTPase, middle, PH, GED, PRD domains. Dynamin related proteins have GTPase, middle and GED domain.

### **1.3.1.1 The GTPase domain:**

Dynamamin, being a large GTPase, harbors an N-terminal GTPase domain which resembles Ras-like GTPases (34). It can be sub-divided into four relatively conserved elements, the P-loop (G1 motif), switch-1 (G2), Switch-II (G3) and the nucleotide binding motif (G4) (34, 35). The dynamamin GTPase domain additionally contains sequences between G2 and G3, and downstream of G4 which are responsible for regulatory function of this domain. The bundle signalling element (BSE) includes the G-domain. The BSE consists of 3 helices which are derived from the N and C terminal sides of the G-domain and the C-terminal region of the GED (36, 37). This stretch participates in GTP dependent conformational switch and self-assembly of dynamamins. G-domain dimerization is an indispensable step which precedes the self-assembly of dynamamins (38) and allows bringing the opposing membranes closer (39).

### **1.3.1.2 The middle domain (MD):**

The middle domain is an essential component of the stalk and is required for self-assembly. It shares its 3 helices along with one from the N-terminal portion of the GED to form an antiparallel four-helix bundle called the stalk (36, 40, 41). This structure is required for self-assembly of dynamamins via dimerization, tetramerization, and subsequent formation of higher-ordered structures into rings or spirals (42). The middle domain is further divided into N-terminal half which is more conserved than the C-terminal half among isoforms dynamamin 1 (92%) and dynamamin 2 (72%) (43, 44) and contains a coiled-coil (aa 320-350) involved in self-assembly. This region contains alternative splicing sites for the classical dynamamin isoforms (45, 46).

#### **1.3.1.3 Pleckstrin homology (PH) domain:**

Pleckstrin homology (PH) domains are a hallmark of membrane binding proteins (47-49). In classical dynamins, PH domain bridges the MD and GED. This domain is sufficient for interaction of the dynamins with the target membranes (50-52). This highly conserved domain binds to negatively charged head group of phosphatidylinositol-4-5-bisphosphate (PIP<sub>2</sub>) on the plasma membrane (50, 53, 54). Mutations in the PH domain that abolish membrane binding show inhibitory effects on clathrin-mediated endocytosis (51, 55-58). The PH domain membrane binding is mediated by a variable loop (VL1) which inserts into the membrane bilayer. Membrane insertion of the VL1 helps in generation of membrane curvature during endocytosis (59). Although Drps do not have a distinct PH domain, they too contain a stretch of positively charged residues in their disordered loop region which mediates membrane binding (60).

#### **1.3.1.4 The GTPase effector domain (GED):**

Dynamain family of proteins are distinguished from other GTPases as they function as a GTPase activating protein (GAP) for themselves (26). GED promotes the GTPase activity of the protein. This domain interacts with GED domains of other dynamain molecules via an arginine finger motif to bring about oligomerization of dynamains into rings and spirals (61, 62).

#### **1.3.1.5 The Proline rich domain (PRD):**

The PRD of dynamain, as the name suggests, is rich in proline and basic amino acids. They provide a binding site for SH3-domain containing proteins which play important regulatory roles in functioning of dynamains (63). Some of the SH3 proteins that interact with classical

dynamins include amphiphysin, Grb2, and PLC (64-67) . These interactions assist dynamin to localize at endocytic sites (68) and facilitate dynamin inter-molecular interactions during self-assembly (69).

## **1.4 Biochemical properties of dynamin family proteins**

### **1.4.1 Self-assembly**

Dynamin family proteins remodel their target membrane (2, 70) and organise themselves into their functional forms which are either helical spirals (71, 72) or ring structures (73, 74). Formation of these self-assembled structures occur on their site of action, but in cytoplasm they mostly remain as monomers or dimers. Higher-order oligomerization proceeds by interaction of these protomers (monomers or dimers) into tetramers via not-so conserved interfaces. Structural studies in dynamin 1, MxA, Drp1, hGBP and Mgm1 have shown that these interfaces mostly reside in the stalk region which is comprised of the middle domain and the GED (37, 40, 75-77). The stalks of two dimers along with other domains orchestrate the criss-cross arrangement as observed in tetramers (37, 40). Dimerization, which is independent of the membrane binding, occurs in the cytoplasm through G-domain interactions (38). G-domain dimerization although independent of higher-order assembly is essential to bring two membrane layers closer to bring about fission or fusion (Fig.1.4.1.1) (2, 78). Other domains such as the PH and PRD although not found in Drps are essential for stabilizing the self-assembled structures in classical dynamin (50, 79).

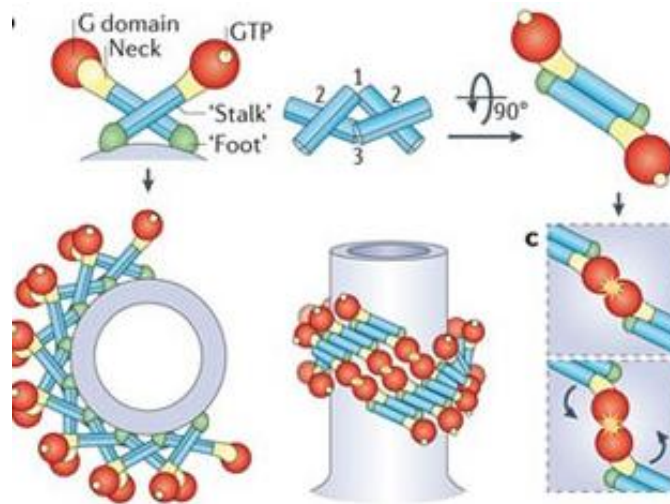


**Figure 1.4.1.1: Self-assembly of dynamins.** The diagram shows oligomerization of dynamin around the template membrane to form higher ordered structures through interaction between their stalk and G-domain. Inter G-domain interactions and GTP binding followed by GTP hydrolysis constricts the membranes (Adapted from Ferguson SM *et al.* 2011)

#### 1.4.2 GTP binding and hydrolysis:

Membrane remodelling by dynamins is an energy dependent process (80, 81). The GTPase domain of dynamins which are conserved among the members (26, 27) harbors the motifs responsible for carrying out GTP binding as well as hydrolysis (82, 83). Dynamin 1 shows very low affinity for GTP and a robust basal GTPase activity ( $\sim 0.4\text{--}1 \text{ min}^{-1}$ ) which is further stimulated by more than 100-fold by higher order self-assembly stimulated by either low salt conditions or membrane binding (43, 71, 84). Its recruitment to the endocytic sites occur in GDP-bound form which is followed by self-assembly and GTP exchange. The GTP hydrolysis activity of the protein is activation dependent. Its interaction with microtubule enhances its activity by 16-fold (24). This enhancement in activity is achieved by positive cooperativity of the protein molecules to form higher ordered structure (43) upon interaction with microtubules or phospholipids, although, this does not change co-operativity of GTP binding (44). Similarly, dynamin like proteins such as Drp1, MxA also show high basal level

GTPase activity which further increases upon self-assembly. GTP binding brings conformational changes in dynamins that allow GTP hydrolysis (38, 85-87). MxA, known for tubulation of membranes, shows higher affinity for GTP than GDP (88). Membrane binding and self-assembly stimulates the GTPase activity to almost 100 fold in dynamin 1 (71). Inability of dynamins to bind GTP (as shown by mutations at K44, S45 residues of dynamin 1) leads to inhibition of function (89, 90). This difference in preference of dynamins for GTP indicates that GTP binding and hydrolysis events are regulated to modulate the generation of the force required for membrane remodelling during their fission, fusion or tubulation functions.

### **1.4.3 Membrane binding and remodelling**

Fission or fusion activities of dynamins require them to bind to their target membranes. Their interactions with lipids allow them to remodel the membrane by redistribution of lipids specifically clustering them on the membranes (70, 91-93). Classical dynamins possess a dedicated PH domain which is responsible for membrane recognition and binding (50, 94). Dynamins work as curvature sensing enzymes (95). The PH domain can bind to flat membrane surfaces by electrostatic interactions, but this interaction is not stable. For stable binding to PIP<sub>2</sub> in the plasma membrane, dynamin uses its variable loop-1 region which resides in the PH domain (58). This stretch of residues (variable loop-1) consists of hydrophobic amino acids which inserts into the membrane bilayer and creates an anchor thereby limiting dynamin conformations (58). This restricted conformation upon membrane binding is essential for self-assembly of the protomers into higher-order structures. VL1 uses hydrophobic membrane interactions to perform sensing of high curvature of budding vesicles (96). In dynamin related proteins, which lack a distinct PH domain, positively charged residues in the unstructured loop regions of the stalk domain participate in membrane

binding. For example in the mitochondrial fission protein, Drp1, the lysine residues within the B-insert region are essential for its interaction with cardiolipin (97). These loop residues provide a lipid interface equivalent to dynamins and form electrostatic interactions with the lipid head group for binding (98, 99). Though these dynamins require membrane binding to oligomerize and stimulate GTPase activity (43, 44), they remodel their target membranes in different ways. Albeit these differences in the membrane binding sequences among the dynamin members, a common mechanism can be seen where the dimers anchored on the juxtaposed membranes contact the dimers on the opposite membranes upon GTP hydrolysis and brings about membrane fission or fusion (Fig.1.4.3.1) (39, 100, 101).

## **1.5 Function of the dynamins and dynamin related proteins**

### **1.5.1 Vesicle Scission**

In mammals, classical dynamins (dynamin 1, 2 and 3) perform scission of vesicles from plasma membrane during endocytosis (102, 103). They perform their function by translocating in nucleotide bound form and oligomerization on the budding vesicle. GTP hydrolysis occurs to generate force which allows dynamin to constrict the neck of the vesicles required for scission from the plasma membrane (104-106). The binding of dynamin to the budding vesicle requires its interaction with the PH domain. Initially, dynamin is recruited to its site of action as a tetramer, and upon membrane binding via PH domain these interact with each other to form helical spirals around the neck of the coated-pits (42). Studies have shown that this helical structure reduces in diameter upon GTP hydrolysis which acts as a scaffold for constricting the underlying membrane (Fig.1.4.3.1) (104-106).

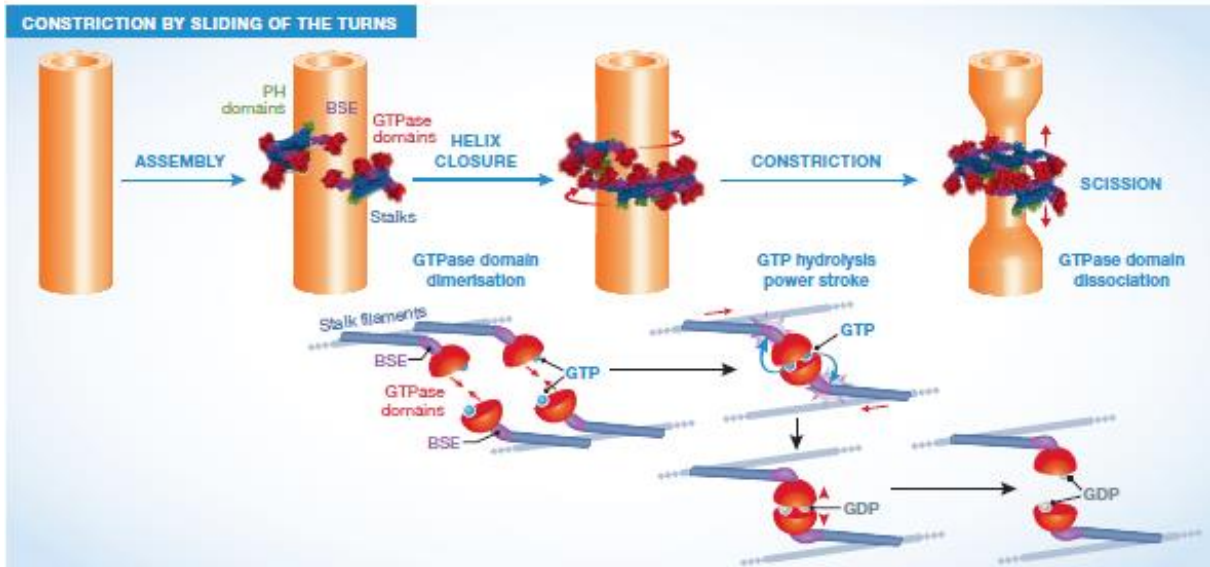


**Figure1.4.3.1: Constriction of vesicles by dynamin.** The diagram shows how dynamin self-assembles around the template membrane through interaction of conserved interfaces. GTP binding and hydrolysis upon self-assembly generates a force that constricts the underlying membrane (Image source: Bruno Antony *et al.* 2016 (39))

Apart from functioning as endocytic dynamin, the ubiquitously present dynamin 2 also performs scission of transport vesicles from trans-golgi network (107). Although dynamin 1 is considered as the universal endocytic dynamin, it is absent in yeast (108, 109). Vacuolar Protein Sorting -1 (Vps1), a golgi localizing dynamin related protein associates with endocytic proteins as well. Apart from endocytosis, this Vps1 also causes membrane fission within the golgi, vacuole, endosome and peroxisomal systems (110-114).

In plants, dynamin-related protein 2A and 2B (DRP2A and DRP2B) are homologous to the classical dynamin 1 (115, 116). These Drps are involved in post-golgi vesicle trafficking and are also important for endocytosis (117). Though a direct role of this protein has not been

established, their association with actin bundles at the plasma membrane is essential for active trafficking of vesicles (117).

The involvement of more than one kind of dynamins in vesicle scission in different systems indicate that these proteins, although lack sequence similarity, are capable of performing similar functions with their mechanism of operation being essentially similar.

### **1.5.2 Mitochondrial maintenance**

Mitochondria are dynamic organelle which are compartmentalized by double membrane system where the outer membrane and the inner membrane are separated by the inter-membrane space. Mitochondrial maintenance by fission and fusion form the basis for cell survival. Mitochondrial fission process is required to carry out its distribution during cell division, to generate ROS and to facilitate mitophagy (118, 119). Fusion of mitochondria allows mixing of content to overcome accumulation of mutations in the mitochondrial DNA (120). These processes require protein machinery to carry out membrane remodeling to cause fission or fusion. First dynamin to be discovered as mitochondrial fusion dynamin was Mgm1 (named after the gene mutation in yeast that caused mitochondrial genome maintenance defect) (121). This defect was later found to be due to abnormal fusion of inner mitochondrial membrane to which Mgm1 is anchored (122). Human homolog of Mgm1 is Opa1, its defective form leads to dominant optic atrophy (123, 124).

Outer Mitochondrial membrane fusion is carried out by a different set of dynamin family proteins. First fusion dynamin was discovered in sperm cells of *Drosophila* and was called fuzzy onions for their appearances due to fragmented mitochondria (125). Its homolog in yeast and *C.elegans* is called Fzo1 (126, 127), whereas, mammals have 2 homologs namely,

Mitofusin 1 and 2 (128, 129). Unlike mitochondrial membrane fusion machinery which are specific for inner and outer mitochondrial membranes, eukaryotes use a single drp for mitochondrial fission. Yeast Dnm1 was the first one to be discovered as mitochondrial fission dynamin (130,131). Mammalian homolog is named as Drp1/DLP1/Dnm1L/DVLP1/Dymple(132-136). Fission proteins bind to their target membrane via adapter proteins. The membrane binding domain of the fusion proteins Mgm1 and Opa1 are specific for cardiolipin (137, 138). On the other hand, the outer membrane fusion proteins Fzo1 and Mitofusins perform this function via their trans-membrane segments located at the N-terminus of GTPase domain (139). Yeast Dnm1 forms multimeric structures to tubulate the membranes (140). It differs from the endocytic dynamin in terms of spiral size. While the spirals formed by endocytic dynamin is 50nm in diameter, Mgm1 forms spirals which measure 120nm (140, 141). This wide diameter is expected as, unlike endocytic dynamin, Mgm1 wraps around double membrane system keeping both, inner and outer membranes intact. These fusion dynamins oligomerize on the opposing membranes and pull them together (142).

### **1.5.3 Antiviral activity**

Mx proteins are interferon-induced dynamins. The Myxovirus resistance (Mx) genes were discovered in mice for their resistance to infection by influenza viruses. The observation that in comparison to the wild mice, the inbred mice were more susceptible to these infections mapped the locus on chromosome 16 of mouse (143-145). Mice chromosome consists of two Mx genes, Mx1 and Mx2 (146, 147). Although they both have antiviral activity, they show different localization and recognize distinct virus groups. While Mx1 is a nuclear localizing Drp that inhibits Thogoto virus and Influenza viruses (148-150), Mx2 is a cytoplasm

localizing Drp which restricts Rift Valley fever virus, Vesicular stomatitis virus and La Crosse virus (151-153). These genes are conserved across the vertebrates and their expression is induced by type I and type III interferons (154, 155). In humans, there are two genes namely MxA and MxB (156). MxB in humans, apart from inhibiting the reported viruses, is known to inhibit HIV-1 infection by reducing integration of viral DNA (157) and Hepatitis C virus (158). Although they both are largely anti-viral proteins, their subcellular localization determines their specificity. MxA mostly exists as cytoplasmic protein, partly associated with the plasma membrane and recognizes the NP proteins via its L4 loop (159-161). MxB, on the other hand, exists as two forms where the long form includes an N-terminal NLS (162). It primarily localizes on the nuclear envelope on its cytoplasmic face (163). MxA acts like a gate-keeper protein in the cytoplasm by blocking the vRNPs in the infected cells (164). MxA organizes itself in ring-like structures around the tubular vRNPs to block their function (74). This organization is induced by the helical nucleocapsids where the nearby MxA contact each other to form an active MxA form (165). MxB prevents infection by blocking nuclear import of DNA from the viruses (166-168). MxA and MxB differ on many other aspects apart from localization differences. As for example, GTP hydrolysis is an requirement essential for MxA activity but it is dispensable for activity of MxB (168).

#### **1.5.4 Endoplasmic reticulum (ER) fusion:**

The ER forms a continuous membrane system in the cell, which also remains continuous with the nuclear envelope. It forms flat sheet structures, and extensive tubules network throughout the cytoplasm. ER function is essential for cellular processes like lipid synthesis, transmembrane and secreted proteins synthesis, calcium homeostasis, post-translational modification of proteins (169, 170).

ER fusion is mediated by a class of dynamin-like GTPases, Atlantin (ATL) (171, 172). Its depletion or mutations in ATL leads to fragmented ER (173). Atlantin localizes on opposing

membranes to form *trans*-oligomeric complexes (172). To perform this membrane tethering activity, Atlastin requires GTP hydrolysis (172, 174). Mutations in the *atlastin* gene which render Atlastin functionally defective, lead to a neurodegenerative disease, hereditary spastic paraplegia where the axons are shortened in cortico-spinal motor neurons (175, 176).

### **1.5.5 Cytokinesis:**

Cell-cycle culminates into physical separation of cellular contents into progeny cells. Dynamins play essential roles in cell division of plants and the protists like *Dictyostelium discoideum* (177-180). They translocate to cleavage furrow and cell plate axis for cytokinesis. In animals, classical dynamins interact with endocytic proteins like clathrin, syntaxin, and endobrevin during fusion events at the time of cell division (181, 182). Dynamins in plants participate in the generation of tubulo-vesicular network which acts as precursors for the cell-plate formation. The first cytokinesis dynamin discovered was Phragmoplastin, a homolog of DRP1 (183). This dynamin accumulates at the cell plate axis and mediates tubulation of membranes which eventually are flattened to form membranes of the dividing cell (184, 185). In *Arabidopsis*, role of Drp1 in cytokinesis has been extensively studied. It localizes to the plane of spindle fibres and phragmoplast, and serve as an anchor for golgi-derived vesicles to accumulate and help in cell-plate formation (185, 186).

### **1.6 Regulation of dynamins by post-translational modifications**

Dynamins remodel their target organelle membranes upon receiving appropriate cellular signals. Their properties like self-assembly, GTPase activity or membrane binding are tightly regulated by various factors including binding with their partner proteins, protein translocation, degradation. Post-translational modifications (PTMs) provide a mechanism to regulate activity of dynamins by reversibly attaching groups at specific sites of the proteins.

In response to cellular signals, dynamins are known to undergo modifications like phosphorylation, ubiquitination, sumoylation, S-nitrosylation. Cells employ various protein machineries to attach and detach these groups depending on cell-stage. An overview of regulation of dynamins by PTMs (187) is tabulated in Table 1.4.1

### **1.6.1 Phosphorylation**

Phosphorylation is most common PTM where phosphate group is attached at serine, threonine and tyrosine residues of a protein by various kinases and is removed by phosphatases bringing about structural and functional changes. Classical dynamins, found exclusively in metazoans, are the first to be reported to undergo phosphorylation. For example, dynamin 2 undergoes phosphorylation at Y597 to regulate endocytosis by modulating its binding to Cav1. This phosphorylation enables localization of Dyn2 to the plasma membrane and hence becomes essential for caveolae scission (188). Phosphorylation of its serine residues in the GED regulate its binding with syndapin and amphiphysin through conformational changes (189, 190). Aberration in mitochondrial dynamics, which causes various diseases like Charcot-Marie tooth disease, Parkinson's disease, Alzheimer's disease is regulated by fission and fusion dynamins (123, 191-194). Drp1, a fission drp, undergoes phosphorylation at S585 which stimulates fission by enhancing interaction with adapter proteins (195). Phosphorylation at S637 and S635 in GED perturbs inter-domain interactions and determine differential localization of Drp1 (196, 197). Mitochondrial fusion proteins Mitofusin 1 and 2 also undergo regulation by phosphorylation during apoptotic cell death (198, 199).

### 1.6.2 Ubiquitination

Ubiquitination regulates protein function by adding ubiquitin at lysine residues. This PTM conventionally is linked to proteasomal pathway for degradation of proteins. Apart from this function, ubiquitination also regulates localization, stability, interaction of partner proteins, and also degradation of proteins by lysosomal pathway (200). MARCH-V mediated ubiquitination of Drp1 at the mitochondrial fission sites regulates assembly at these sites (201). In oxygen glucose deprivation and reperfusion (OGDR) condition, another E3 ligase Parkin ubiquitinates Drp1 to degrade it which in turn protects the cell from mitochondrial dysfunction (202). Enhancing mitochondrial fission during cell cycle requires reduction in fusion activity of Mfn1. MARCH-V mediated ubiquitination of Mfn1 allows its degradation to facilitate mitochondrial fragmentation (203). During hypoxic stress, deacetylation by HDAC6 which recognizes MARCH-V, prevents Mfn1 ubiquitination to enhance mitochondrial fusion activity (204). MARCH-V mediated ubiquitination of Mfn2 at K192 facilitates maintenance of ER- mitochondrial contact sites during mitochondrial fusion by upregulating self-assembly (205, 206). This ubiquitination is specific for the Mfn2 bound to mitochondrial membrane. This implies that regulation by ubiquitination by a common E3 ligase like MARCH-V can regulate both fission and fusion of mitochondria. This specificity might be determined by cellular stress, apoptotic signals, cell cycle signals and specific lipid interactions. Homolog of Mfn in yeast, Fzo1 is deubiquitinated at K398 by Ubp2 and at K464 by Ubp12. Ubiquitination at K398 leads to inhibition in mitochondrial fusion by promoting proteasomal degradation whereas Mdm-30 mediated K464 ubiquitination imparts stability to the protein which promotes mitochondrial fusion (207).

### **1.6.3 SUMOylation**

SUMOylation is a reversible PTM which is carried out by covalently conjugating Small Ubiquitin-like Modifier (SUMO) at lysine residues of a protein. It provides an efficient method of modulating the activity, stability and subcellular localization, of a wide variety of substrate proteins. Mitochondrial fission drp, Drp1, is a target for SUMOylation by 3 SUMO forms, SUMO 1, 2, 3. The recruitment and dissociation of Drp1 on the mitochondrial membrane is regulated by sumoylation by SUMO and de-sumoylation by SENP5(208). Drp1 SUMOylation occurs at 4 lysine residues (K594, K597, K606, and K608) which reside in the B-insert region (209). SUMO-1 attaches to Drp1 at the onset of cell cycle which stabilizes Drp1 in the mitochondrial membrane to promote fission (210). During oxygen glucose deprived stress, when fusion of mitochondria is more favoured than fission, Drp1 is withheld in the cytosol by SUMO2/3 addition (211). The non-canonical drp, MxA, involved in antiviral activity, is sumoylated at K48 in its GTPase domain, although its role remains unknown.

### **1.6.4 S-Nitrosylation**

S-nitrosylation is a reversible and targeted PTM wherein nitric oxide (NO) is covalently bonded to a thiol group of cysteine residue (S—NO) of target protein. Addition of NO exerts its effects during processes like DNA repair, host defence, endocytosis, and neurotransmission by modulating a protein's stability and localization (212). Endocytic dynamin, dynamin 1, is a target for S-nitrosylation during receptor mediated endocytosis. NO synthase mediated S-nitrosylation of dynamin 1 at C607 (in the PH domain) stimulates its membrane binding, GTPase activity and oligomerization (213). While S-nitrosylation at another site in the GTPase domain (C86) regulates endocytosis favouring survival of the

endothelial cells (214). Mitochondrial fission drp, Drp1 is a substrate for S-nitrosylation (215, 216). This nitrosylation occurs in response to beta-amyloid oligomers during conditions like Alzheimer's and Huntington disease to promote mitochondrial fragmentation leading to neuronal damage (217). It promotes Drp1 dimerization and GTPase activity. The GED, which is responsible for self-assembly, undergoes nitrosylation at residue C644 of Drp1 allowing dimerization of Drp1 to promote further self-assembly (217, 218).

### **1.6.5 Acetylation**

Acetylation (also referred to as *N* $\epsilon$ -lysine acetylation) is the addition of an acetyl group to the amino group of a lysine side chain. It neutralizes the positive charge that disrupts salt bridges and introduces steric bulk leading to altered protein–protein interactions, enzymatic activity and stability (219-221). OPA1 resides in the inner mitochondrial membrane and is crucial for maintenance of cristae formation. Its membrane fusion activity is regulated by a balance between acetylation and de-acetylation. Hyper-acetylation of OPA1 at K931 is observed during cardiac pathological conditions like cardiac hypertrophy. This PTM reduces mitochondrial fusion and GTP hydrolysis activity, and leads to abnormal mitochondrial distribution and fragmentation. This is restored by de-acetylation by SIRT3 de-acetylase (222, 223).

Modification	Protein	Residues	Effect on function	Mechanism
Phosphorylation	Dynamamin 1	Tyr 597	Promotes clathrin-mediated endocytosis	Increases self-assembly and GTP hydrolysis
	Dynamamin 2	Tyr 597 Tyr 231 Ser 774/778	Promotes caveolae-mediated scission - Inhibit endocytosis	Increases translocation to plasma membrane Enhances Dyn2-Cav1 interaction Impair interaction with Amphiphysin and Syndapin, inhibit its membrane recruitment
Ubiquitylation	Yeast Vps1	Ser 599	Promotes vesicle scission from trans golgi	Enhances interaction of Vps1 with Amphiphysin partner Rvs167
	Drp1	Ser 585(Rat) or Ser616(Human) Ser 637	Promotes mitochondrial fission during mitosis. Inhibits mitochondrial fission	Facilitates interaction with other adaptor proteins
	Mfn2	Ser 600 Ser 635(Rat) or Ser617(human) Ser 27	Promotes mitochondrial fission Promotes mitochondrial fission during apoptosis Promotes mitochondrial fission during apoptosis	Inhibits interaction of GED and GTP binding domain and reduces GTPase activity Facilitates Drp1 association with adapter Fis1 Dissociates sequestered Drp1 from microtubule and recruits to mitochondria Promotes ubiquitylation of Mfn2 by E3 ligase Huwe1 and targets for proteasomal degradation
S-nitrosylation	Mfn1	Thr 111/Ser442 Thr562	Promotes mitochondrial fragmentation during apoptosis Promotes mitochondrial permeabilization and apoptosis	Phosphorylated form acts as a receptor for E3 ligase Parkin Promotes recruitment of BAK to mitochondrial membrane
	Dynamamin1 Drp1	Cys 86/Cys 607 Cys 644	Stimulates endocytosis Promotes mitochondrial fission and causes synaptic damage	Induces self-assembly and GTPase activity Promotes Drp1 dimerization, self-assembly and stimulates GTPase activity
Sumoylation	Drp1	-	Induces mitochondrial fragmentation	Promotes Drp1 association with mitochondria
	Fzo1	Lys 398 Lys 464 Lys 594, Lys 597, Lys 606, Lys 608	Inhibits mitochondrial fusion Promotes mitochondrial fusion Promotes Cyt C release from inter mitochondrial membrane space during apoptosis	Targets for proteasomal degradation Stabilizes Drp1 on the mitochondrial membrane Stabilizes Drp1 association with mitochondria and facilitates Bax oligomerization on mitochondria
Acetylation	OPA1	Lys 926, Lys 931	Promotes mitochondrial fragmentation	Inhibits GTPase activity of OPA1
	Mfn1	Lys 491	Inhibits mitochondrial fusion	Targets Mfn1 for MARCH-V-mediated proteasomal degradation

Table 1.4.1: Overview of post-translational regulation of Dynamins. Source: Kar et al., 2017

## 1.7 Nuclear envelope remodelling:

A distinguishing feature of the eukaryotes is the compartmentalization of their genetic material. The nuclear envelope (NE), a semi-permeable bilayer membrane is highly selective. This membrane system is continuous with the endoplasmic reticulum. Cell division in all the eukaryotes requires division of the genetic material among the progeny cells. This requires the nuclear content to replicate and get distributed to new cells. NE on the basis of its integrity during this process can undergo either closed mitosis or open mitosis (Fig.1.7.1). Closed mitosis occurs in yeast and lower eukaryotes where the NE remains intact throughout the cell division (224, 225). Here, the spindle bodies embedded in the NE initiates spindle formation inside the nucleus. On contrary, open mitosis occurs in higher eukaryotes including mammalian cells and proceeds by nuclear envelope breakdown followed by disassembly of the nuclear lamina and nuclear pore complexes. Closed mitosis requires the intact nucleus to expand to accommodate the replicated genetic material and form two new nuclei from the pre-existing one whereas open mitosis proceeds by disassembly followed by reassembly of NE around the genetic material.

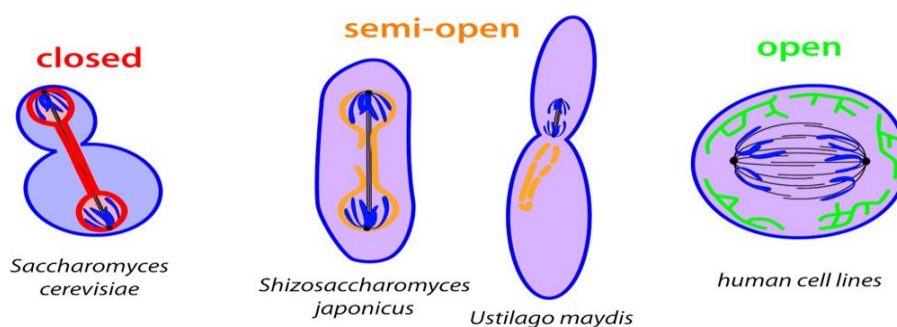


**Figure 1.7.1: Eukaryotes undergo division of nucleus by closed, semi-open or open mitosis.** The image shows the modes by which nuclei divide by maintaining the nuclear envelope (closed, red), partial disintegration of NE (semi-open, yellow) or complete

disintegration of NE (open, green) in different organisms.(Image source Boettcher B *et al.* 2013)

*Tetrahymena thermophila*, a ciliate protozoa, undergoes closed mitosis. It has a large, somatic, polyploid macronucleus called the MAC and a small germline diploid micronucleus called the MIC. MACs being somatic, are transcriptionally active whereas the MICs are transcriptionally inactive in vegetative cells. The MIC DNA get actively transcribed during sexual reproduction. In vegetative cells, MIC and MAC replicate at separate time points of the cell cycle. The MAC division occurs before MIC, without functional centromeres. Copies of MAC chromosomes get partitioned randomly between the two progeny cells. Due to random segregation of alleles, vegetative heterozygous progeny after conjugation becomes pure for one of the allele within approximately 100 cell fissions (226). This genetic phenomenon is known as phenotypic assortment.

### **1.8 Nuclear expansion in *Tetrahymena***

*Tetrahymena* undergoes sexual reproduction by forming conjugating pairs with the mating partners. The otherwise transcriptionally inactive MIC elongates to almost 50 folds to attain a crescent shape during meiosis (227). At this stage chromosome pairing and recombination occur in MIC. Following this meiotic division, four nuclei are formed, of which, three degenerate and one is selected for inheritance. This selected nucleus undergoes mitosis to produce two pronuclei which are genetically identical. Of these two, one is transferred to the partner cell which fuses with the resident micronucleus to yield a zygotic MIC. This zygotic nucleus undergoes two rounds of mitosis which results in 4 MICs. Out of these four MICs, two expand ~15 folds to become MACs. This stage is termed as ‘macronuclear expansion’ (Fig.1.8.1). This expansion is necessary for accommodating the increased genetic material.

MAC expansion which occurs by increase in the volume of the nucleus, requires addition of new membrane. This process although occurs during closed mitosis and interphase stages of cell cycle during open mitosis, remains yet to be fully understood.

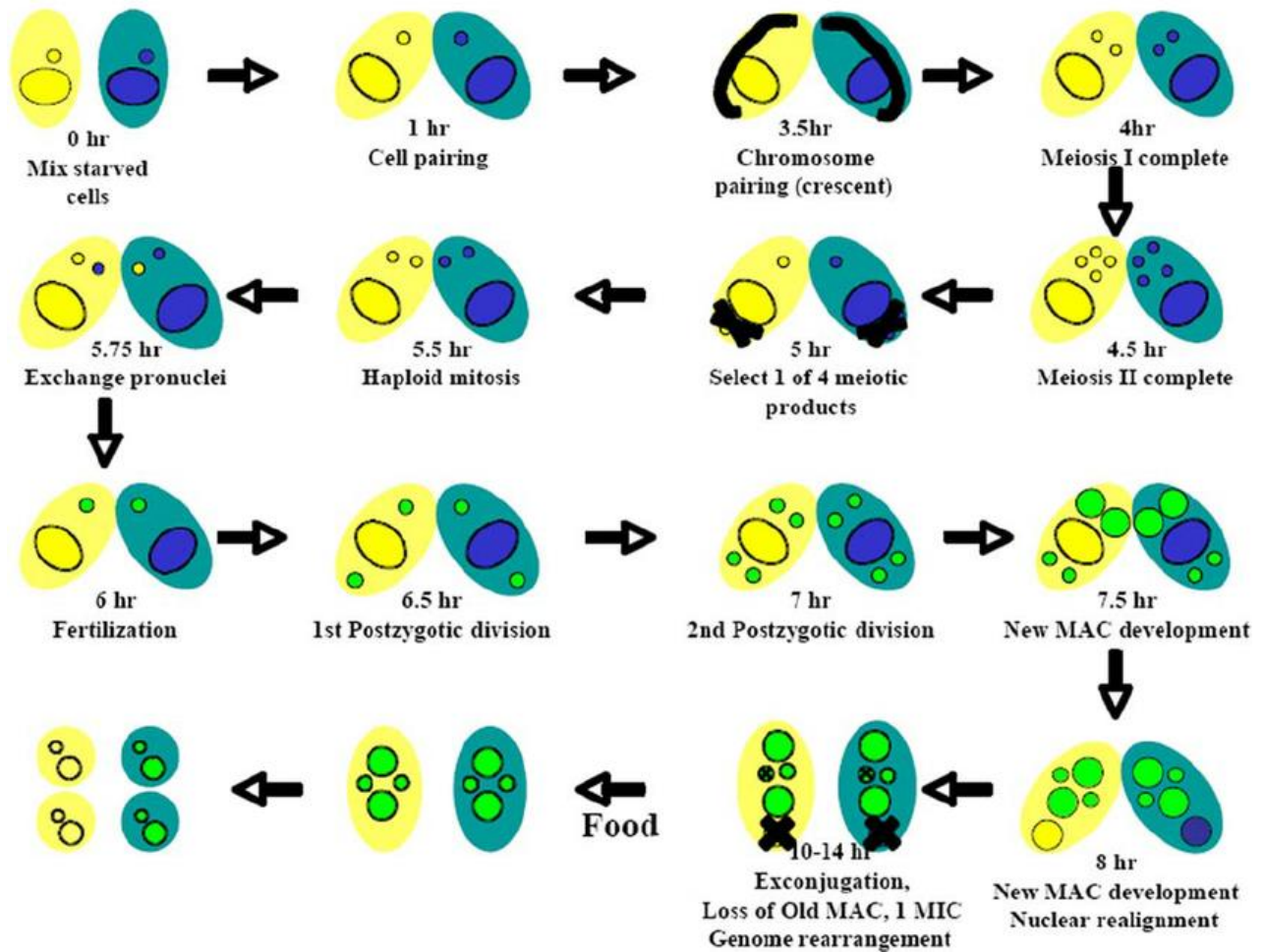


**Figure 1.8.1: Stages of nuclear division during conjugation in *Tetrahymena thermophila*.**

The diagram shows stages during conjugation of *Tetrahymena* where it undergoes mitosis and meiosis and forms new MAC during macronuclear development stage of conjugation (8hr). Yellow and dark green colors show opposite mating-type cells. (Image source: Wei Miao *et al.*, 2009)

This bi-nucleated protozoa has evolved a well-organised membrane-trafficking system. This is evident from the presence of several Rab GTPases (228). Along with these, *Tetrahymena* harbors eight dynamins which further indicates towards well evolved membrane organization. TtDrp1 performs important role during endocytosis, whereas TtDrp2 localizes on parasomal sacs. Drp3-6 form a lineage specific group which might have evolved to perform specific functions (229) (Fig.1.8.2). Drp7 and Drp8 are known to localize in subcortical mitochondria and might have functions in mitochondria.

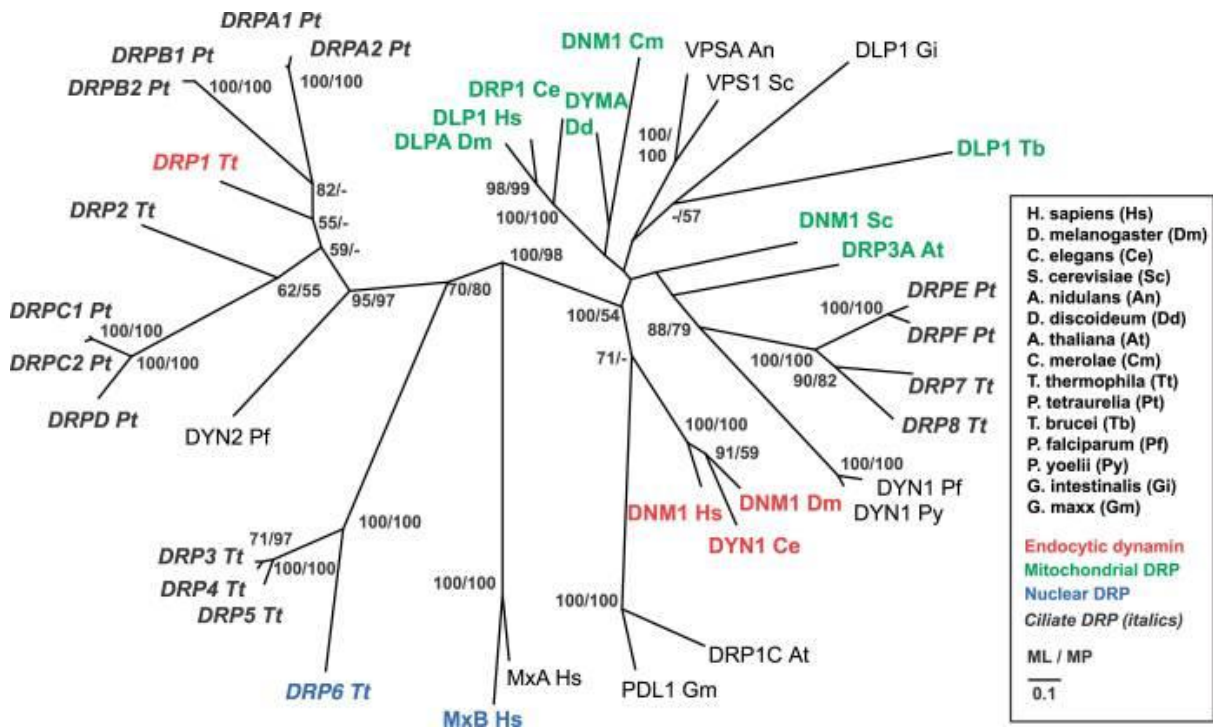


**Figure 1.8.2: *Tetrahymena* contains 8 Dynamin Related Proteins.** Phylogenetic tree showing different members of dynamin family of proteins. Drp3-6 of *Tetrahymena* form a separate clade and have evolved to perform specific functions.(229) (Image source: Elde NC *et al.* 2005)

Dynamamin related protein 6 (Drp6) is a nuclear localizing dynamamin in *Tetrahymena thermophila*. Macronuclear expansion in cells lacking Drp6 or expressing its dominant negative form remains inhibited, indicating its role during this stage (230). Drp6 is required for expansion of the nuclear envelope during transition from MIC to MAC. Its localization during the vegetative state is at the nuclear envelope with a lesser population present as the cytoplasmic puncta. Depending on the cell cycle stage, this protein keeps switching between its cytoplasmic and nuclear membrane localization. Apart from the localization, its function is also cell cycle regulated. It shows peak in activity in starved conditions or during macronuclear expansion (230).

In this thesis, we investigated how the localization and activity of Drp6 is regulated in *Tetrahymena thermophila*. The chapters in the following sections were an attempt to study how Drp6 regulation in terms of localization and activity can be brought about by various factors like post-translational modifications, lipid specificity, self-assembly and interaction with cytoskeletal proteins like microtubule and dynein. The findings of the study has been divided into the following objectives:

1. Mechanism of Drp6 function and regulation by post-translational modifications
2. Mechanism of cardiolipin interaction specificity and nuclear recruitment of Drp6.
3. The role of G domain and middle domain in the self-assembly and nuclear recruitment of Drp6.
4. Mechanism of nuclear expansion by Drp6 and role of microtubule structure.

## *CHAPTER 2*

# *Mechanism of Drp6 function and regulation by post- translational modifications*

## 2.1 Introduction

Post-translational modifications (PTMs) provide mechanisms to regulate the activities of proteins in response to various cellular cues after they are synthesised in eukaryotic cells.

The vast arrays of protein PTMs namely ubiquitylation, S-nitrosylation, phosphorylation, SUMOylation, acetylation are known to regulate protein function. Dynamin family proteins that perform membrane remodelling functions are also regulated by various post-translational modifications. Several examples of how phosphorylation affects the functioning of dynamins are known. Dynamin 1 and 2 undergo phosphorylation at Y597 which leads to increased endocytosis by actuating self-assembly and GTP hydrolysis during caveolae mediated or ligand activated receptor endocytosis but not constitutive endocytosis. In dynamin 2 this phosphorylation is required for Cav1 binding and its translocation to plasma membrane (188). This indicates that phosphorylation is capable of regulating dynamin function in specific processes (231). In post-mitotic neurons, residues S774 and S778 in GED of dynamin 1 are phosphorylated by CDK5 leading to impairment of its membrane recruitment by impairing its interaction with amphiphysin and syndapin. Whereas calcineurin-mediated dephosphorylation is required for restoring these interactions and hence recruitment to target membrane (189, 190, 232). Vps1 in yeast mediates clathrin mediated endocytosis as well as trans-golgi protein trafficking (114, 233, 234). An inter-play of phosphorylation and dephosphorylation at S599 determines its binding with amphiphysin Rvs167 to regulate the progression of endocytosis (235). Mitochondrial dynamics regulation if impaired, lead to various disorders like Optic atrophy, Charcot-Marie tooth disease, Alzheimers's disease, etc. (123, 191, 192). Mitochondrial fission dynamin, Drp1 undergoes phosphorylation at S585 by multiple kinases at different cell stages and under cellular stress (236, 237), which stimulates its fission activity without affecting its GTPase activity. Loss of this phosphorylation leads to reduction in mitochondrial fission probably by augmenting its interaction with the adapter

proteins. Phosphorylation at a particular residue can lead to many opposing downstream effects. For example, Drp1 phosphorylation at S585 by CDK5 in neuronal cells leads to fragmentation upon injury (238) whereas in healthy cells, it inhibits fragmentation by inhibiting self-assembly (239). Another impact of phosphorylation on self-assembly of Drp1 can be seen at S637 in GED. It augments its interaction with GTPase domain which inhibits both GTPase activity and oligomerization (240). Dephosphorylation of S637 by calcineurin during apoptosis translocates Drp1 to mitochondria.

Mitofusin 2, upon pro-apoptotic signals during cellular stress, undergoes phosphorylation at S27. This phosphorylation in turn activates ubiquitination mediated proteasomal degradation of Mfn2 to promote mitochondrial fragmentation (199).

During *Tetrahymena* conjugation, the activity of Drp6 is most pronounced at a stage when the MIC (2n) expands to form a polyploid MAC (45n). Elimination or inhibition of Drp6 activity inhibits this nuclear transition. This protein is present in the vegetative growth phase of the cells as well indicating its requirement at this stage. Drp6 localizes to nuclear envelopes of growing cells with a subset of population that localizes as cytoplasmic puncta. The proportion of this cytoplasmic subset increases during starvation when the NE locating population starts falling off. At early conjugation stages, Drp6 completely loses its NE localization and remains cytoplasmic. During the MIC to MAC transition stage called the nuclear expansion stage, Drp6 begins to re-associate specifically with the new developing MAC and Mic. Apart from differential localization, Drp6 exhibits differential activity as well. Its rapid assembly on the NE during starvation and MAC expansion stage but not vegetative condition further points towards its highly regulated function. Earlier in the lab it has been shown that Drp6 undergoes phosphorylation and ubiquitination. This chapter attempted to elucidate the role of phosphorylation in regulating function and localization of Drp6.

## **2.2 Materials and methods**

### **2.2.1 Materials**

- pRSETB vector was a kind gift from Prof. M.S.Shaila, IISc, Bangalore.
- 3xmCherry 2xHA Neo4 vector was a kind gift from Prof. Aaron Turkewitz, University of Chicago, USA
- PCR reagents and restriction enzymes were purchased from New England Biolabs.
- Primers were purchased from Eurofins MWG.
- Lipids and extruder apparatus used in the assays were purchased from AvantiPolar Lipids.
- Proteose peptone, Yeast extract were purchased from BD Bacto. Glucose and Fe-EDTA were purchased from Sigma-Aldrich.
- Luria Bertani broth and agar were from Himedia.
- All other chemicals unless otherwise mentioned were from Sigma-Aldrich.
- TEM accessories were from Ted Pella, Inc.

### **2.2.2 Methods:**

#### **(A) Cloning and generation of point mutants**

Codon optimized DRP6 was synthesized and supplied in pUC57 vector by Eurofins (MWG). It was cloned in pRSETB using KpnI and EcoRI sites. Stratagene quickchange protocol was used to design primers for incorporation of point mutations to generate phosphomimic mutation (serine to aspartate) and Phosphonull mutation (serine to alanine). Primer details are listed in Table 2.2.1.1. Mutations were incorporated in DRP6-pRSETB construct using the following PCR protocol.

**Table 2.2.1.1.1: PCR reaction mix and program**

Component	Volume
Template (50ng/ $\mu$ L)	1 $\mu$ L
dNTP mix (10mM)	1 $\mu$ L
Forward primer	1 $\mu$ L
Reverse primer	1 $\mu$ L
MgCl <sub>2</sub> (50mM)	1 $\mu$ L
5x Phusion polymerase buffer	10 $\mu$ L
Hotstart Phusion Polymerase	1 $\mu$ L
Deionised water	34 $\mu$ L

<b>PCR program:</b>	
95°C	30 s
95°C	30 s
55°C	1 min
72°C	3 min

PCR was performed for 18 cycles.

20  $\mu$ L of the PCR products were treated with 0.5 $\mu$ L DpnI for 7-8 hours at 37 °C. 3  $\mu$ L of the DpnI treated PCR product was transformed in DH5 $\alpha$  competent cells. Mutations were confirmed by sequencing.

### **(B) Expression and purification of recombinant Drp6 and its variants.**

For expression of protein, chemically competent *E. coli* C41-DE3 cells were transformed with the pRSETB constructs and grown on ampicillin (100  $\mu$ g/ml) containing LB agar plates

for 16 hours at 37 °C. Under sterile conditions, few colonies were picked and transferred to 800ml LB broth supplemented with ampicillin (100 µg/ml) and allowed to grow at 37 °C at 220 rpm till the OD<sub>600</sub> reached 0.2. Culture was then transferred to 18 °C and incubated for 40 mins. Protein expression was induced with 0.5mM IPTG (at 0.4 O.D<sub>600</sub>) and grown at 18 °C for 16 hours. Cells were harvested at 12000 rpm at 4°C and used for protein purification.

Harvested cells were resuspended in ice-cold buffer A (25mM HEPES pH 7.5, 300mM NaCl, 2mM MgCl<sub>2</sub>, 2mM β- mercaptoethanol.) supplemented with 1mM PMSF (Sigma-Aldrich) and EDTA- free protease inhibitor cocktail (Roche). Lysis was carried out using sonication at 4 °C and a clear lysate was obtained by centrifugation at 15000 rpm at 4 °C for 1h. Lysate was incubated with Ni-NTA agarose resins (Qiagen) for 2 hours at 4 °C. Resins were collected at 4000 rpm, 4 °C and washed with 100 bed volumes of wash buffer (50mM imidazole in buffer A). Protein was eluted with buffer A containing 250mM imidazole. For assessing the purity of the proteins, SDS-PAGE gels were imaged using QuantityOne software, Biorad. Protein band intensity measurement was done using ImageJ image (NIH) software to assess the purity of Drp6 band against the contaminant proteins in the same lane. Protein was dialyzed in lysis buffer at a concentration of 150 µg/ml.

### **(C) Measurement of GTPase activity**

GTPase activity of Drp6 and its variants were performed using 1 µM protein and 1mM GTP (Sigma- Aldrich) in Buffer B (25mM HEPES pH 7.5, 150mM NaCl, 2mM MgCl<sub>2</sub>). The reaction mix was incubated in 37°C. For time kinetics assay, 20µL aliquots were collected at different time intervals and 0.5mM EDTA was added to stop the reaction. 1 mL of Biomol Green reagent was added to samples and incubated for 20min at RT before measuring the absorption at 620nm. The amount of phosphate released was estimated using a standard

curved prepared using the phosphate supplied with the kit. The assays were performed more than three times for analysis.

#### **(D) Size-exclusion chromatography**

Size-exclusion chromatography was performed using Superdex 200 GL 10/300 column (GE Life Sciences). The column was equilibrated with buffer A. 500 $\mu$ L of 0.4mg/ml protein was loaded on the column and  $A_{280}$  was monitored. Void volume was determined using dextran blue and the positions of molecular weights by various protein molecular weight standards.

#### **(E) Determination of nucleotide binding affinity**

Binding affinity of Drp6 and Drp6-S248D for GDP and GTP $\gamma$ S was determined by Micro-Scale Thermophoresis (MST) (NanoTemper). 200nM of His-tagged protein in Buffer B was incubated with nucleotides varying in concentration from 15nM to 500 $\mu$ M. Fluorescence of each sample capillary was recorded upon subjecting to temperature variation.  $F_{\text{norm}}\%$  was plotted against ligand concentration for analysing the results. Experiments were performed thrice.

#### **(F) Liposome co-floatation assay**

Floatation assay was performed using liposomes comprising 70% PC and 30% PE or with 70% PC and 20% PE along with 10% CL or PS or PA. 2.5mg of total lipid were re-suspended in chloroform and used to create a thin film in a 50ml round bottom flask. The flask was exposed to nitrogen for 30mins or until the chloroform smell disappeared. 1 mL of pre-warmed buffer B was added to the film and the flask was subjected to freeze thaw cycles until the lipid film fully resuspended into the buffer. To obtain 100nm liposomes, this solution was extruded 17-21 times using 100nm filter in Avanti Polar Lipid Extruder. The liposomes were checked for size uniformity using DLS.

To set up the floatation reaction, a 500 $\mu$ L reaction in buffer B was set up using 1 $\mu$ M protein, 1mM GTP and 0.5mg (200 $\mu$ L) of liposomes. The reaction mix was incubated at RT for 1 hour.

For setting up the sucrose gradient, the reaction mix was adjusted to contain 40% sucrose. The reaction mix was placed at the bottom of ultra-centrifuge tubes and overlaid with 2mL each of 35%, 30%, 25%, 20%, 15% and 10% sucrose solutions (in buffer B) . The gradient was subjected to ultra-centrifugation using SW41 rotor at 35000rpm, 4 °C for 15 hours in a Beckman Coulter Ultra-centrifuge. 1mL fractions were collected from the top and analysed by western blotting using anti-His antibody (Sigma-Aldrich). Quantitation of protein bands were performed using Quantity One software. Experiment was performed at least thrice for quantitation.

### **(G) *In vitro* membrane fusion assay**

A polyvinyl alcohol (5% w by w) solution in hot water was prepared and was used to coat the inner surface of petri plates . The plates were allowed to dry overnight.

A smear of the lipid solution in chloroform having 10% CL, 20% PE, 70% PC with 18 mol% R18 dye was made on this dried surface and kept in vacuum for 2 hours. 1 ml of buffer B was added to the dried lipid film and allowed to hydrate for 5 mins. The GUV solution was collected in a tube. To remove the excess dye, the GUV solution was dialysed in the same buffer. For the fusion assay, reaction using 1 $\mu$ M protein, equal volumes of R18 labelled and unlabelled GUVs, 1mM GTP/GDP/GTP $\gamma$ S/GMPPCP (added just before fluorescence measurements) was performed on ice. Fluorescence measurements were carried out using  $\lambda_{exc}$  at 560 nm and  $\lambda_{em}$  at 585 nm for 2 hours at RT using Varioscan (Thermo Scientific).

### **(H) TEM imaging**

For TEM experiments, purified recombinant Drp6 and Drp6-S248D were concentrated to 4.5 $\mu$ M in buffer A and kept overnight at 4 °C. 20 $\mu$ L sample containing 1 $\mu$ M of protein and 1mM GTP $\gamma$ S in buffer B was incubated at RT for 45 mins before adsorbing onto the copper coated 200 mesh grid by placing the grid on the sample for 2 min followed by placing on 2% Uranyl Acetate (MP Biomedicals) for 2 min. Excess stain was removed using a Watman filter paper and the grid was dried for 10min before imaging in TEM (JEOL JEM transmission electron microscope).

### **(I) Liposome tubulation assay**

Liposomes comprising 70%PC, 20%PE, 10%CL was prepared as mentioned earlier. A 20 $\mu$ L reaction was set-up using 1 $\mu$ M purified recombinant protein, 9 $\mu$ L of liposomes, 1mM GTP $\gamma$ S. The reaction was incubated for 2hours at RT and sample grids were prepared as mentioned above.

### **(J) *Tetrahymena* strains and culturing**

Wild-type *Tetrahymena* cells (CU428.1 and B2086.1) were procured from *Tetrahymena* stock centre, Cornell university, USA. SPP media containing 2% Proteose peptone, 0.2% Yeast extract, 0.1% glucose and 0.003% Fe-EDTA was sterilised by autoclaving for 40 min at 121°C. Cells were grown in conical flasks at 30 °C.

### **(K) Expression of Drp6 and its mutants from the endogenous locus**

To perform studies on localization of Drp6, the gene was endogenously tagged with mCherry at C-terminus followed by Neo4 cassette for selection. For this purpose, a vector consisting of 3x mCherry, 2x HA and Neo4 was used. For studying the effect of phosphorylation on

localization of Drp6, point mutations were generated using Stratagene QuickChange protocol in DRP6-pENTRD TOPO vector. Serine at 248 was replaced by alanine for phosphonull mutant and by aspartate for phosphomimic mutant. The mutant fragments were cloned after PCR amplification in the 3x mCherry, 2x HA Neo4 vector using SacI and XbaI sites. 3'UTR of Drp6 (1kb) was amplified from the genomic DNA and cloned C-terminus to NEO4 cassette using EcoRV and XhoI sites.

For transformation, 25µg of plasmid was digested with SacI and XhoI restriction enzymes. The DNA was ethanol precipitated and resuspended in 13µL of sterile deionised water. For coating of gold particles, 10µL of the DNA was used along with 62.5µL of 2.5M CaCl<sub>2</sub> and 32.5µL Spermidine. Particle coating was carried out at 4 °C by vortexing for 10min. Particles were then spun at 3000rpm for 5s and the supernatant was completely removed. The particles were washed with 150 µL of 70% ethanol followed by 150µL of 100% ethanol to finally resuspend in 40 µL of 100% ethanol. 10 µL of particles were evenly spreaded on the microcarrier and allowed to dry. *Tetrahymena* cells were grown in SPP media and starved using DMC for 14-16 hours. Cells were centrifuged at 1100g for 1 min at RT and were resuspended in 500 µL of DMC to use  $1 \times 10^7$  cells for a single transformation. Cells were spread at the centre of a Watman filter paper in 100mm petri-dish. Filter was soaked in DMC and particle delivery was carried out using BioRad PDS1000/He Biolistic particle delivery system. Cells were then transferred to 50mL of SPP media supplemented with streptomycin-penicillin-fungizone and revived at 25 °C for 14 hours. To the cells 120µg/mL paromomycin sulphate and 1µg/mL cadmium chloride were added and grown at 30 °C in 96 well plate. Transformants were selected and subjected to increasing concentration of paromomycin sulphate (200µg/mL) each passaging keeping the cadmium concentration

same). Once the cells were grown at 1mg/ml paromomycin, cadmium chloride concentration was reduced successively till it reached 0.1µg/mL concentration. At this stage, paromomycin sulfate concentration was further increased till concentration reached at 3.5mg/mL. Cells were passaged without drug and complete replacement of the transgene was confirmed by RT-PCR analysis. The cells were grown to a density of  $2 \times 10^5$  cells/mL. Cells were fixed using 4% paraformaldehyde for 20min at RT. Cells were then stained with DAPI and imaged using confocal microscopy.

## 2.3 Results

### 2.3.1 Drp6 is a fusion dynamin:

Classical dynamins and Drps function by remodeling of their target membranes to bring about change in curvature. Remodeling involves in fission, fusion or tubulation of the membranes. *Tetrahymena thermophila* macronucleus undergoes expansion not only during conjugation but also during vegetative cell division. Although the expansion during nuclear transition from micronucleus to macronucleus is much more pronounced than the macronuclear division during fed-state, both the cases require active nuclear remodeling. As a result, activity of Drp6 is more prominent during nuclear transition phase. Macronucleus expansion requires addition of new membranes to the existing nucleus. Since absence of Drp6 inhibits nuclear expansion (230) an *invitro* membrane fusion assay was performed to understand if Drp6 is a fusion dynamin. GUV composed of 10% CL, 20% PE, 70% PC were mixed with a set of same GUV additionally labelled with R18 dye. This R18 dye, when used in high concentrations shows self-quenching property. So, fluorescence can be detected only when the dye is de-quenched upon dilution (Fig. 2.3.1.1). The fusion assay was performed by mixing equal amounts of labelled and unlabeled GUVs. When Drp6 was added to this reaction, fluorescence was observed under confocal microscope (Fig. 2.3.1.2A). Along with this, many hemi-fusion states were also observed in presence of Drp6 (Fig. 2.3.1.3A). In absence of Drp6, fluorescence was not observed and hemi-fusion population was also less frequent (Fig. 2.3.1.3B). The increase in fusion activity in presence of Drp6 with time was measured by increase in fluorescence intensity. Addition of Drp6 led to enhanced fluorescence intensity over time indicative of an increased fusion activity (Fig.2.3.1.2B). These results establish that Drp6 functions as a fusion dynamin.

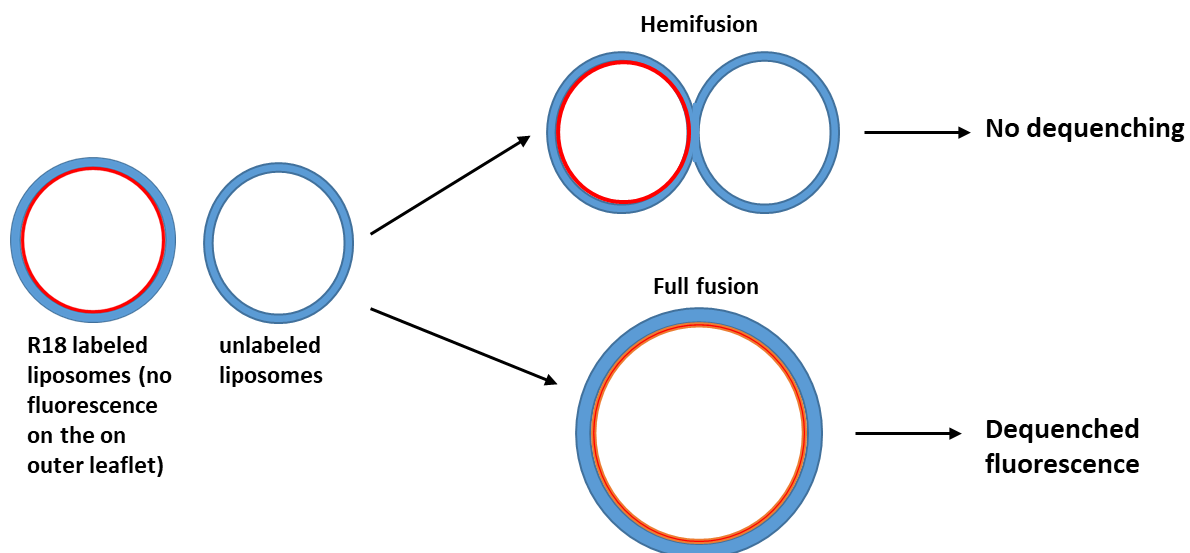
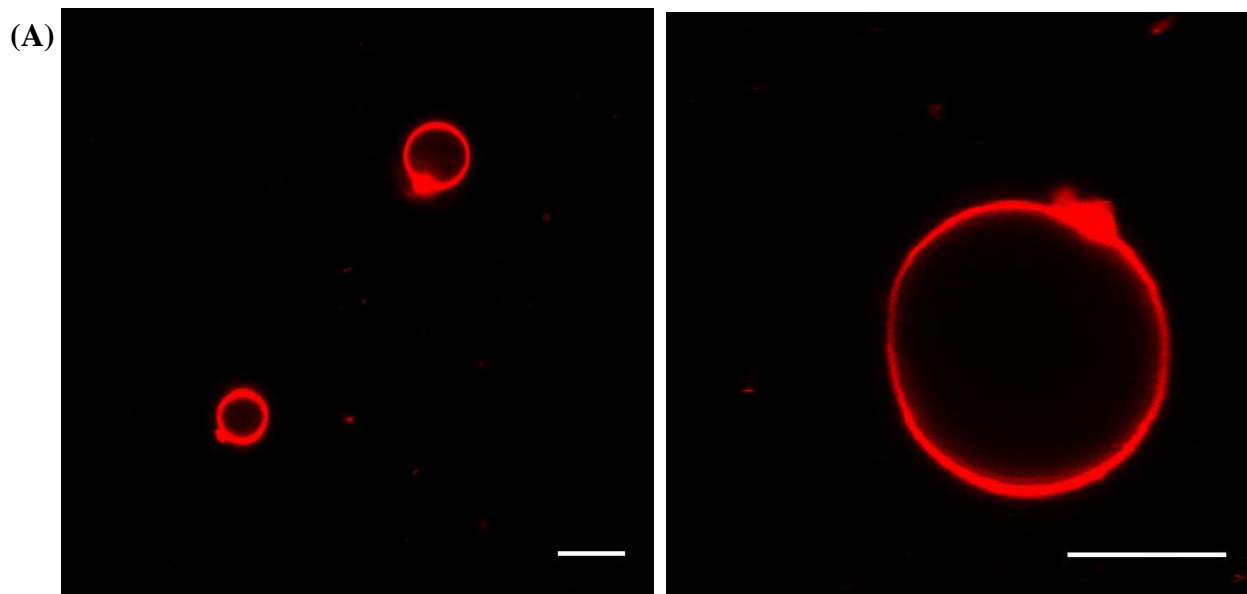


**Figure 2.3.1.1: Schematic representation of R18 dye dequenching during *in-vitro* membrane fusion assay.** Fusion of R18 labeled GUVs with unlabeled GUVs dequenches the dye in an event of full fusion which leads to detectable fluorescence. While hemifusion doesnot dequench the dye and hence doesnot give any detectable fluorescence.



(B)

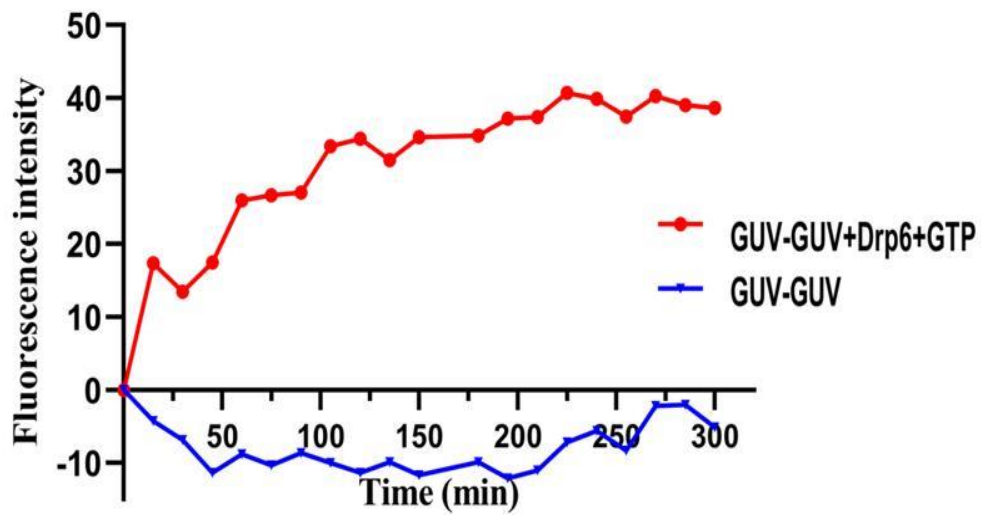
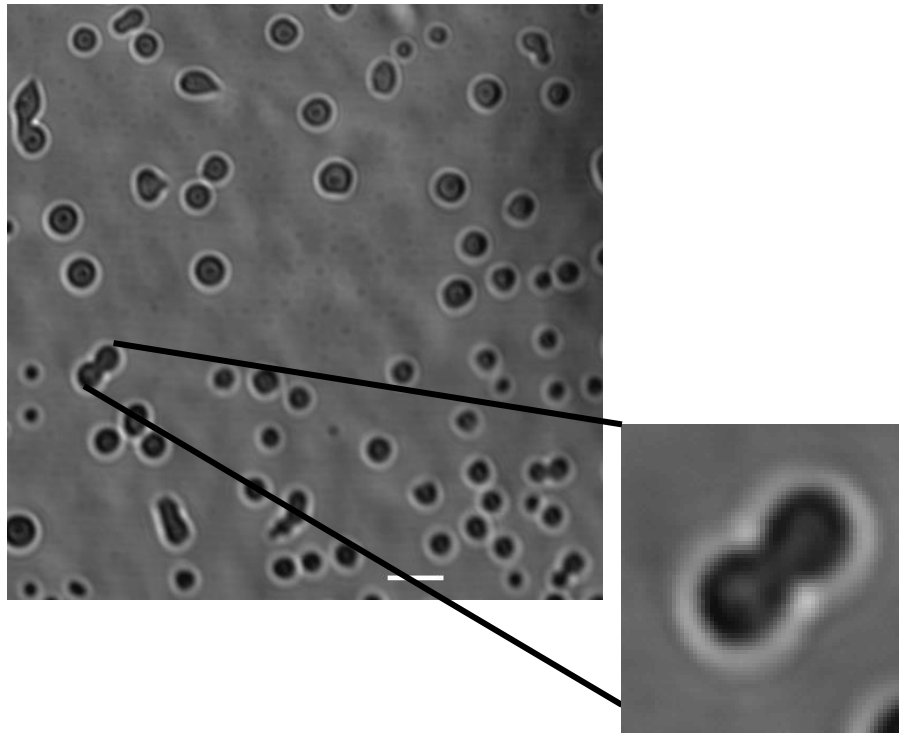


**Figure 2.3.1.2: *In-vitro* membrane fusion by Drp6.** (A) Confocal images showing fluorescence of R18 labelled GUVs upon fusion with unlabeled GUVs after addition of Drp6. Bar=10 $\mu$ m.

(B) Graph showing fluorescence intensity with time either in presence of Drp6 (GUV-GUV+Drp6+GTP) or in absence of Drp6 (GUV-GUV).

(A)



(B)

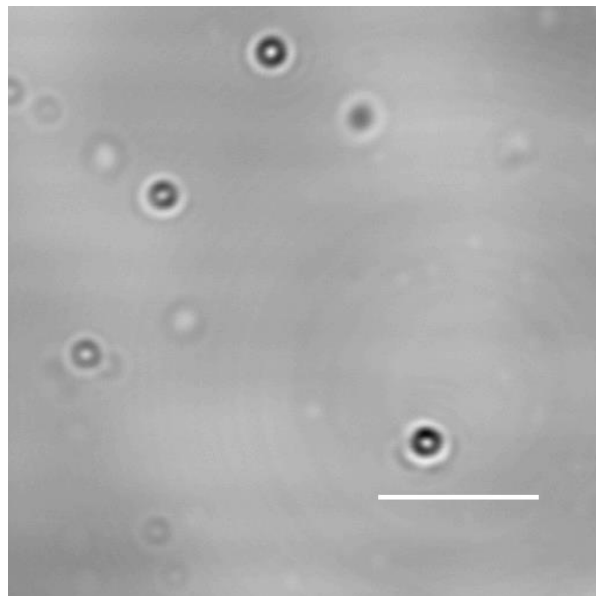
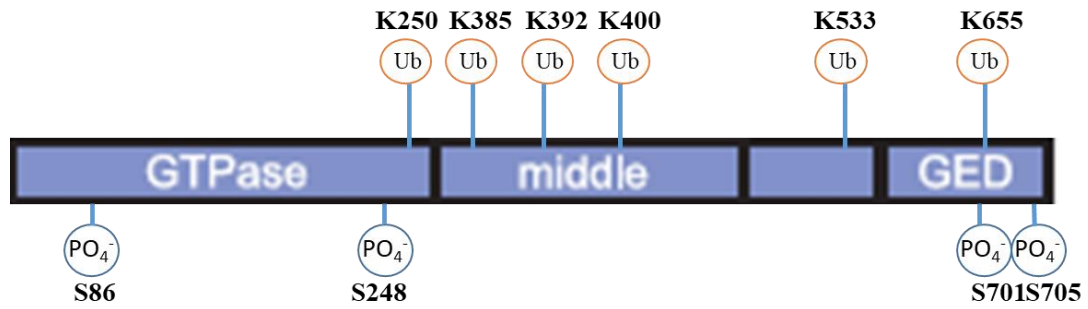


**Figure 2.3.1.3:**(A) DIC image showing GUV fusion *in-vitro*.The fusing population is more abundant when Drp6 is added to the GUVs. The inset shows a magnified image of the fusing GUVs. Bar=10 $\mu$ m (B)Image showing GUVs in the absence of Drp6, fusion states are less and the GUVs are smaller. Bar=5 $\mu$ m

### 2.3.2 Effect of phosphorylation on self-assembly of Drp6

*In vitro* phosphorylation assay and mass-spectroscopic analysis have established that Drp6 undergoes phosphorylation at four serine residues along with ubiquitination at six lysine residues (done previously in lab). Phosphorylation was identified at S86, S248, S701, and S705 (Fig. 2.3.2.1A). Self-assembly of dynamins into higher-order structures is pre-requisite for their function. In most of the dynamins, self-assembly depends on binding to the target membrane. Drp6, unlike other dynamins, does not require association with membrane for its self-assembly. To understand the role of phosphorylation on self-assembly property of Drp6, phosphomimic forms of Drp6 were generated by replacing the serine residue with aspartate. The negative charge of aspartate mimics the negative charge imparted to the protein upon phosphorylation. Different phosphomimic variants along with wildtype were expressed as N-terminal His<sub>6</sub> tagged proteins in *E.coli* C41 DE3 cells. The proteins were purified to approximately 80% purity as estimated by using Fiji software (Fig. 2.3.2.1B). Size-exclusion chromatography in Superdex 200 analytical gel-filtration column was performed with these recombinant phosphomimic mutant proteins and compared with that of wildtype protein. All the four phosphomimic mutant proteins eluted in the void volume (Fig. 2.3.2.2). The elution profile was similar to that of the un-phosphorylated form suggesting that phosphorylation does not inhibit self-assembly property of Drp6.

(A)



(B)

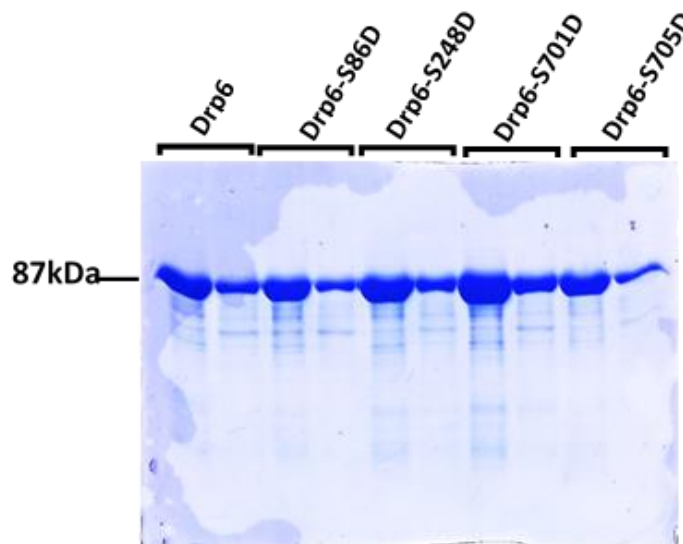


**Figure 2.3.2.1:** (A) Schematic representation showing residues of Drp6 which undergo phosphorylation and ubiquitination as identified by mass-spectrometry. (B) Coomassie stained SDS-PAGE gel showing Drp6 and the phosphomimic variants (as indicated on top of the gel) purified from *E.coli*. Marking on the left indicates the molecular weight of the proteins.

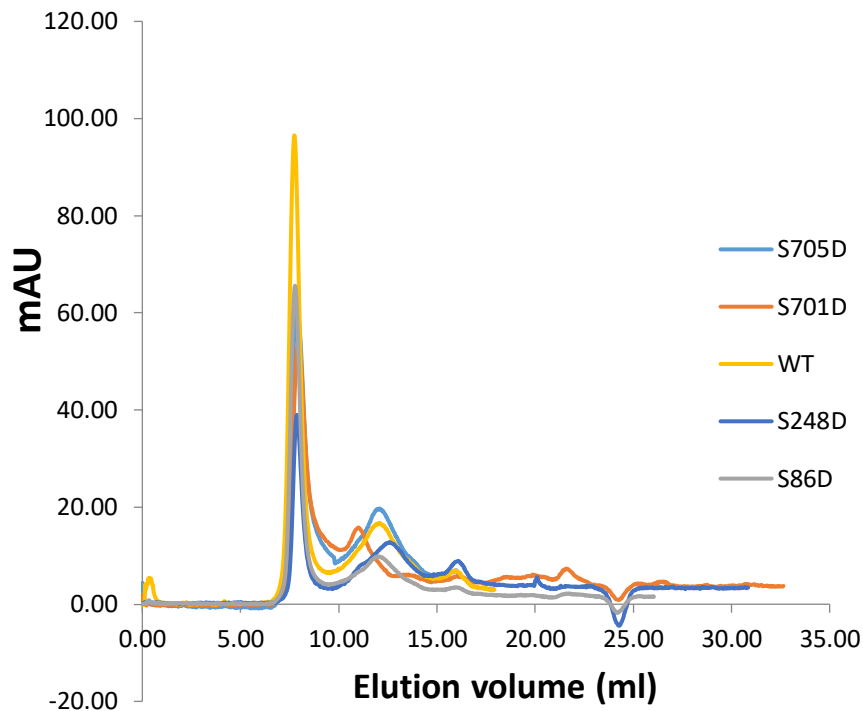


**Figure 2.3.2.2: Size-exclusion chromatography of phosphomimic variants.** Analytical gel-filtration was performed using Superdex 200 column for the four phosphomimics and the un-phosphorylated Drp6. Color code on the right indicates the proteins. The mutants eluted majorly in the void fraction as the un-phosphorylated Drp6.

### 2.3.3 Effect of phosphorylation on GTPase activity of Drp6

GTP hydrolysis is an intrinsic property of all the dynamin family proteins. Drp6 also hydrolyses GTP *in vitro*. To study the effect of phosphorylation on basal GTPase activity of Drp6, His-tagged phosphomimic forms were expressed and purified. GTP hydrolysis activity was measured using colorimetric assay and compared to that of wildtype Drp6. Phosphate release was  $0.056 \pm 0.002$  nmol/min/  $\mu$ M protein for S86D,  $0.057 \pm 0.0016$  nmol/min/  $\mu$ M protein for S701D,  $0.059 \pm 0.0021$  nmol/min/  $\mu$ M protein for S705D (Fig.2.3.3.1A,B) The phosphomimics, S86D, S701D, and S705D showed very similar activity and did not differ

significantly from the non-phosphorylated wild-type form ( $0.058 \pm 0.0017$  nmol/min/  $\mu$ M protein). However, S248D showed 50% of the GTPase activity as compared to the wildtype protein ( $0.029 \pm 0.0014$  nmol/min/  $\mu$ M protein) (Fig.2.3.3.1A,B). The inhibition in activity was also observed when TAP tagged Drp6-S248D and Drp6 were purified from *Tetrahymena thermophile* and their GTPase activities were assessed (Fig.2.3.3.2). These results lead us to conclude that phosphorylation of serine residue at 248<sup>th</sup> position inhibits GTPase activity of Drp6.

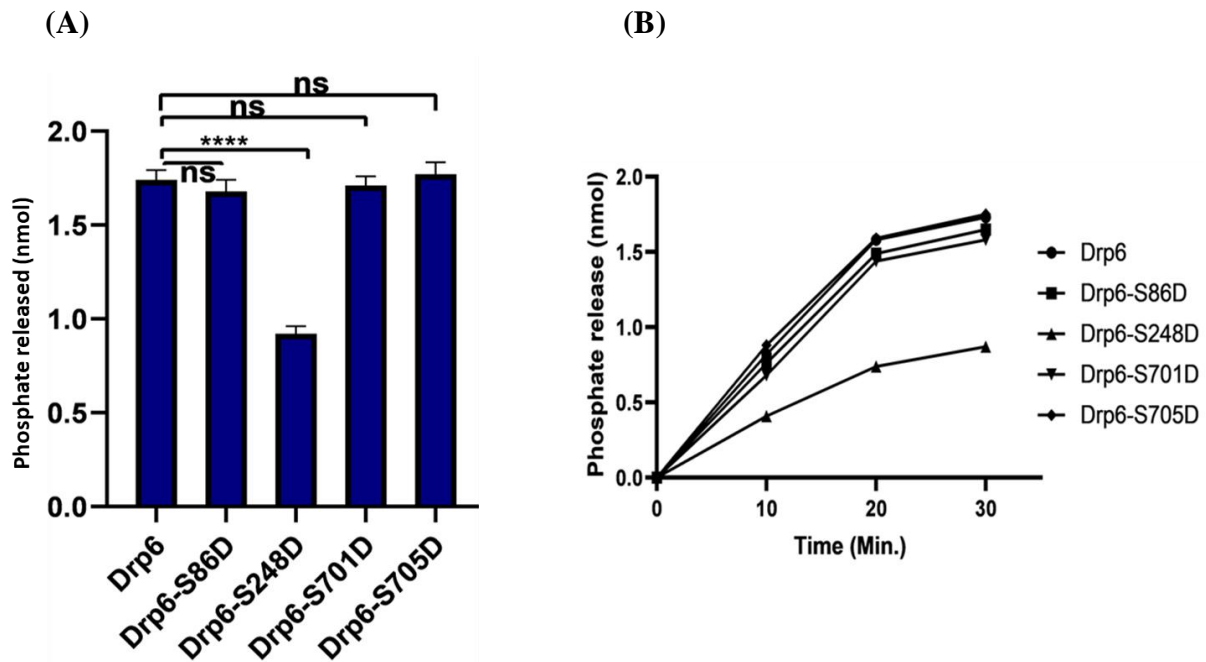


**Figure 2.3.3.1: GTPase activity of Drp6 and phosphomimic variants.**(A) The graph shows phosphate released by Drp6 and the phosphomimics in 30mins. Statistical significance of Drp6-S248D compared with Drp6 was  $<0.0001$  (\*\*\*\*), for other mutants it was non-significant (ns). (B) Graph shows phosphate released by Drp6 and the phosphomimic variants (as indicated on right) from 0 to 30 min. Assays were performed at least three times.

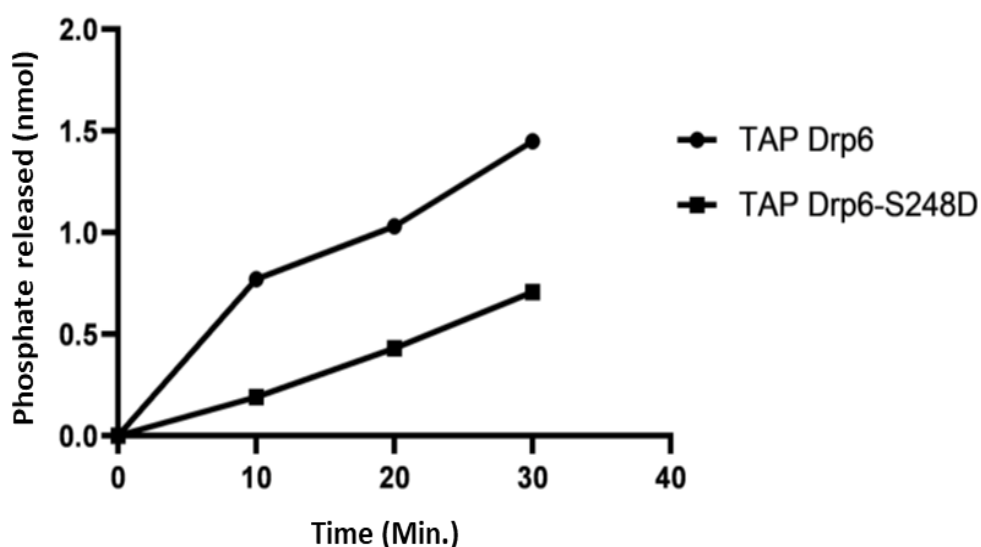


**Figure 2.3.3.2: TAP-tagged Drp6-S248D purified from *Tetrahymena* shows reduced GTPase activity.** TAP-Drp6 and TAP-Drp6-S248D were purified from *Tetrahymena* and their GTPase activity (phosphate release in nmol) was assessed for 0 to 30 min.

### 2.3.4 Inhibition in GTPase activity is not due to reduced GTP binding

Inhibition in GTPase activity can be either due to reduced GTP hydrolysis or due to reduced GTP binding affinity. Dynamins have lower affinity for GTP than GDP. The GDP bound molecules exchange GDP for GTP upon self-assembly on the target membranes. To understand if phosphorylation at S248 inhibits activity by reducing GTP binding affinity, Micro-Scale Thermophoresis (MST) experiments using GTP $\gamma$ S (non-hydrolyzable GTP analog) were performed and compared with that of Drp6. The dissociation constant ( $K_D$ ) of 1.3 $\mu$ M for Drp6-S248D was comparable to 0.697  $\mu$ M of Drp6 (Fig. 2.3.4.1). Affinity of Drp6 for GDP (2.7  $\mu$ M) was also comparable to that of S248D (1.89 $\mu$ M). These results suggest that phosphorylation at Ser248 reduces GTPase activity by reducing GTP hydrolysis and not GTP binding.

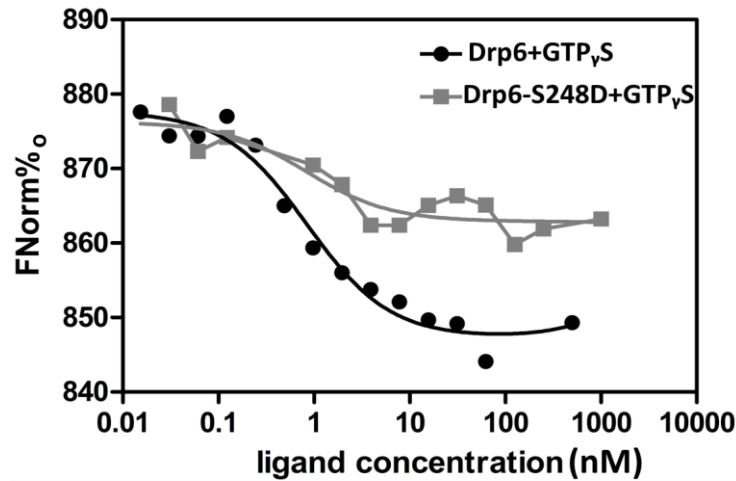
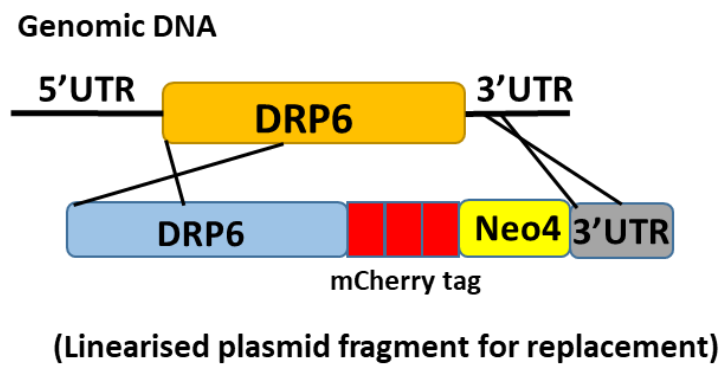


**Figure 2.3.4.1: Phosphomimic Drp6-S248D binding to GTP $\gamma$ S is similar to Drp6.** Micro-scale thermophoresis (MST) measurement of Drp6-S248D and Drp6 binding affinity with GTP $\gamma$ S was performed.  $K_D$  was computed from this binding curve using NanoTemper binding affinity software.

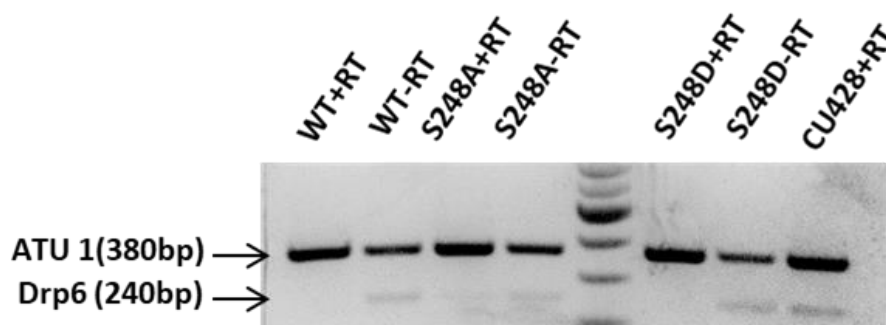
### 2.3.5 Effect of phosphorylation on localization of Drp6

Drp6 exhibits differential localizations in different cell cycle stages and expected to be regulated by post-translational modifications. To observe if phosphorylation at S248 affects the localization, Drp6-mCherry or Drp6-S248D-mCherry or Drp6-S248A-mCherry was incorporated into the genome by replacing the cellular copies of Drp6. The Schematic representation of the homologous recombination based endogenous tagging of Drp6 is shown in the figure 2.3.5.1 The complete replacement was confirmed by RT-PCR analyses (Fig.2.3.5.2). The localization of the endogenously expressed tagged proteins was assessed by confocal microscopy. As shown in the figure 2.3.5.3, Drp6-S248A-mCherry failed to associate with nuclear envelope suggesting that phosphorylation at S248 is important for nuclear recruitment of Drp6. Although as expected both Drp6-mCherry and Drp6-S248D-

mCherry were recruited into the nuclear envelope, S248D were visibly more prominent in the nuclear envelope as compared to the wild type Drp6 (Fig.2.3.5.3). These results further confirm that phosphorylation of Drp6 at S248 enhances nuclear association of Drp6.

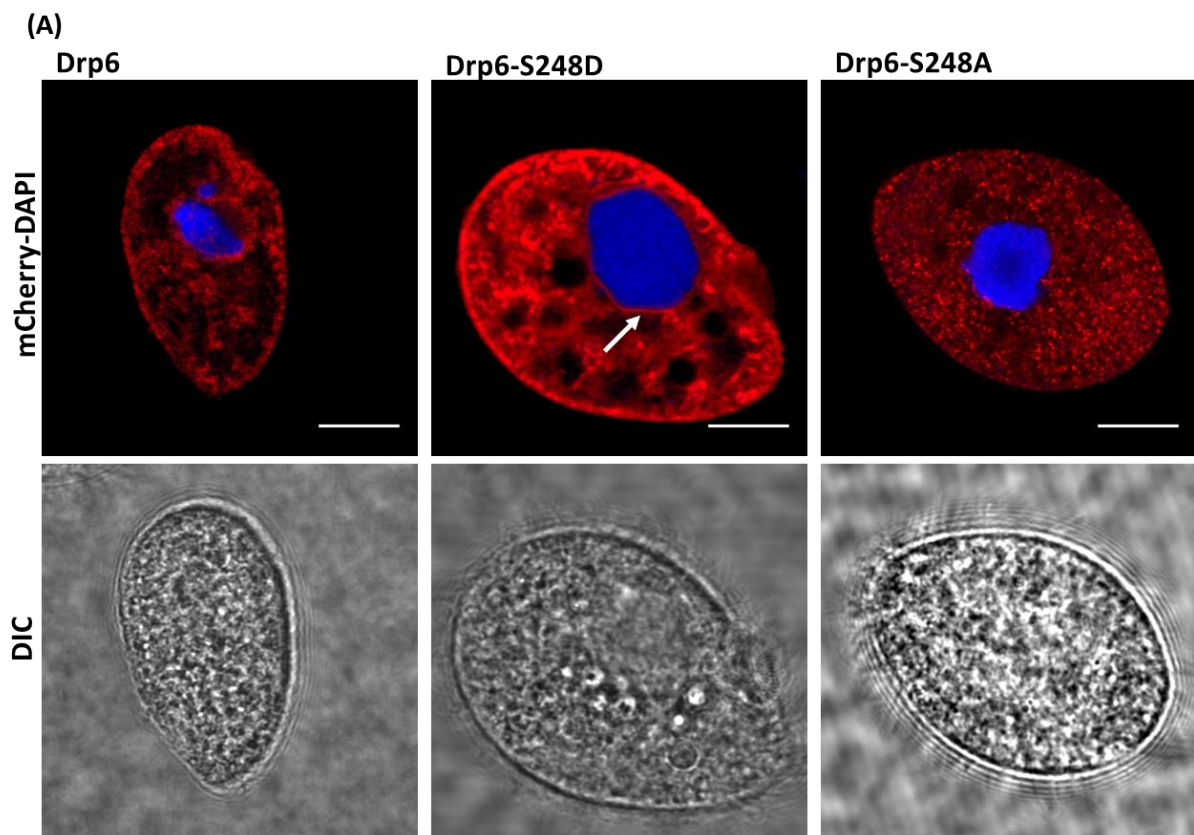


**Figure 2.3.5.1: Schematic representation of strategy used for mCherry tagging of endogenous Drp6.** Homologous recombination based strategy was used to replace genomic copy of Drp6 with mCherry tagged Drp6 using a construct containing DRP6 gene sequence followed by 3x mCherry-tag, Neo4 cassette and 3'UTR sequence.



**Figure 2.3.5.2: confirmation of endogenous replacement of Drp6 by semi-quantitative PCR.** Semi-quantitative RT-PCR was performed using cDNA synthesized from RNA

isolated from *Tetrahymena* cells expressing either mCherry-Drp6 (WT+RT) or mCherry-Drp6-S248A (S248A+RT) or mCherry-Drp6-S248D (S248D+RT). Cu428+RT represents RT-PCR performed using cDNA synthesized from the wild-type *Tetrahymena* without replacement. +RT represents the PCR amplification from cDNA template generated using the reverse transcriptase (RT) enzyme. -RT represents the PCR amplification from template which lacked RT enzyme and served as control. ATU1 is tubulin gene used as control.



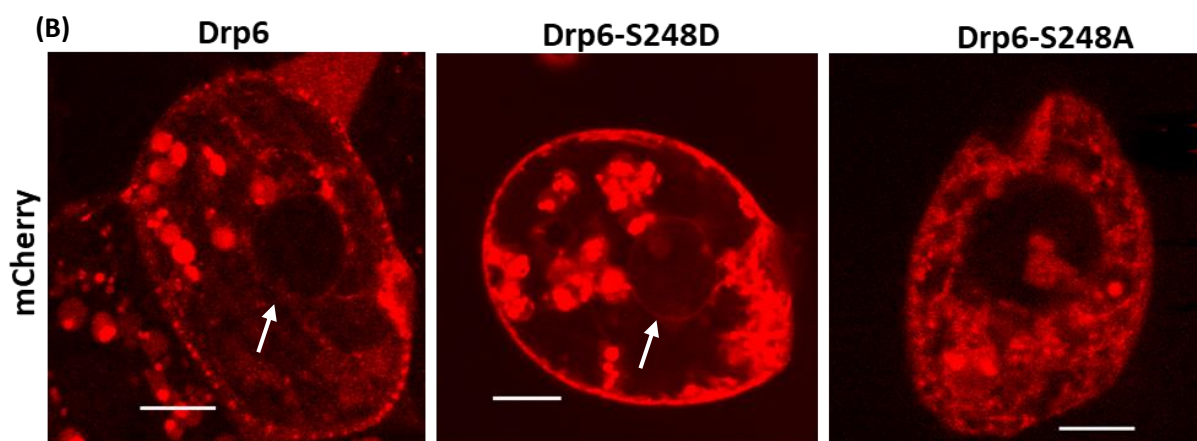


**Figure 2.3.5.3: Localization of Drp6 in presence or absence of phosphorylation at S248.**

Confocal images showing either fixed DAPI stained (A) or Live *Tetrahymena* cells (B) expressing mCherry-Drp6 or Drp6-S248D or Drp6-S248A. Bar = 10μm. Arrow indicates nuclear envelope localization.

### 2.3.6 Phosphorylation at S248 enhances cardiolipin binding affinity

Recruitment of Drp6 to the nuclear envelope is mediated by interaction with cardiolipin(241)also discussed in detail in chapter 3. To check if phosphorylation enhances nuclear association by increasing cardiolipin binding affinity of Drp6, we have performed *in vitro* membrane binding assaywas performed by liposome floatation assay. Drp6 associates with three phospholipids namely cardiolipin (CL), phosphatidic acid (PA) and phosphatidylserine (PS). The co-floatation assay of Drp6 in presence or absence of GTP showed that GTP enhances Drp6 interaction with CL-membrane *in vitro* (Fig.2.3.6.1). To examine the effect of phosphorylation at S248 on membrane binding affinity, either recombinant Drp6 or its phosphomimic variant (S248D) were used for binding to liposomes either containing CL or PS or PA. Quantitative estimation of floatation assay showed that 35-

42% of Drp6 associates with CL containing liposomes. The floatation of 55-60% Drp6-S248D in the same assay suggests that phosphorylation enhances cardiolipin binding affinity of Drp6 (Fig 2.3.6.2A). The effect of phosphorylation at other serine residues (S86, S701 and S705) was also assessed and it was found that phosphorylation at these positions did not show significant difference in CL binding when compared with wild type Drp6 (Fig.2.3.6.3). Interestingly, interactions of S248D with PS liposomes or PA liposomes was similar to that of wild type Drp6 (Fig.2.3.6.2B,C). These results suggest that phosphorylation at any of the four serine residues does not change over all membrane binding of Drp6 except enhanced CLbinding due to phosphorylation at S248. Taken together, it can be concluded that phosphorylation specifically at S248 enhances nuclear recruitment by increasing CLbinding affinity.

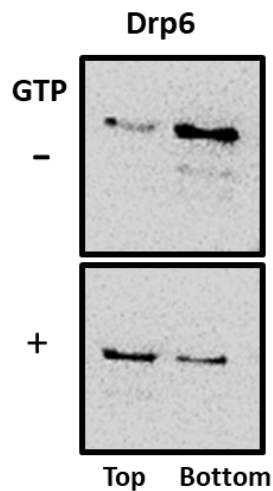
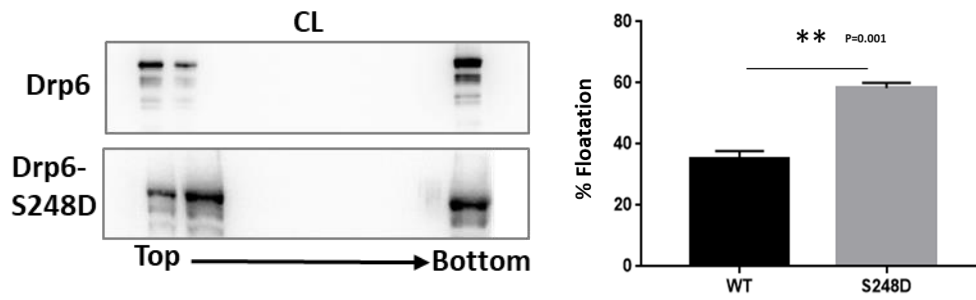
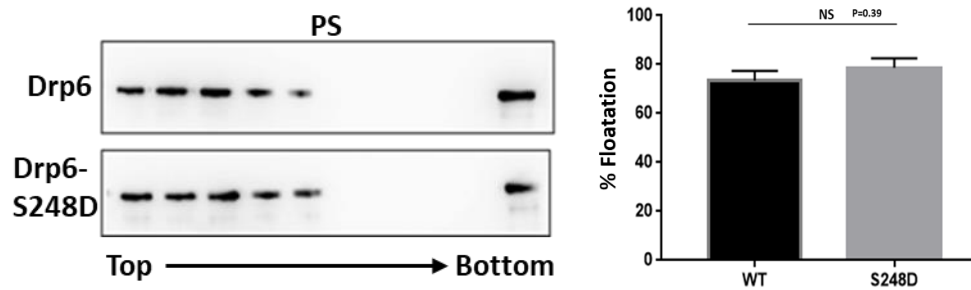


**Figure 2.3.6.1: GTP enhances Drp6 binding with CL.** Liposome co-floatation assay was performed with liposomes containing 70% PC 20% PE supplemented with 10%CL in presence (+GTP) or absence (-GTP) of GTP showing that GTP enhances binding of Drp6 with CL. Western blot analysis of the collected fractions was performed using anti-His antibody.

(A)



(B)



(C)

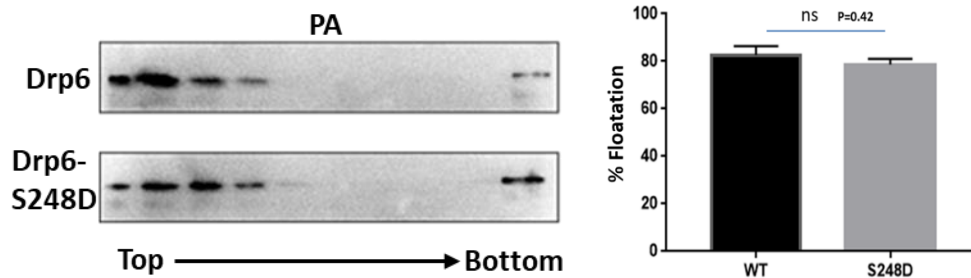


**Figure 2.3.6.2: Drp6 S248D shows enhanced binding specifically with cardiolipin. (A)**

Liposome co-floatation assay of Drp6 and Drp6-S248D was performed with liposomes containing 70% PC, 20% PE supplemented with 10% CL. Fractions were collected from the top and analyzed by western blotting using anti-His monoclonal antibody. Quantitation using ImageJ software is shown on the right. P value = 0.001 (\*\*).

(B) Same as (A) except liposome containing 70% PC, 20% PE supplemented with 10% PS was used for the assay. Western-blot was performed and analysed as mentioned above. P value= 0.39 (ns)

(C) Same as (A) except liposome containing 70% PC, 20% PE supplemented with 10% PA. Western-blot was performed and analysed as mentioned above. P value= 0.42 (ns)

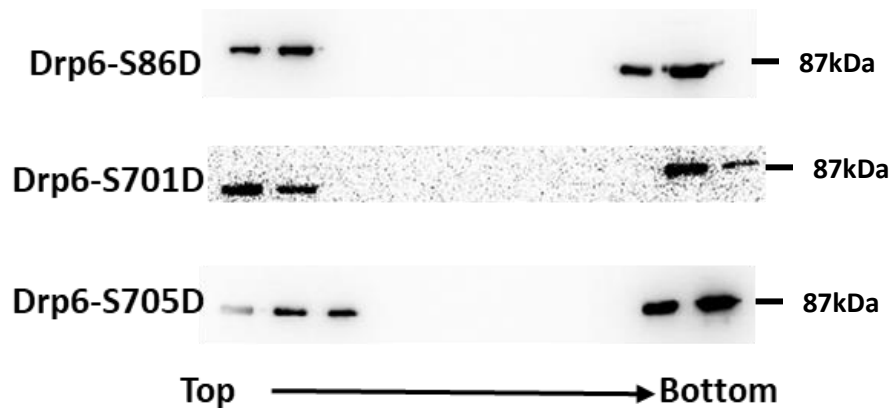


**Figure 2.3.6.3: Liposome co-floatation assay of Drp6-S86D, Drp6-S701D and Drp6-S705D.** Liposomes containing 70% PC, 20% PE supplemented with 10% CL were used for the assay. Fractions were collected from the top and analyzed by western blotting using anti-His monoclonal antibody. Molecular weights are indicated on the right.

### 2.3.7 Phosphorylation at S248 enhances membrane fusion activity of Drp6

Drp6 is essential during the transition of micronucleus to macronucleus that requires nuclear expansion. The nuclear expansion involves addition of new membrane to the existing nuclear membrane. Therefore, it can be hypothesized that Drp6 performs membrane fusion during

nuclear expansion. Since phosphorylation enhances the recruitment of Drp6 to the nuclear membrane implying enhanced nuclear expansion, we examined the effect of this phosphorylation on the membrane fusion activity of Drp6. For this purpose, an *in vitro* membrane fusion assay was carried out as mentioned in the methods. The results showed that when the mixture of R18 labelled and unlabeled GUVs were incubated with Drp6 either in presence or absence of GTP, the fusion activity (as measured by fluorescence intensity) increased with time only when GTP was added in the reaction. When Drp6-S248D was assessed under the same assay conditions, the fusion activity was found to be higher (~2 fold) as compared to that of un-phosphorylated Drp6. It has been shown that phosphorylation at S248 inhibits GTPase activity of Drp6. It can be argued that if the enhanced fusion activity by phosphorylation was due to inhibition in GTPase activity, then the GTPase activity of un-phosphorylated Drp6 would increase when GTP is replaced with GTP $\gamma$ S (non-hydrolysable GTP analog). Interestingly, the fusion activity of un-phosphorylated Drp6 increased almost 2 fold (Fig.2.3.7.1) in presence of GTP $\gamma$ S strongly suggesting that phosphorylation at S248 enhances membrane fusion function by inhibiting GTPase activity. Taken together, the results suggest that phosphorylation at Ser248 promotes membrane fusion during nuclear expansion by inhibiting hydrolysis of GTP.

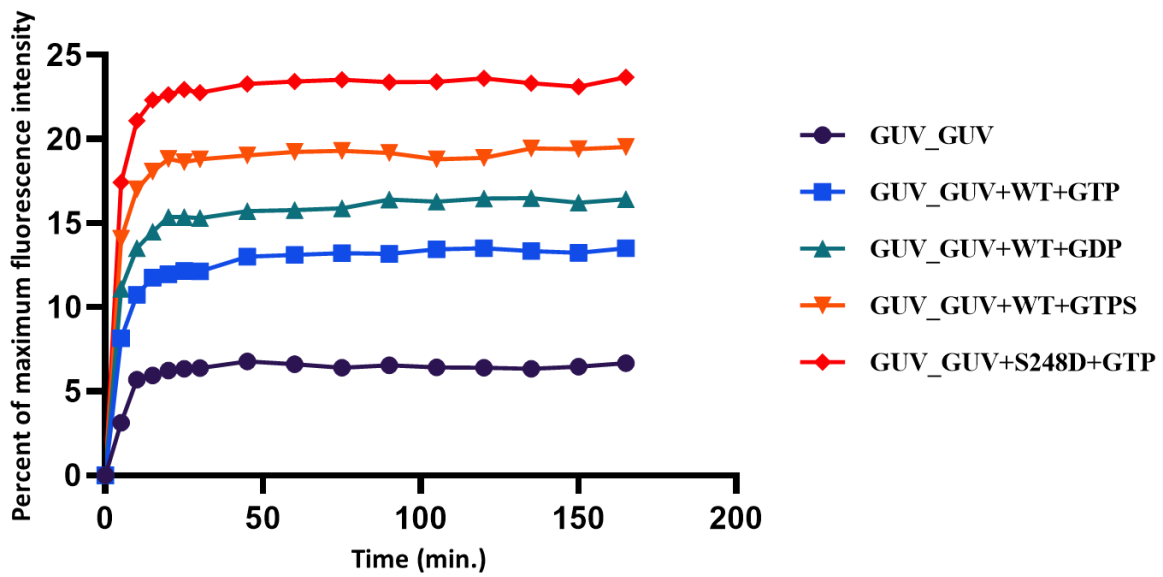
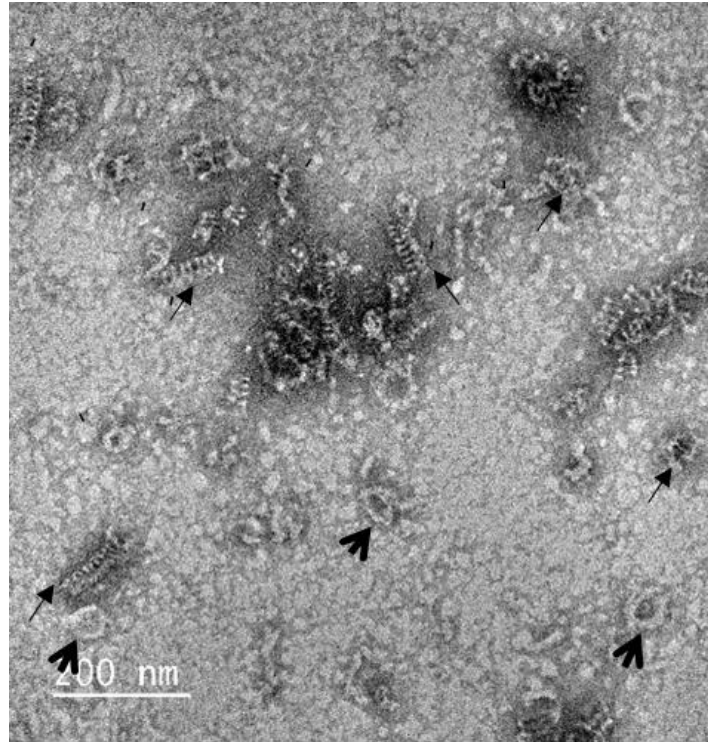


**Figure 2.3.7.1: Phosphorylation at S248 (Drp6-S248D) enhances membrane fusion activity.** *In-vitro* membrane fusion assay was performed with GUVs containing 70% PC, 20% PE and 10% CL. The assay was performed by mixing R18 labeled and un-labeled GUVs either in absence (GUV\_GUV) or in presence of Drp6 and GTP (GUV\_GUV+WT+GTP) or in presence of Drp6 and GDP (GUV\_GUV+WT+GDP) or in presence of Drp6 and GTP $\gamma$ S (GUV\_GUV+WT+GTPS) or in presence of Drp6-S248D and GTP (GUV\_GUV+S248D+GTP). Percent of maximum fluorescence intensity was derived using fluorescence after treatment with TritonX100.

(A) Drp6



(B) Drp6-S248D

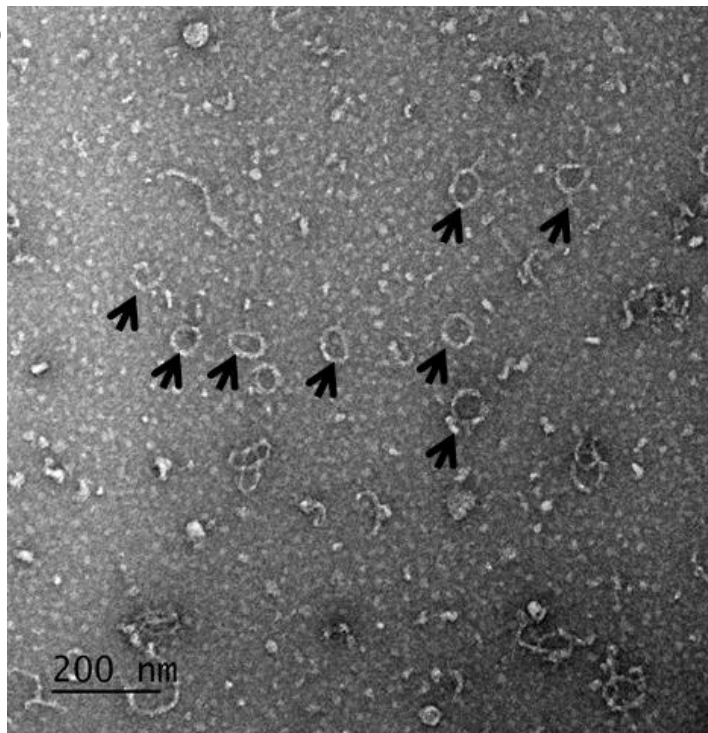


**Figure2.3.8.1: Drp6-S248D stabilizes self-assembled ring structures.** Electron micrograph of Drp6(A) and Drp6-S248D(B) in physiological salt concentration. Drp6 forms helical spirals(long arrows) as well as ring structures (short arrows) whereas Drp6-S248D forms stable ring structures. Bar=200nm.

### **2.3.8 Phosphorylation at S248 stabilizes the self-assembled ring structures**

The dynamin superfamily of proteins is distinguished as self-assembly activated GTPases. Functional structures of dynamins are helical spirals and ring structures which are usually formed upon membrane binding. Drp6 in contrast self assembles into helical spirals and rings even in absence of membranes. As discussed in the earlier section, similar to Drp6, Drp6-S248D also elutes in the void fraction suggesting that it is also capable of forming oligomeric structures. To visualize and find out if the Drp6-S248D is capable of forming ordered assemblies like wild type Drp6 and is not mere irregular aggregates, TEM experiments with purified proteins were performed. The results showed that Drp6 under physiological salt concentration forms rings and helical spiral structures upon incubation with non-hydrolyzable GTP analog. These helical spirals varied in length between 70nm to 110nm and had a diameter of roughly 35-50nm whereas the ring structures were about 55-65nm in diameter. The Drp6-S248D under same conditions formed predominantly ring structures albeit with a very less number of helical spirals. These rings were measured to be around 50-70nm in diameter (Fig.2.3.8.1).

To study dependence of Drp6 on nucleotide for self-assembly, Drp6 was imaged after negative staining in absence or presence of GDP or GMPPNP. In nucleotide-free state, Drp6 remains mostly in open, long, filament-like structures varying in lengths whereas Drp6-S248D was able to organize itself in ring structures which were either closed or partially closed structures with a diameter ranging from 60-70nm. Addition of GDP yielded structures which were similar in both Drp6 and Drp6-S248D. Most abundant structures found in both the cases were filament like structures and comma shaped (incomplete rings) structures with occasional presence of ring structures throughout the scanned fields. Upon addition of GMP-PNP (a non-hydrolyzable GTP analog), Drp6 could form helical spirals of various lengths in

addition to rings, whereas Drp6-S248D showed mostly ring structures of about 55-70nm (Fig.2.3.8.2). Drp6-S248D also formed open rod like structures which might be precursor for the formation of ring structures. While some dynamins require helical spirals for function, ring structures are the functional forms for other family members. As for example, the classical dynamins like dynamin 1 is active in its helical spiral form whereas MxA forms ring like organization during membrane fusion. Therefore, it was concluded that phosphorylation of serine residue at 248<sup>th</sup> position enhances membrane fusion activity of Drp6 by stabilizing its ring structures.

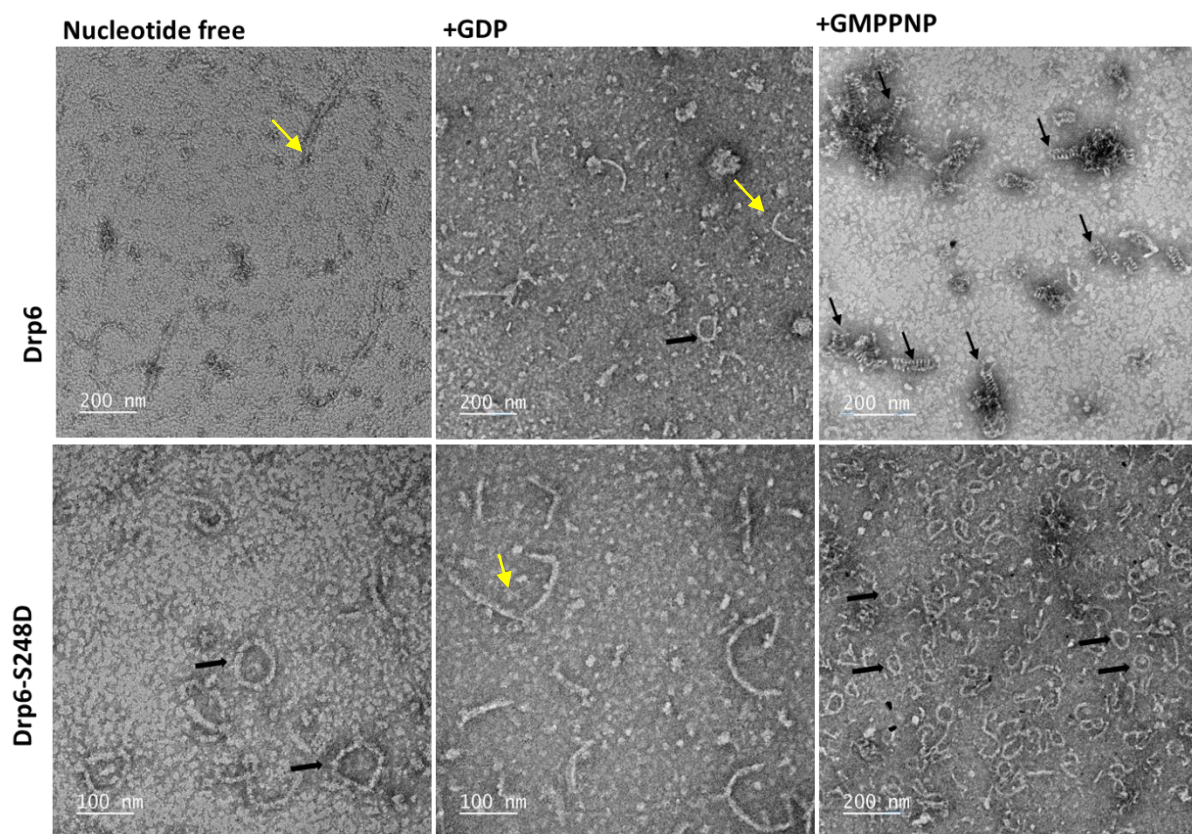


**Figure 2.3.8.2:**Electron micrograph of Drp6 (top) and Drp6-S248D (bottom) either in absence of nucleotide (Nucleotide free) or in presence of GDP (+GDP) or in presence of GMP-PNP (+GMPPNP). Arrows indicate helical spirals and thick arrows indicate the rings. Yellow arrow indicates helical-rod like structures.

### **2.3.9 Phosphorylation at S248 enhances membrane tubulation and tubular network formation**

Fusion dynamins perform their function by membrane tubulation and bringing two opposing membranes together via G-domain dimerization. To understand how phosphorylation at S248 enhances membrane fusion activity, Drp6 and Drp6-S248D were assessed for their membrane tethering activities by electron microscopic analysis. For this purpose, electron micrographs of negatively stained liposomes were evaluated after incubation with Drp6 or Drp6-S248D. Negative stained electron micrographs showed that Drp6 tethers liposomes to form fusion precursors, a property shown by fusion dynamin. When Drp6-S248D was incubated with liposomes under similar condition, extensive tubulation of the liposomes were observed along with tethering (Fig.2.3.9.1). These tubulated structures appeared mostly as networks with three (or more) way connections, resembling endoplasmic reticulum (ER) network. Moreover, fusion of liposomes in these networks were readily visible confirming membrane fusion activity of Drp6.

Taken all the results together discussed in this section it can be concluded that Drp6 is a fusion dynamin and phosphorylation of serine residue at 248<sup>th</sup> position enhances nuclear recruitment of Drp6 by enhancing cardiolipin binding affinity and membrane fusion activity by enhancing membrane tethering and membrane tubulation function of Drp6 possibly by stabilizing its GTP bound ring structures.

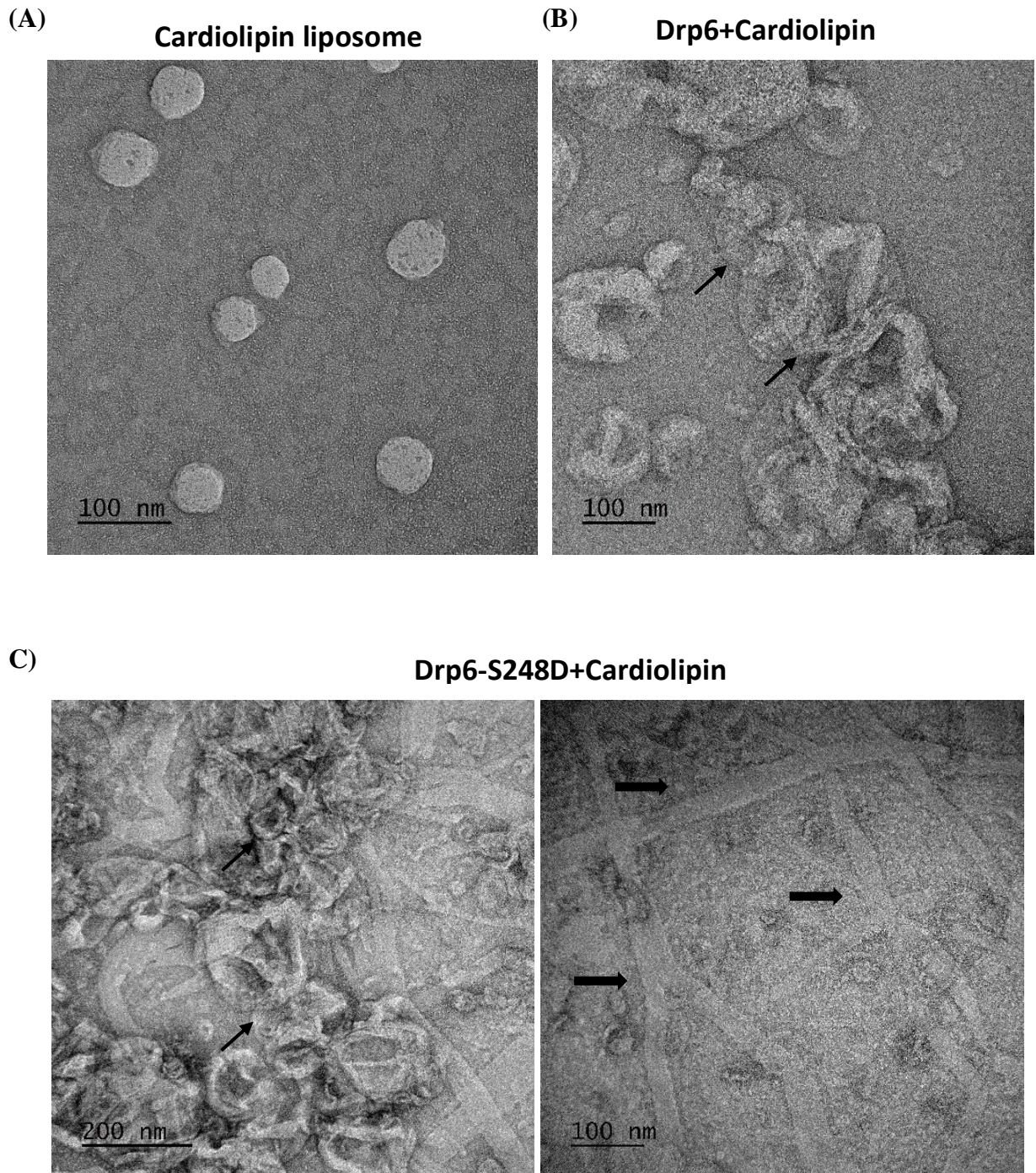


**Figure 2.3.9.1:** Electron micrographs of CL containing liposomes either in absence of any protein (A) or in presence of Drp6 (B) or in presence of Drp6-S248D (C). Arrows indicate the tethered liposomes. Membrane tubulation and networks are indicated as thick arrow.

## 2.4 Discussion

Dynamins perform their function in cell under highly regulated conditions. Regulation encompasses factors like protein synthesis, activation, translocation and degradation following appropriate cellular signals. Post-translational modifications allow modulation of their functions as well as presence in the cell. Drp6 like other dynamins undergoes phosphorylation at four serine residues which are, S86, S248 in the GD and S701 and S705 in the GED. This study attempted to understand the mechanism and regulation by phosphorylation of Drp6 function. *In vitro* membrane fusion assay established that Drp6 is a fusion dynamin since it could tether as well as fuse the membranes. This result support the role of Drp6 in nuclear expansion during transition of micronucleus to macronucleus which requires many-fold increase in the membrane surface area. The fusion of ER derived vesicles with the nuclear membrane would enable addition of new membranes to the nucleus thereby causing nuclear expansion. Comparison of GTPase activity of phosphorylated Drp6 with unphosphorylated forms showed that phosphorylation at S248 reduces the GTPase activity of Drp6. This inhibition in GTPase activity is due to inhibition in catalytic activity of Drp6 and not due to inhibition in GTP binding. Though dynamins are oligomerization stimulated GTPases, size-exclusion chromatography results showed that the inhibition in GTPase activity due to phosphorylation does not arise from defective self-assembly. Phosphorylation at S248 enhanced nuclear envelope localization of Drp6 by increasing cardiolipin binding affinity. This phosphorylation also leads to increase in membrane fusion function and hence nuclear expansion. The increase in membrane fusion was attributed to increased membrane tubulation possibly by stabilizing the self-assembled ring structures. All the results together discussed in this chapter unravels the mechanism of nuclear expansion in which the Drp6 associates with cardiolipin containing membrane and brings about fusion of ER vesicles

either with each other or with nuclear membrane by homotypic interaction and expands the nuclear membrane by incorporating new membrane. This study also reveals that phosphorylation in a single serine residue in the GTPase domain (particularly serine at 248<sup>th</sup> position) enhances membrane fusion function by enhancing tubulation of cardiolipin containing membrane and also by inhibiting GTPase activity possibly by stabilizing the ring structures of the protein Drp6.

## *Chapter 3*

*Mechanism of cardiolipin*

*interaction specificity and*

*nuclear recruitment of Drp6*

### 3.1 Introduction

Dynamin family of proteins require binding to their target membranes to perform their function. As discussed in earlier sections, dynamin-1 wraps around the neck of the invaginated endocytic vesicles. This association is carried out by signature PH domain which binds to the plasma membrane through PIP2 recognition (50, 53, 54). However, the PH domain does not rely on its lipid-binding property for targeting of endocytic dynamin to the clathrin-coated pits suggesting that membrane specific targeting of endocytic dynamins is carried out by protein-protein interactions.

Other members of this family also show functional activation upon membrane binding. These include the mitochondrial fission protein Drp1, yeast dynamin Vps1, mitochondrial fusion protein Opa1 being some of them (97, 235, 242, 243). Although they do not contain a defined PH domain, they contain at an equivalent position, a region termed Insert B. This region is variable among the proteins with a very low sequence complexity. Evidences indicate that this association arise from the direct interactions between this region and specific lipids on the membrane, and are essential for the full functionality of the protein in membrane remodelling. For example, Drp1 interacts with membranes enriched in cardiolipin using a 4 lysine residues within the Insert B region (97). MxA, which is also a member of the dynamin superfamily, interacts with lipids via stretch of 4 lysine residues in the unstructured loop L4 that lies in an equivalent position of the Insert B regions and PH domains (73). Vps1 in yeast localize to both endocytic sites and endosomes, and bind to and tubulate liposomes (243). The membrane binding and deformation occurs by two mechanisms by direct binding of the proteins with the target membrane. One mechanism depends on the electrostatic interactions between the membrane-binding domains of the protein and the anionic lipids in the membrane. Direct insertion of protein into the membrane is another mechanism for

inducing membrane curvature. Here, the hydrophobic protein residues inserts into the membrane, thereby enlarging the area of the bilayer and inducing membrane deformation (244).

Most of the effect of PH domain on membrane binding property of dynamin has been studied in dynamin 1 and 2. By mutational analysis of this domain, the key residues have been identified that perturb their functions (51, 59). Curvature generation is a hallmark of dynamins and dynamin 1 with a functionally defective PH domain surprisingly shows membrane fission when it binds to highly curved membrane surfaces (95, 59). These findings have led to a conclusion that PH domains of dynamin 1 or 2 do not directly cause membrane binding but induce membrane curvature to cause membrane fission (59). A key residue I533 in the disordered loop 1 region shows a dominant negative phenotype when replaced with other hydrophobic residues. Depending on the hydrophobicity introduced by these mutations, the inhibition in its activity is observed thus highlighting the importance of the presence of hydrophobic residue at this position.

Drp6 is a nuclear localizing dynamin in *Tetrahymena* which carries out macronuclear expansion during sexual reproduction (230) in which 2 of the 4 micronuclei expand 10-15 folds in volume to form the somatic macronuclei (245). Apart from the localization on the nuclear envelope, a sub-set of the protein also associates with ER vesicles (230). This dynamin functions as a GTPase, and self-assembles into higher-ordered rings and helical spirals (246). This chapter elucidates the significance of interaction of Drp6 with lipids and the consequent effect of these interactions on the localization of Drp6. The study explains the mechanism by which Drp6 distinguishes its interaction with cardiolipin for its recruitment to the nuclear envelope. It also identifies a single amino acid in the membrane binding domain that determines cardiolipin binding specificity and nuclear recruitment.

## 3.2 Materials and methods

### 3.2.1 Materials

Same as 2.2.1

### 3.2.2 Methods

#### (A) Generation of point mutations

To introduce point mutation, Stratagene Quickchange protocol was followed to design the primers with the desired mutation using either Drp6-pRSETB (for His-tag protein purification) or Drp6-pENTRD TOPO (for gateway cloning in pIGF vector) as template. A 50 $\mu$ L PCR reaction was set-up and the following PCR program was used to amplify the DNA with the desired mutation.

PCR program:	
95°C	30 s
95°C	30 s
55°C	1 min
72°C	3 min

PCR was performed for 18 cycles.

20  $\mu$ L of the PCR products were treated with 0.5 $\mu$ L DpnI for 7-8 hours at 37 °C. 3  $\mu$ L of the DpnI treated PCR product was transformed into *E. coli* DH5 $\alpha$  competent cells. Incorporation of desired mutations were confirmed by sequencing. The list of mutations and the corresponding primers are mentioned in the table below.

**Table:3.2.1 List of primers used for point mutations**

<b>Mutation</b>	<b>Primer sequence</b>
Tt I553A- Forward	5'AAATCATTATGGAATGGACTGTTTAAGAAGCAATGATAAAAGCAGAAAATTT ATGTAATG3'
Tt I553A- Reverse	5'CATTACATAAAATTTCTGCTTTTATCATTGCTTCTTAAACAGTCCATTCCATA AATGATTT 3'
BD6M554L- Forward	5' GGAATGGACCGTGCAGGAAATTTTGATTAAAGCGGAAAACCTG 3'
BD6M554L- Reverse	5' CAGGTTTTCCGCTTTAATCAAAATTTCTTGCACGGTCCATTCC3'
BD6E552D-Forward	5' GGAATGGACCGTGCAGGACATTATGATTAAAGCGG 3'
BD6 E552D-Reverse	5' CCGCTTTAATCATAATGTCCTGCACGGTCCATTCC 3'

**(B) Gateway cloning into pIGF vector for GFP-tagging.**

For generating C-terminal GFP tagged proteins, 150ng of entry clone was added to 220ng of pIGF vector. 1µL of LR clonase enzyme (Invitrogen) was used (the enzyme was vortexed for 2s and placed on ice immediately, it was repeated twice) and the reaction volume was adjusted to 5 µL using plasmid elution buffer. The reaction was carried out at 25°C for 7-8 hours and terminated using 0.5 µL ProteinaseK enzyme at 37 °C for exactly 10min. 3 µL of the reaction mix was used for chemical transformation of *E. coli* DH5a cells. Individual colony was grown in 3mL LB broth to isolate the plasmid. The positive clone was confirmed by restriction digestion using ApaI and XhoI.

**(C) Transformation and expression of GFP-tagged Drp6 variants in *Tetrahymena***

To study the localization of the GFP-tagged proteins, CU428 and B2086 strains were grown to a density of  $4 \times 10^5$  cells/mL in SPP media at 30 °C, 90rpm. The cells were starved using

DMC media at a density of  $2.5 \times 10^5$  cells/mL for 14-16 hours under same conditions. To initiate conjugation, 40 mL of each strain was mixed in a 1L conical flask and kept at 30 °C without rotation. At 9 hour 40 min post-mixing, 50mL cells were pelleted at 1100g for 1min and washed in 10mM HEPES, pH7.5 and resuspended in 300  $\mu$ L in the residual buffer. 18-22  $\mu$ g of plasmid was resuspended in 125  $\mu$ L of the same buffer. 125  $\mu$ L each of cells and the plasmid were added and mixed in 2mm electrocuvette. Electroporation was carried out at 250 V, 275  $\mu$ F capacitance, 13  $\Omega$  resistance, 4ms. SPP was added 1 min post-pulse to recover the cells. Cells were plated in 96 well plate (125  $\mu$ L cells /well) and incubated at 30 °C in a well hydrated closed chamber for 16-18 hours. Cells were drugged next day using 100  $\mu$ g/mL paromomycin sulfate and incubated in the same condition to select the transformants. To induce expression, the cells were passaged twice in presence of drug and then grown in 5mL media to a density of  $2.5 \times 10^5$ . Expression was induced using cadmium chloride at a concentration of 1  $\mu$ g/mL for 4 hours at same conditions. For imaging, cells were pelleted at 1100g for 2 min. For fixation, 3mL of 4% paraformaldehyde was added to the cells and incubated for 20 min at RT. Cells were washed with 10mM HEPES, pH 7.5 before imaging.

#### **(D) Protein expression and purification**

Protocol mentioned in 2.2.1.2 was followed.

#### **(E) Fluorescence spectroscopy**

For measuring the intrinsic fluorescence, 300  $\mu$ L of protein (in buffer A) at a concentration of 0.2  $\mu$ M was used in 10mm quartz cuvette. The samples were excited at 295nm with a 2 nm band pass using FLS-1000 fluorescence spectrophotometer (Edinburgh Instruments Ltd., UK) and emission was recorded at 310-400nm with 10nm band pass. Experiment was performed at least thrice.

### **(F) Acrylamide quenching assay**

For this assay, 1.5  $\mu\text{M}$  protein in presence of varying concentrations of acrylamide (0mM-400mM) was used in Cary-Eclipse fluorescence spectrophotometer, Agilent technologies. The excitation was at 295 nm. Emission at 332nm was considered for *Stern-Volmer* plot using the following equation:

$$F_0 / F = 1 + K_{sv}[Q]$$

$F_0$  indicates fluorescence without a quencher,  $F$  indicates fluorescence in presence of quencher.  $Q$  is the quencher concentration in  $\text{M}$ .  $K_{sv}$  denotes the *Stern-Volmer* constant. The values were plotted using GraphPad Prism 8.  $K_{sv}$  was derived from the slope of the graph. Quenching constant was derived using the following equation:

$$k_q = K_{sv}/\tau$$

$k_q$  denotes quenching constant (in  $\text{Mol}^{-1} \text{ns}^{-1}$ ) and  $\tau$  is tryptophan life-time (ns), value used here is 2.7 ns. Experiment was done twice.

### **(G) Circular Dichorism (CD) spectroscopy**

145  $\mu\text{g/mL}$  protein was used in buffer A for CD measurements using Jasco J-1500 instrument (Jasco Inc. USA). Ellipticity in millidegrees was recorded between 260nm -250nm. Mean Residue Ellipticity was derived using the following formula:

$$[\theta]_{\text{MRW}} = \theta.100.M_r.(c.l.N_A)^{-1}$$

$\theta$  denotes ellipticity in mdeg.  $M_r$  shows the molecular weight in Da,  $c$  is concentration of protein in mg/ml,  $l$  is path length (cm),  $N_A$  denotes number of residues in the protein. Experiments were performed thrice.

#### **(H) Fractionation of membrane protein and soluble protein**

GFP-drp6 or GFP-DTD expressing *Tetrahymena* cells were lysed in 500  $\mu$ l of ice-cold lysis buffer containing 25 mM Tris–Cl pH 7.5, 300 mM NaCl, 10% glycerol supplemented with protease inhibitors (pepstatin, E-64, aprotinin, protease inhibitor cocktail (Roche) and PMSF, by passing through a 12mm ball-bearing homogenizer. The lysates were centrifuged at 16,000 g for 15 min, 4°C, the supernatant was collected as soluble protein fraction and the pellet representing membrane fraction was resuspended in 500  $\mu$ l of lysis buffer. The proteins in both soluble fraction and membrane fraction were separated using 12% SDS–PAGE gel and analyzed after western blotting using anti-GFP polyclonal antibody (1:4000; Sigma–Aldrich). Experiment was done twice.

#### **(I) Measurement of GTPase activity and size exclusion chromatography**

Protocols mentioned in 2.2.1.3 and 2.2.1.4 were followed. Assay was done atleast thrice for plotting the graph.

### 3.3 Results:

#### 3.3.1 Drp Targeting Determinant (DTD) of Drp6 is the membrane binding domain

Unlike the classical dynamin, Drp6 lacks a distinct membrane binding PH domain (Fig.3.3.1.1A). Earlier it has been shown in the lab that the DTD of Drp6 interacts with three phospholipids namely CL, PS and PA (241). It was also shown that DTD alone is not able to associate with nuclear membrane. To assess if DTD is the membrane binding domain of Drp6, GFP-Drp6-DTD and GFP-Drp6 were expressed in *Tetrahymena* and the cell lysate was subjected to fractionation. As expected, the wildtype Drp6 was found in the membrane fraction along with in the soluble fraction. Similar to wild type Drp6-DTD was also present in the membrane fraction. Therefore, it can be concluded that DTD is the membrane binding domain of Drp6 (Fig.3.3.1.1B).

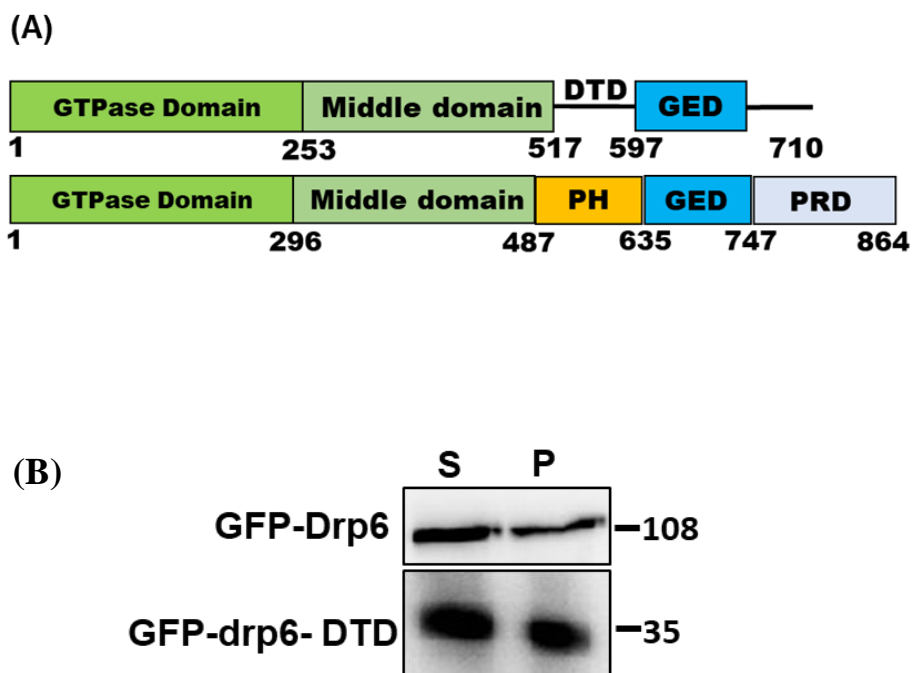


**Figure 3.3.1.1: (A) Domain organization of Drp6 (top) and HDyn1 (bottom).** Diagrammatic representation of domain organization of Drp6 and Hdyn1. Numbers indicate the positions of amino acids in the protein. **(B) Sub-cellular fractionation of GFP-Drp6 (top) and GFP-**

**Drp6-DTD (bottom).** The soluble fraction (S) and pellet fractions containing membrane fraction (P) were analysed using western blotting using anti-GFP polyclonal antibody. Molecular weights are indicated on right.

### **3.3.2 Identification of a hydrophobic patch in the DTD.**

Drp6 lacks PH domain and adopted a loop (DTD) in the equivalent position. A hydrophobic patch in the PH domain of dynamin is known to be important for membrane association/insertion. To find out if a similar hydrophobic patch is also present in the membrane binding domain of Drp6, the DTD sequence was aligned with PH domain. Since there was very less sequence similarity between them, the equivalent hydrophobic patch in Drp6 was not evident from sequence alignment. The 3D structures of all the dynamin family proteins are conserved. A 3D model of Drp6 was generated using human dynamin 1 as template and compared the membrane binding domain of Drp6 with PH domain. In the 3D model three hydrophobic residues IMI (amino acid residues 553-555) (Fig.3.3.2.1B) were found that is located around the position where the hydrophobic patch (IGI) in PH domain of human dynamin is present. This hydrophobic patch in human dynamin 1 contains a critical isoleucine at 533<sup>rd</sup> position (Fig.3.3.2.1A) which is important for membrane insertion. In the subsequent sections, we have analysed the importance of hydrophobic patch in membrane binding and nuclear recruitment of Drp6.

(A)

Drp6	CICSKMIDIHETESKCLKQNHVYLQN	527
Hdyn1	TNHEDFIGFANAQQRSNQMNKKKTS	512
	..*.: : : : : * : .	
Drp6	DNQQKKVL--YEYI-----SKNK-----SFMWTVQE-----IMTKAE-----	558
Hdyn1	GNQDEILVIRKGWLTINNIIGIMKGGKEYWFLTAENLSWYKDDEEKEKYMLSVDNLKL	572
	.**.: : : : * . . . * : : * : . :	
Drp6	-----NLCNVPITMSDLQNTYTKA-----	577
Hdyn1	RDVEKGFMSKHFALFNTEQRNVYKDYRQLELACETQEEVDSWKASFLRAGVYPERVGD	632
	*.: : : : : *	
Drp6	EEK	580
Hdyn1	KEK	635
	:**	

(B)

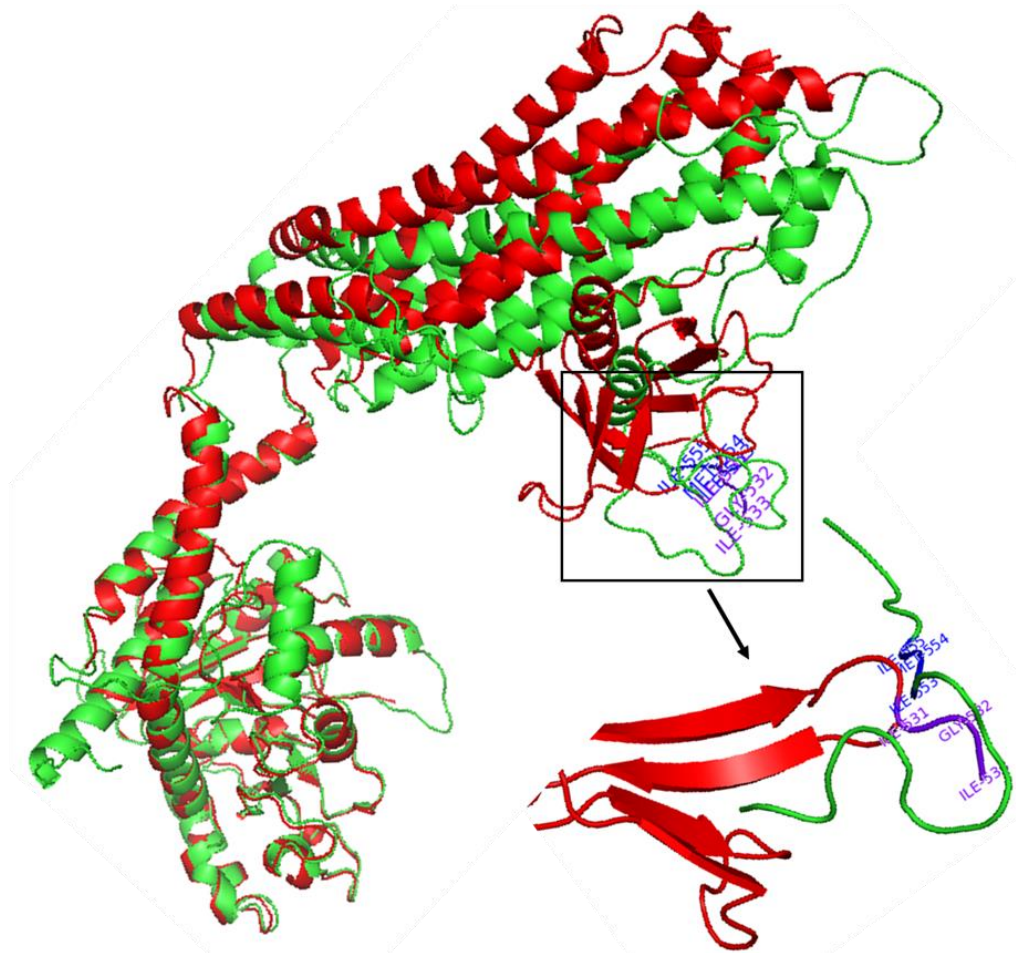


**Figure 3.3.2.1: (A) Drp6 contains a hydrophobic patch.** Protein sequence alignment of Drp6 (top) and Hdyn1 (bottom) using clustal omega showing the hydrophobic patch in the membrane binding domain of Drp6 and HDyn1 (marked within the box).

**(B) 3-D structure of Drp6 generated using I-TASSER.** Homology model of Drp6 (green) was generated using HDyn1 (red) as template. The region marked within the box shows the loop region containing the hydrophobic patch (numbers indicate the amino acid residues of the patch) in the PH domain of HDyn1 (red) and the membrane binding domain of Drp6 (green). The inset shows a magnified view of the amino acid residue positions (Purple indicates residues in HDyn1 and Blue indicates residues in Drp6)

### **3.3.3 An isoleucine residue at 553<sup>rd</sup> position is essential for nuclear recruitment and cardiolipin binding specificity of Drp6.**

It was earlier shown that a mutation isoleucine to methionine at 553<sup>rd</sup> position results in loss of nuclear recruitment and cardiolipin binding. However, it was not clear if the loss was due to absence of isoleucine or due to incorporation of methionine. Another mutant was generated at 553<sup>rd</sup> position where isoleucine was replaced with alanine, and evaluated its nuclear envelope localization after expressing it as GFP tagged protein (GFP-Drp6-I553A) in *Tetrahymena*. GFP-Drp6-I553A localizes mostly as cytoplasmic puncta but does not localize on the nuclear envelope (Fig.3.3.3.2) which is similar to GFP-Drp6-I553M. This result confirms that isoleucine at this position is critical for nuclear recruitment of Drp6.

To assess if the loss of nuclear recruitment of I553A is also due to loss of CL binding, a floatation assay was performed. Earlier floatation assays were performed using total *Tetrahymena* lipid supplemented additionally with either CL or PS. To rule out the role of other *Tetrahymena* lipids in Drp6 binding if any, liposomes with PC and PE supplemented with either CL or PS or PA were prepared and used for floatation assays. The results showed that Drp6 does not interact with membrane containing only PC and PE, but require CL or PS or PA for membrane binding (Fig.3.3.3.1A). The membrane binding of Drp6-I553M was

evaluated and confirmed that the mutation causes loss of interaction specifically with CL without affecting its interaction with PS and PA (Fig.3.3.3.1B). To examine if the loss of I553A nuclear recruitment is also due to lack of interaction with CL, floatation assays with the liposomes were carried out. Similar to I553M, I553A also specifically lost interaction with CL but retained interactions with PS and PA. All these results suggest that isoleucine at 553<sup>rd</sup> position of Drp6 is important for interaction with cardiolipin (Fig.3.3.3.3)

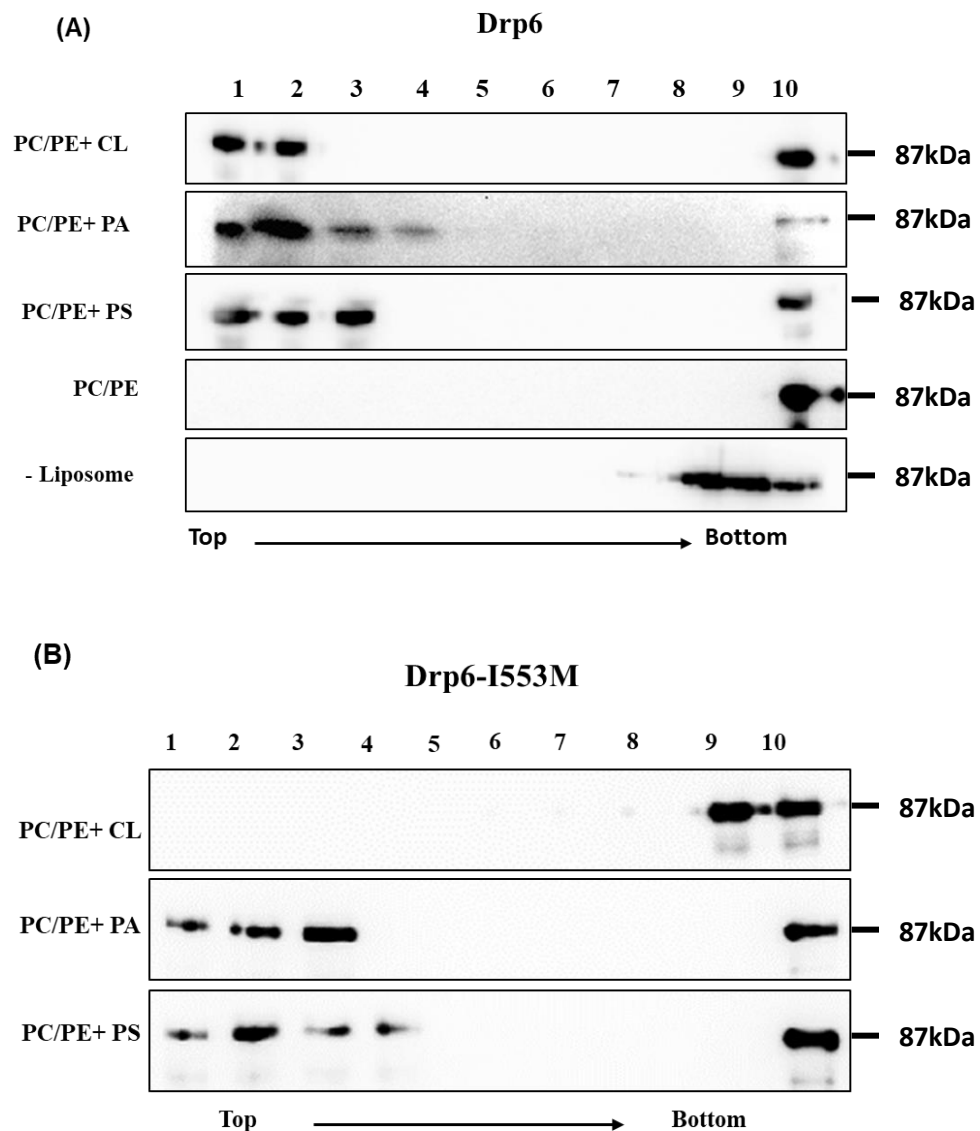


**Figure 3.3.3.1: Liposome co-floitation assay of Drp6 (A) and Drp6-I553M (B).** Liposome co-floitation assay was performed with purified His-Drp6 using liposomes containing PC and

PE supplemented by either CL or PS or PA without addition of protein to the liposomes (- Liposome) as indicated on the left of the panel. Fractions were collected from the top and analysed by western blotting using anti-His monoclonal antibody. While Drp6 interacts with CL, PS and PA, I553M loses interaction specifically with CL. Molecular weights are indicated on right side of blots.

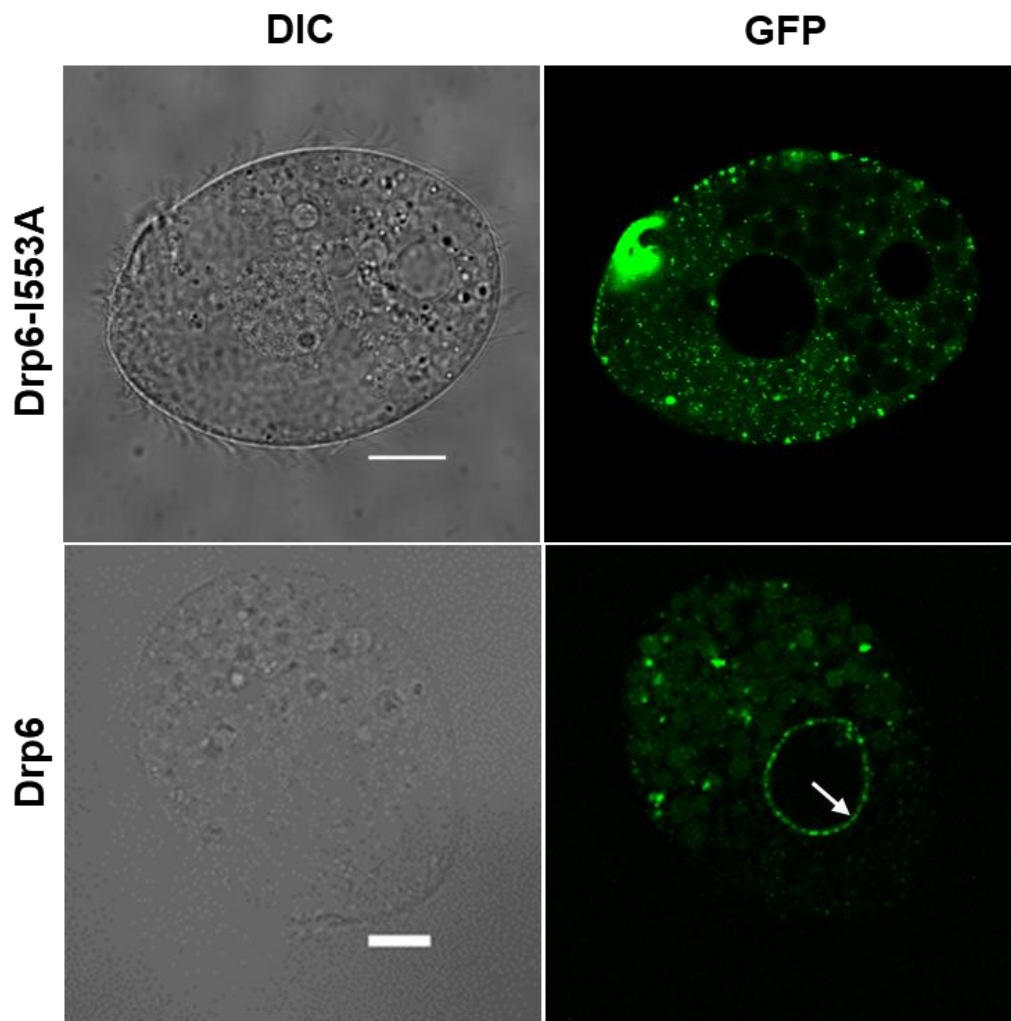


**Figure 3.3.3.2: Drp6-I553A doesnot localize on the nuclear envelope.** Confocal images of live *Tetrahymena* cells expressing GFP-Drp6-I553A(top) or GFP-Drp6 (bottom). Arrow indicates nuclear envelope localization. Bar =10 $\mu$ m.



**Figure 3.3.3.3: Liposome co-floatation assay of I553A-Drp6.** Liposome co-floatation assay was performed in 3.3.3.1 as mentioned above. Liposomes containing PC and PE supplemented with either CL or PA or PS were used as indicated on the left of the panel. Fractions collected (indicated as numbers) and analysed by western blotting using anti-His monoclonal antibody.

### 3.3.4 Mutations at I553 do not affect GTPase activity and self-assembly property

Drp6-I553A resulted in loss of nuclear association by inhibiting CL binding affinity. To examine if the loss of nuclear recruitment is due to cardiolipin binding defect or also due to defect in other biochemical properties, we assessed GTPase activity and self-assembly of I553A mutant was assessed and was compared with that of wild type Drp6 proteins. For measuring the GTP hydrolysis activity, a colorimetric assay was performed using purified recombinant proteins. As shown in Fig. 3.2.4.1A,B, the GTP hydrolysis activity of Drp6-I553A (0.0522 nmol phosphate/ $\mu$ M protein/min) was found to be similar to that of the wild-type Drp6 (0.0524 nmol phosphate/ $\mu$ M protein/min). The self-assembly property of the

mutant was assessed by size-exclusion chromatography using Superdex 200 10/300 gl column.

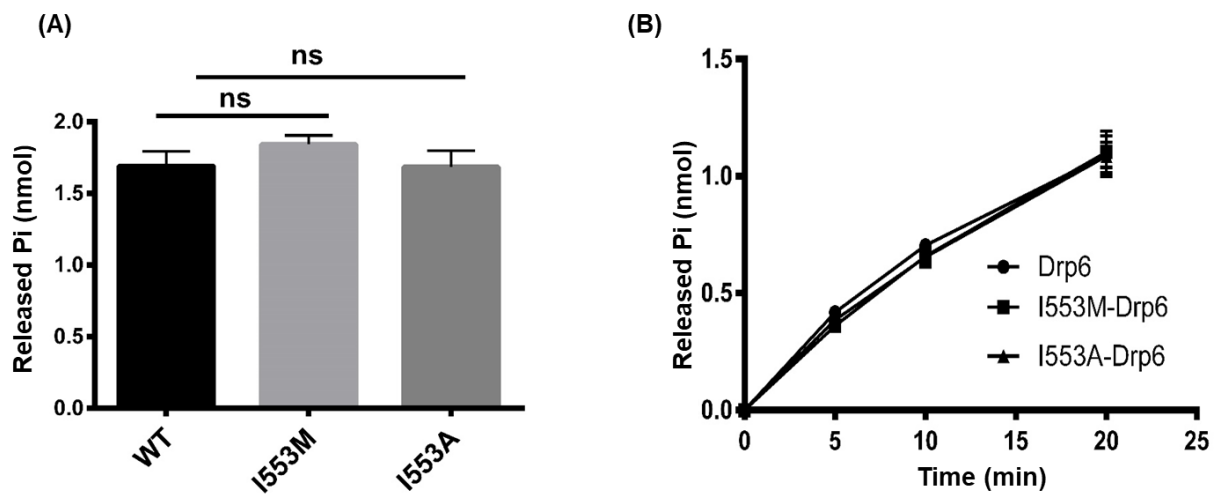


**Figure 3.3.4.1: GTP hydrolysis activity of Drp6 (WT), I553M-Drp6 (I553M) and Drp6-I553A (I553A).** The reaction was either carried out for 30min (A) or 0-20min (B). Statistical analysis was performed using GraphPad Prism 8.0 software.

Similar to the wildtype Drp6, Drp6-I553A also eluted mostly in the void volume indicating the presence of higher ordered structures. A minor fraction eluting as mixture of oligomers indicating presence of dimers at the peak fraction was also observed (Fig.3.2.4.2). These results confirmed that the mutation of isoleucine at 553<sup>rd</sup> position of Drp6 specifically inhibits its interaction with CL. This loss in CL binding does not arise from changes in other known properties of Drp6 such as GTP hydrolysis and self-assembly.

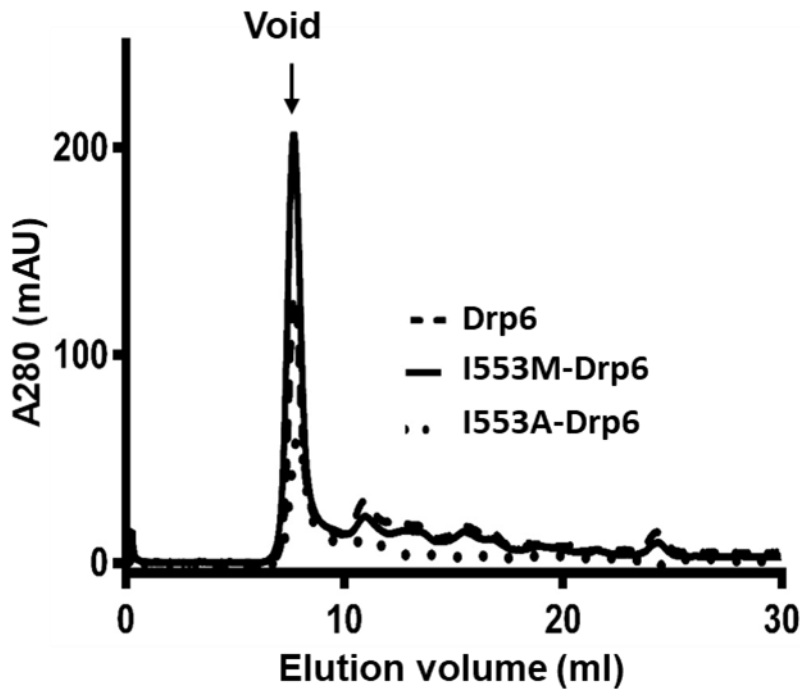


**Figure 3.2.4.2: Size exclusion chromatography of Drp6, I553M-Drp6 and I553A-Drp6.**

Gel filtration of Drp6, I553M-Drp6 and I553A-Drp6 was performed using Superdex 200 10/300 GL column. All the three proteins eluted majorly in the void fraction. Arrow indicates the void volume.

### **3.3.5 Mutations at I553 do not alter the protein conformation**

It could be argued that the loss of cardiolipin interaction and thereby loss of nuclear recruitment of Drp6 due to mutation at I553 may arise from the defect in protein structure and/or conformation. To see the effect of the mutation at I553 on the overall folding of Drp6, far-UV circular dichroism experiments were performed with purified Drp6-I553A, Drp6-I553M and wildtype Drp6 proteins. The CD spectra of Drp6 showed an ellipticity minima at 222nm and analysis of the spectra using K2D suggested presence of both  $\alpha$ -helix and  $\beta$ -sheets as secondary structures. Both the mutants also showed spectra that resemble the spectra of

wildtype Drp6 (Fig.3.3.5.1). Therefore, it can be concluded the mutations at I553 does not affect the folding of Drp6.

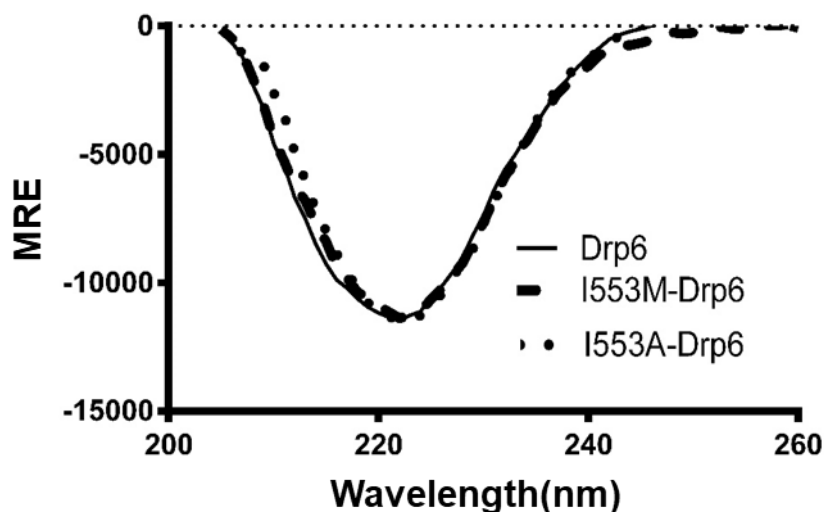


**Figure 3.3.5.1: Far UV-CD spectra of His-Drp6, His-Drp6-I553M and His-Drp6-I553A.**

The graph shows the CD-spectra of His-drp6 (Drp6), His-drp6-I553M (Drp6-I553M) and His-drp6-I553A (Drp6-I553A). The spectra was recorded from 205nm to 260nm. Mean Residue Ellipticity (MRE) was calculated using the formula mentioned in 3.2.1.7 and plotted against wavelength (nm).

To see the effect of the mutation on the overall conformation of the protein, fluorescence spectra were measured using tryptophan residue present in Drp6. Drp6 contains a single tryptophan residue at position 548. The mutants I553M and I553A showed a spectra very similar to that of wildtype Drp6 with a peak at around 332nm, suggesting that mutation at I553 does not change protein conformation. A peak at 332nm signifies that this tryptophan is mostly buried in the protein structure. This further indicates that the stretch of residues near this tryptophan constitutes a hydrophobic environment (Fig.3.3.5.2).

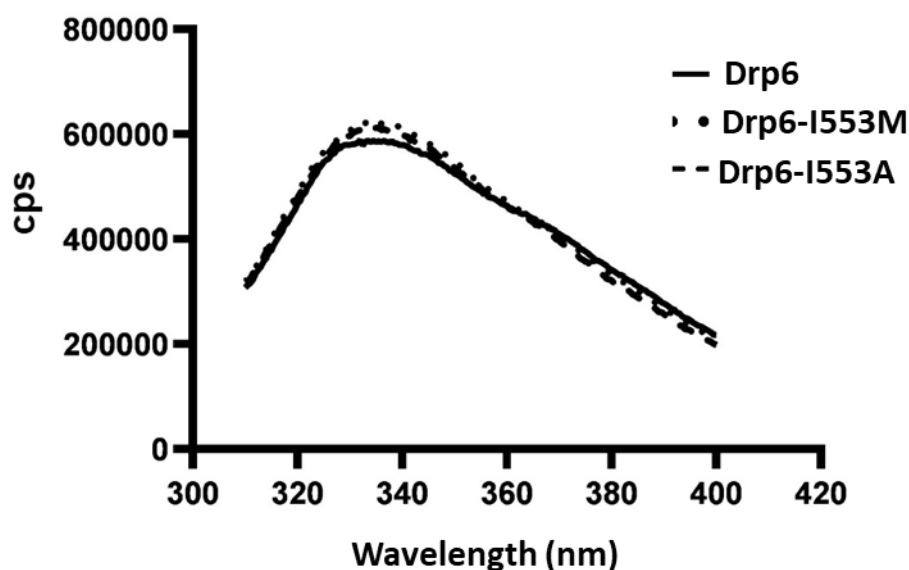


**Figure 3.3.5.2: Tryptophan fluorescence spectra of Drp6, Drp6-I553M and Drp6-I553A.**

The graph shows fluorescence spectra recorded for the intrinsic tryptophan fluorescence of Drp6, Drp6-I553M and Drp6-I553A. All the proteins show a similar spectra with a peak at 332nm.

It is possible that mutation changes local conformation without any visible effect on the fluorescence spectra. To evaluate if there is any change in the local conformation due to the introduction of mutations, acrylamide quenching assay was performed. The accessibility of the tryptophan was studied by measuring intrinsic tryptophan fluorescence at different concentrations of the quencher. The presence of a single tryptophan residue at position 548 served to the advantage in studying the accessibility of the hydrophobic patch, since it resides near I553 residue. The quenching of fluorescence intensity with increasing concentrations of the quencher is shown in Fig.3.3.5.3. The accessibility of the tryptophan was compared by plotting the *Stern-Volmer* plot and deducing the quenching constant ( $k_q$ ). The *Stern-Volmer* plot for the mutants were comparable to that of the wild-type (Fig.3.3.5.4).  $k_q$  for Drp6 was

measured to be  $1.01 \text{ M}^{-1}\text{ns}^{-1}$  whereas it was  $1.11\text{M}^{-1}\text{ns}^{-1}$  for Drp6-I553M and  $1.04\text{M}^{-1}\text{ns}^{-1}$  for Drp6-I553A. A comparable quenching constant suggests that the mutation at I553 does not change the local conformation of Drp6 significantly. Overall, these results suggest that the loss of nuclear envelope localization and CL binding due to mutation at I553 of Drp6 does not arise from changes in conformation or folding of the protein.

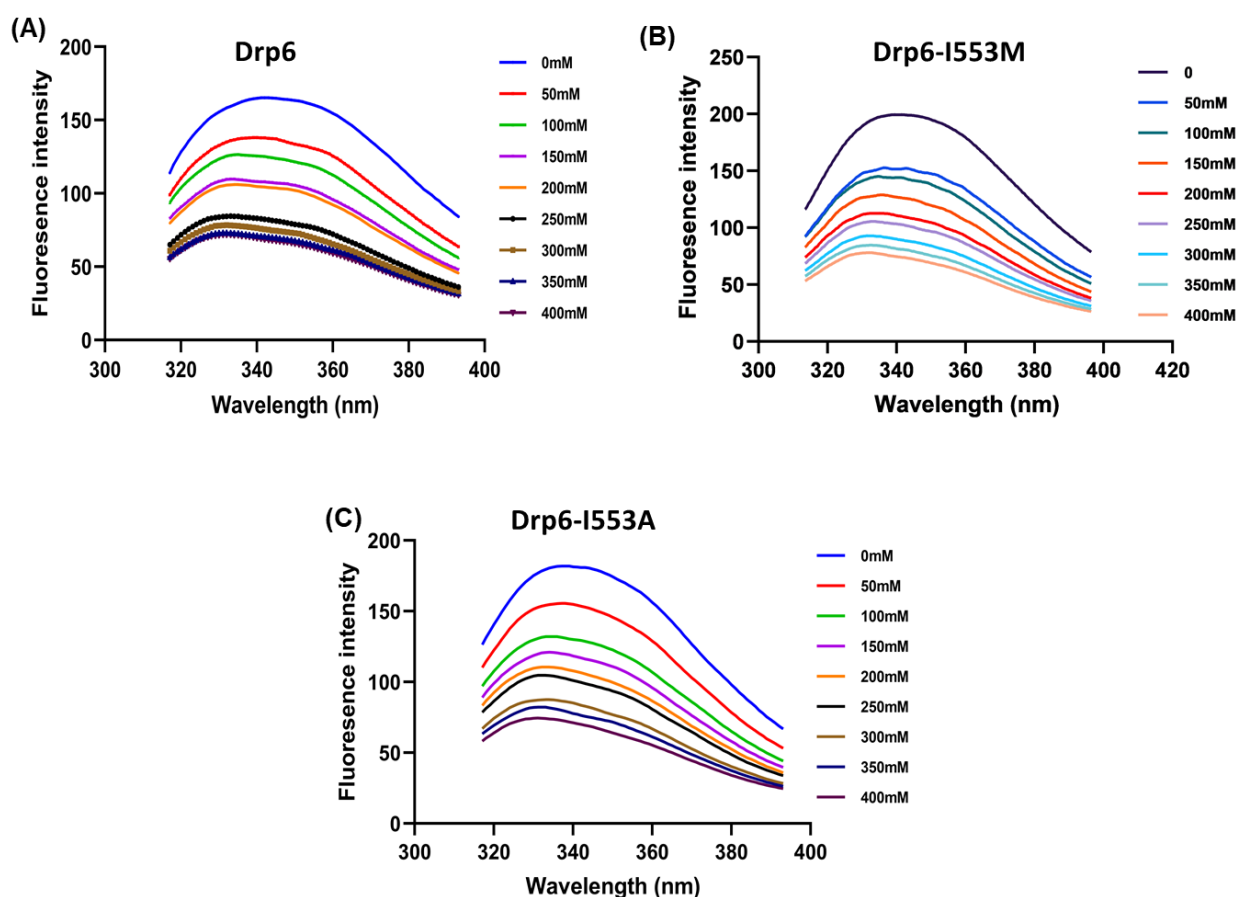


**Figure 3.3.5.3: Effect of acrylamide on tryptophan fluorescence spectra of Drp6 (A), Drp6-I553M (B) and Drp6-I553A (C).** The graphs show the change in intrinsic tryptophan fluorescence upon addition of acrylamide in different concentrations. Color coded lines on the right of the graphs indicate spectra at the respective acrylamide concentrations.

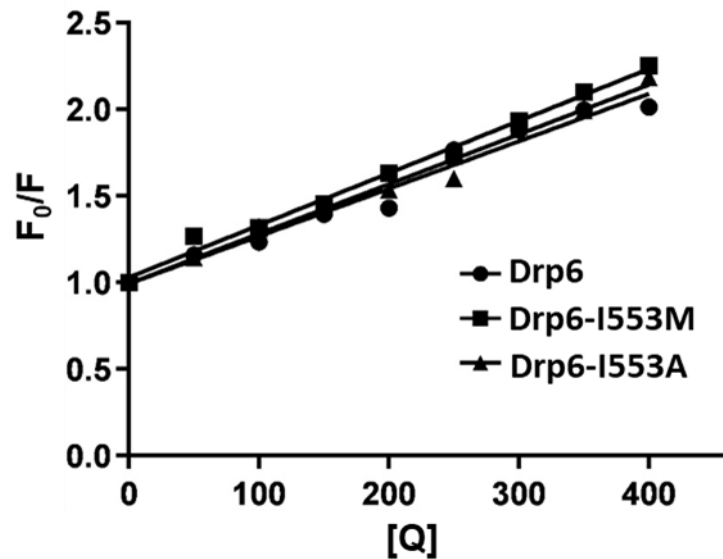
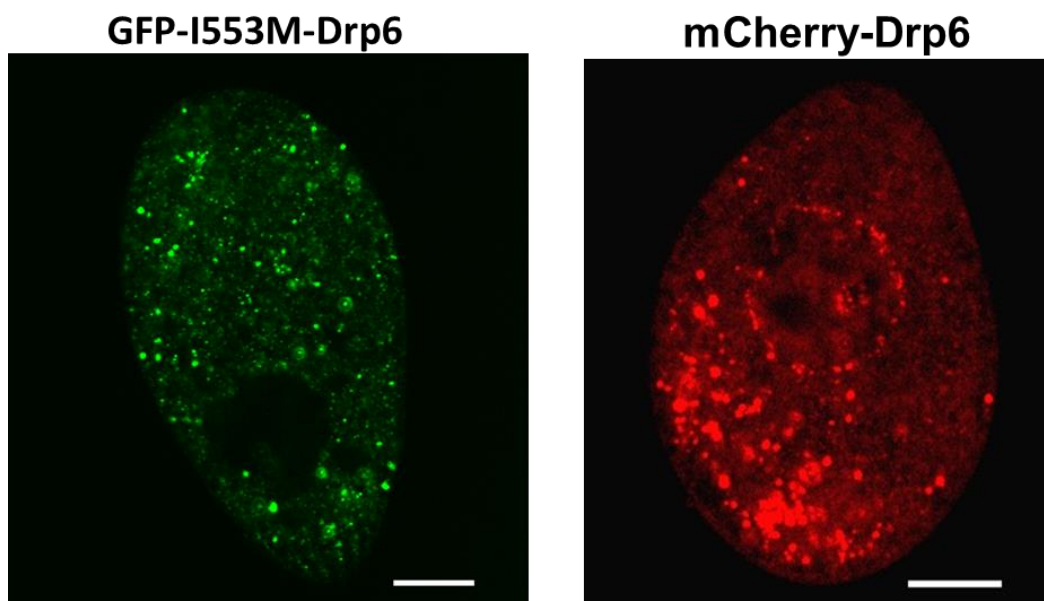


**Figure 3.3.5.4: Stern-Volmer plot for acrylamide quenching of His-Drp6 (Drp6), His-Drp6-I553M (Drp6-I553M) and His-Drp6-I553A (Drp6-I553A).**  $F_0$  is the fluorescence intensity without addition of acrylamide.  $F$  is the fluorescence intensity at a given acrylamide concentration.  $[Q]$  is molar concentration of acrylamide. The graph was plotted using GraphPad Prism8.0

### 3.3.6 Nuclear recruitment of Drp6-I553M mutant is restored by co-expression of wildtype protein.

The mutant defective in CL binding, Drp6-I553M does not show any visible defect in properties like GTP hydrolysis, self-assembly or binding with PS and PA liposomes *in vitro*. If other properties of Drp6 are not affected, then Drp6-I553M should be recruited to the nuclear envelope as a self-assembled complex with wildtype Drp6. To test this hypothesis, *Tetrahymena* was co-transformed with mCherry-Drp6 and GFP-drp6-I553M. The localization was then studied by confocal imaging of the co-transformants. As expected, when Drp6-I553M expressed without co-expression of mCherry-Drp6, it failed to associate

with nuclear envelope. However, Drp6-I553M was able to associate with wild type Drp6 as these two proteins colocalized almost completely including in the nuclear envelope (Fig.3.3.6.1). This confirms our *in-vitro* results that Drp6-I553M does not have major defect in other properties except defect in binding to cardiolipin. More importantly, the GFP-I553M-drp6, which localizes in the cytoplasm puncta could now associate with mCherry-drp6 and translocate to the nuclear envelope (Fig.3.3.6.1). This observation suggests that isoleucine at 553<sup>rd</sup> position of Drp6 is required for localizing to the nuclear envelope. Mutation leading to loss of this isoleucine leads to loss of nuclear envelope localization by specifically inhibiting its CL binding activity and can be restored by its association with Drp6 which binds to the CL on nuclear envelope.



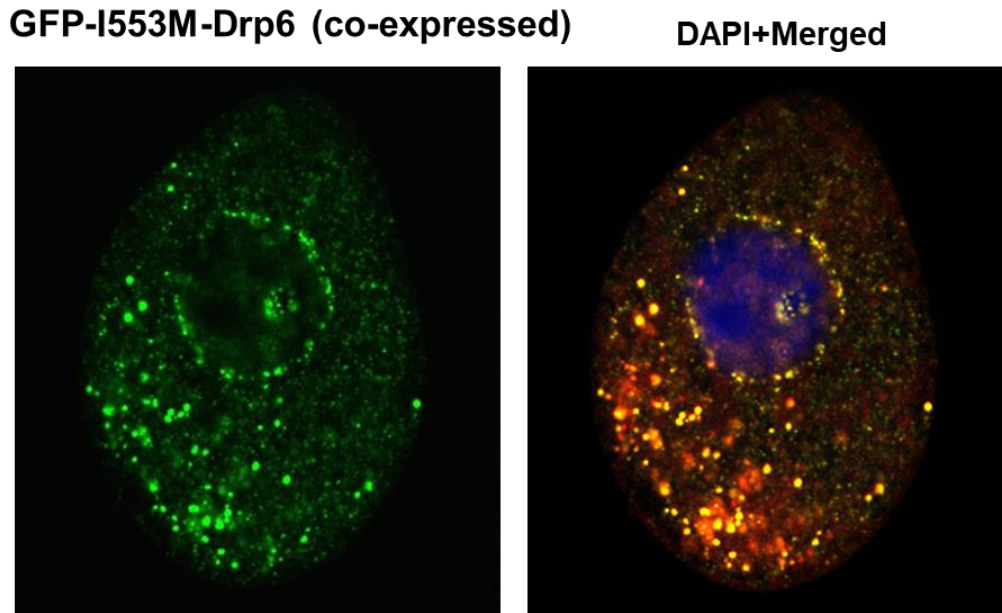


**Figure 3.3.6.1: Co-expression of GFP-Drp6-I553M and mCherry-Drp6 restores nuclear envelope localization of Drp6-I553M.** Confocal images of fixed *Tetrahymena* cells expressing either GFP-Drp6-I553M (top left) or cells co-expressing GFP-Drp6-I553M and mCherry-Drp6 (GFP-I553M-Drp6 (co-expressed) and mCherry Drp6). DAPI+ Merged is the merged image of GFP-I553M-Drp6 (co-expressed) and mCherry Drp6 stained with DAPI. Bar= 10 $\mu$ m

### **3.3.7 Residues in the vicinity of I553 are not essential for nuclear recruitment and cardiolipin binding specificity of Drp6**

An isoleucine residue at 553<sup>rd</sup> position is required for cardiolipin binding specificity and nuclear recruitment of Drp6. To see if the residues surrounding this isoleucine are also essential for providing cardiolipin binding specificity and nuclear recruitment, E552 and M554 were mutated independently (Fig.3.3.7.1A). The glutamate was mutated to aspartate (E552D) and methionine was mutated to leucine (M554L). These mutants were expressed as GFP-tagged proteins in *Tetrahymena* for studying localization and as His-tagged proteins in



**assay of Drp6-M554L and Drp6-E552D.** Assay was performed using liposomes containing 70%PC, 20%PE, 10%CL. Fractions collected from top were analysed by western blotting using anti-His monoclonal antibody.

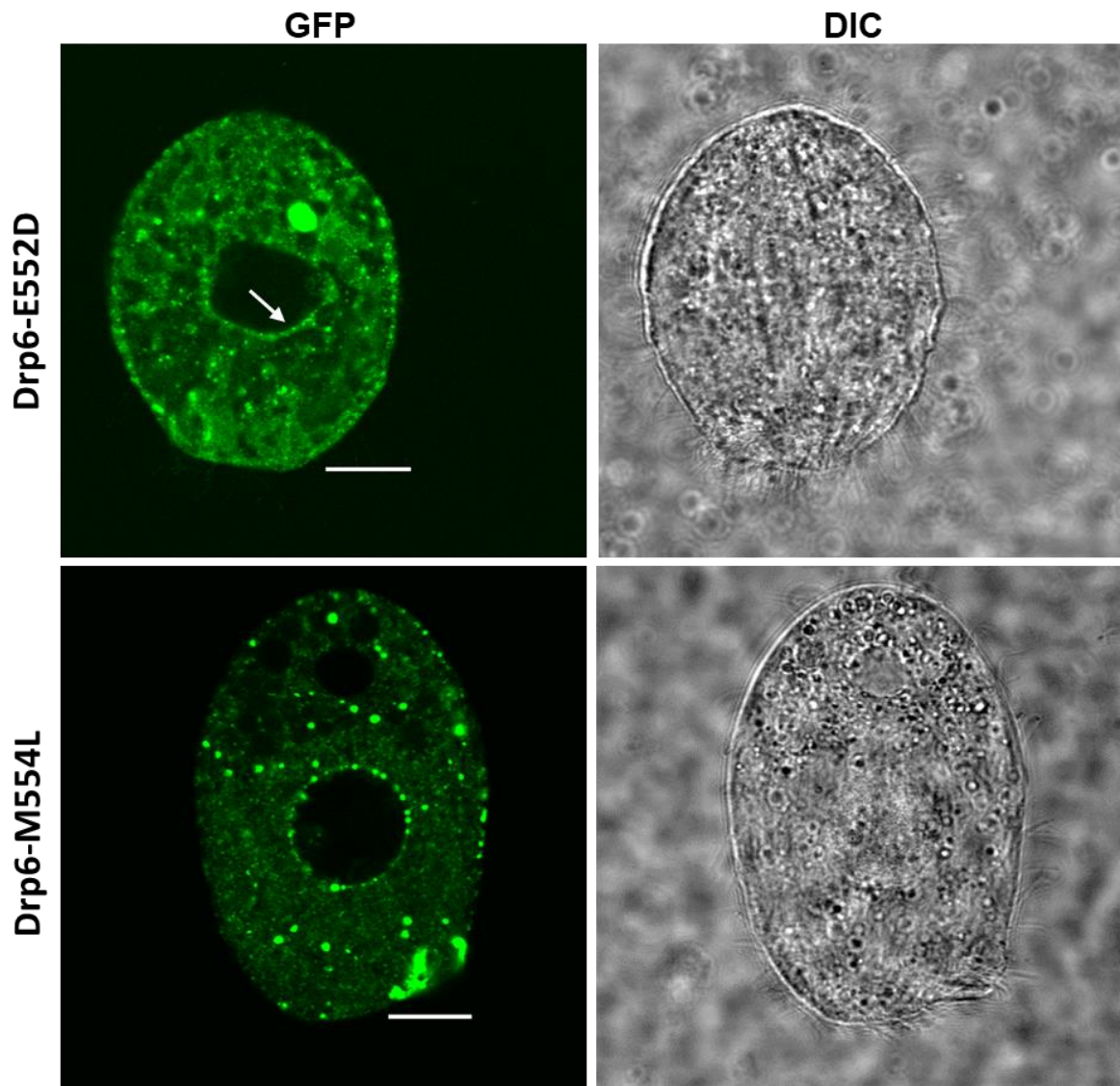


**Figure 3.3.7.2: GFP-Drp6-E552D and GFP-Drp6-M554L localize on the nuclear envelope.** Live cell confocal images of *Tetrahymena* expressing GFP-Drp6-E552D and GFP-Drp6-M554L. Arrow indicates nuclear envelope localization. Bar =10 $\mu$ m

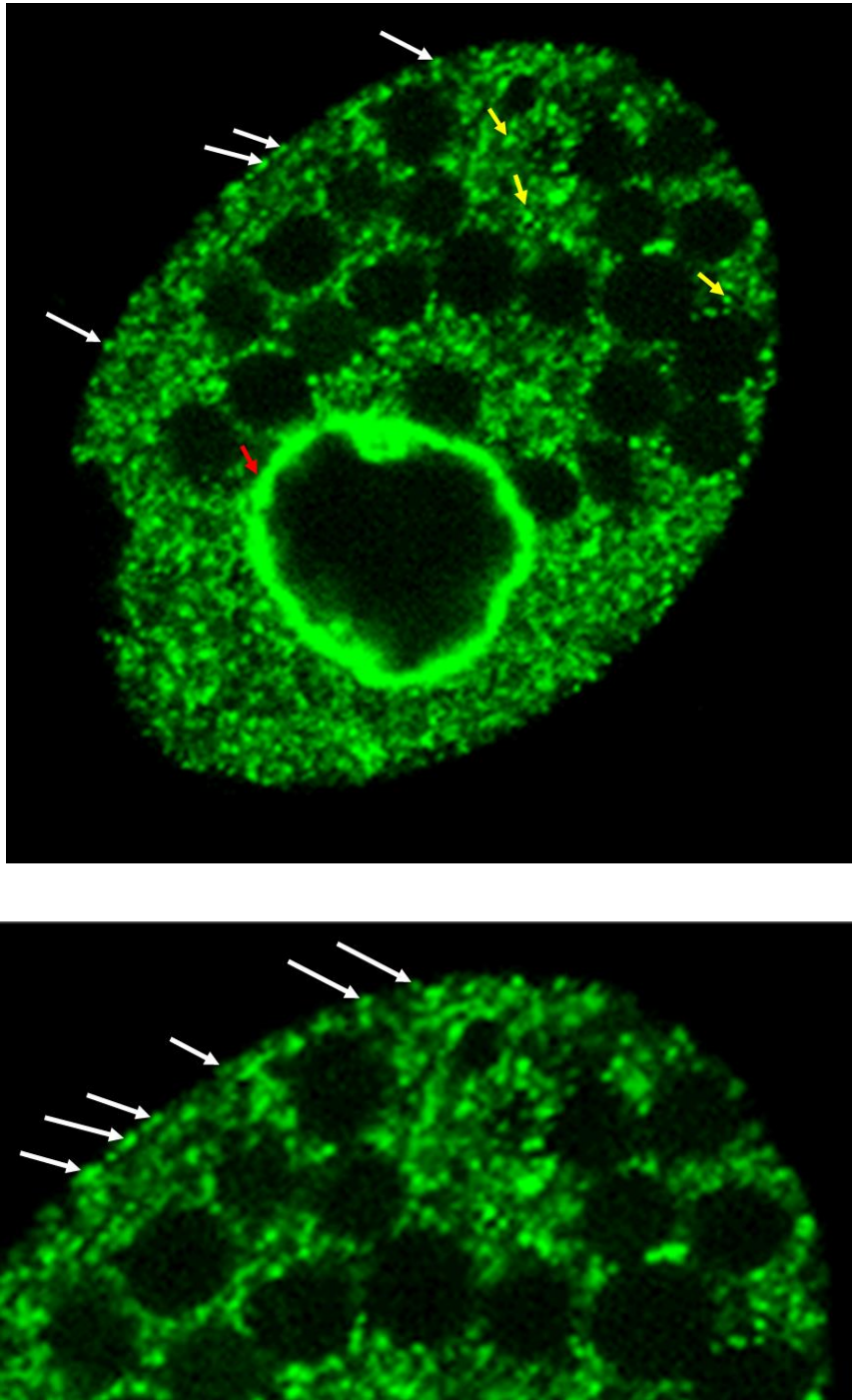


**Figure 3.3.1: Drp6 localizes on nuclear envelope, plasma membrane and ER.** Confocal image of live *Tetrahymena* cell expressing GFP-Drp6. Red arrow indicates localization on nuclear envelope, white arrow on plasma membrane and yellow arrows in ER vesicles.

### 3.4 Discussion

Drp6 is a nuclear localizing dynamin which functions in nuclear remodelling in *Tetrahymena* (230). It interacts with 3 phospholipids (CL, PS and PA). Inhibition of CL or mutation of isoleucine at 553<sup>rd</sup> position (Drp6-I553M) leads to loss of nuclear envelope localization of Drp6 (241). This study was carried out to understand the importance of this single residue in the DTD of Drp6 in CL binding and localization of Drp6. GFP-drp6-I553M, when co-expressed with mCherry-Drp6, can localize to the nuclear envelope indicating that it can co-assemble with the wild-type form. It also indicates that Drp6 molecules self-assemble into higher-ordered structures at the nuclear envelope and binds to CL. Mutations of the neighbouring residues E552 and M554 showed that these residues are not essential for the CL interaction specificity and nuclear envelope localization specificity of Drp6. These results emphasised that the single residue I553 determines specificity for CL interaction of Drp6 which in turn determines its nuclear envelope localization.

Interaction with specific lipids via the membrane binding domains determines target specificity. Although Drps including Drp6 lack a PH domain, they can bind to their target membranes via a membrane binding domain located at equivalent position of the PH domain of dynamin (242). The sequence diversity in the membrane binding domains of various Drps indicates diverse functions of the family members on different target membranes. Nuclear envelope of *Tetrahymena* uniquely contains 3.2% CL (245). Drp6 in *Tetrahymena* has evolved to perform a novel function in nuclear remodelling (230). Drp6, apart from localizing on the nuclear envelope, associates with the ER vesicles and also at the plasma membrane (Fig.3.3.1). The perturbation of interaction specifically with CL by mutation at I553 of Drp6 leads to loss of localization at the nuclear envelope whereas it does not abolish interaction with ER vesicles or plasma membrane. This mutation also retains binding with PS

or PA. These results suggest that localization of Drp6 on ER depends on interaction with PS or PA. Since PA is abundant on the ER (247-249), it is possible that PA is involved in recruitment of Drp6 to ER vesicles. Similarly, plasma membrane is abundant in PS (250) and interaction with PS might determine the localization of Drp6 on the plasma membrane. These observations show that lipids play a critical role in determining the localization of Drp6, and interaction with CL allows Drp6 to localize on the nuclear envelope.

Dynamins are known to interact with target membranes involving a stretch of positively charged residues that recognises anionic head groups of phospholipids like PIP2, CL and PS (51, 57, 73, 97, 243, 251-253). However, the mechanism by which different dynamins distinguish different anionic lipids based on only ionic interactions is not known. Our study shows that a single amino acid residue (I553) mainly determines CL interaction specificity of Drp6. CL is a highly dynamic lipid which strongly interacts with hydrophobic residues (254). However, hydrophobicity alone is not responsible for determining CL specificity since replacing I553 with another hydrophobic residue (M) does not restore its CL interaction (241). Thus, it appears that the side-chain of isoleucine plays an important role in determining the specificity for CL.

The nuclear expansion process in *Tetrahymena* requires the addition of new membranes to the existing one. Our results in the previous chapter has shown that Drp6 is a fusion dynamin. Therefore, it is conceivable that Drp6 interacts with CL on the nuclear envelope and carries out nuclear membrane expansion by performing membrane fusion. Overall, our results suggest the importance of a single amino acid residue (in the membrane binding domain of Drp6) in target membrane selection of a dynamin related protein by providing specificity to bind a specific phospholipid.

## *Chapter 4*

*The role of G domain and middle domain in the self-assembly and nuclear envelope recruitment of Drp6*

## 4.1 Introduction

The self-assembling property is intrinsic to dynamins and is pre-requisite for their functions. Majority of the dynamins are oligomerization stimulated GTPases implying that the rate of GTP hydrolysis is enhanced when they organise themselves into such higher ordered structures (255). The repetitive GTP binding and hydrolysis in-turn regulates homo-oligomerization on the membrane and membrane severing events. Oligomerization of dynamin and Mx proteins initiate from assembly of protomers which are mainly dimeric. The dimers interact to form stable tetramers. Tetrameric forms are capable of translocating to the template organelle membranes and act as a nucleating structure for multimeric organization of the dynamins into rings and spirals. Structural studies conducted on dynamin 1 (37) and MxA (40) show a common pattern of oligomerization where the protein monomers arrange themselves to dimer and tetramer followed by higher-order structures using relatively conserved interfaces. The residue participating in the interface sites are mainly from the stalk region.

The stalk region is comprised of 4  $\alpha$  helices of which 3 are contributed by the middle domain and 1 by N-terminal residues of GED. Four loop regions connect these helices to form linear filament arrangement (37, 40). Self-assembly into dimer, tetramer and further into rings or helical spirals requires interaction of the stalk and other domains mainly through 4 interfaces. Interface 1 is comparatively conserved but does not involve direct contact between the stalk helices. In MxA, this interface is essential for forming rings (the functional form), instead of helices. Contact between the centres of stalk from two monomers generates the interface 2 to form dimers. Loop 1 and 2 contact to form the interface 3 for assembly of dimers to form higher order structures. Disruption of this interface yields stable dimers (37). A unique 4<sup>th</sup> interface is identified in Dnm1L where the helix 2 of the 2 parallel stalk align placing the stalk filaments parallel to form oligomers (256).

The G-domain dimerization is independent of higher order assembly. GTP-binding dependent dimerization of Drps like Drp1 (72), human guanylate binding protein 1 (75) and Atlastin (257) on the opposing membranes is required to bring the membranes closer to cause fission or fusion. Hydrolysis of the bound GTP causes dimer to tetramer transition in human guanylate binding protein 1. GTPase domain dimerization is a higher ordered self-assembly independent process that requires GTP binding (257).

The middle domain which constitutes major part of the stalk initiates criss-cross arrangement of the dynamin molecules during self-assembly. Transition from dimer to tetramer of rat dynamin, human dynamin 1 (258) and Drp1 depends on the middle domain and GED interaction within the stalk region. Disruption of the stalk domain interface in Drp1 shifts the dimer-tetramer equilibrium towards dimer formation (60). Loss of this interaction leads to loss of function as seen in Vps1, Drp1 and dynamin 1 (42, 79, 137), Opa1 dimerization also requires the G-domain and middle domain interaction (259).

The GED, which contributes for the 4<sup>th</sup> helix in the stalk region, is sufficient by itself to form homodimers in dynamin 1 (260, 261). The interaction with other domains are essential for its assembly into functional structures like rings and helical spirals, and for stimulating GTPase activity (262). Mutation in GED of Vps1 blocks its self-assembly, leads to extended invagination due to constitutive binding of GTP, and inhibits scission (79). These mutations in the amphipathic helix of GED don't inhibit tetramerization but affect the stimulated GTPase activity (a result of higher-order assembly) indicating that GED interaction with G-domain is essential for self-assembly stimulated GTPase activity (82). Few positively charged residues within the GED of Mgm1 are critical for its self-assembly (77). In human guanylate binding protein 1, helix 12 and 13 equally positioned as the GED regulate its tetramerization.

Dynamin 1 requires PH domain for its dimerization (50) and it is capable of forming tetramers even in absence of membrane (61). However, further self-assembly requires low salt *in vitro* or target membrane binding *in vivo*. Self-assembly of dynamin 1 and Vps1 (79) requires the PRD interaction with the G-domain. Deletion of this domain leads to loss of localization.

Dependence of dynamins on all the domains for self-assembly imply that dynamins initially dimerize via G-domain but further self-assembly into their functional forms requires participation of all the domains. The self-assembly interfaces are mostly conserved and reside within the stalk region composed of the middle domain and the GED.

Drp6 self-assembles into higher order structures independent of its target membrane binding (246). Lack of GD and MD leads to loss of nuclear envelope localization of Drp6. In this study, the role of GD and MD in self-assembly and membrane binding properties of Drp6 was studied.

## 4.2 Materials and Methods

### 4.2.1 Materials:

- Amylose resin and anti-MBP antibody were purchased from New England Biolabs.
- Ni-NTA resin was purchased from Qiagen.
- Anti-His HRP conjugate antibody was purchased from Sigma Aldrich
- Superdex200 10/300 GL column was purchased from GE lifesciences.
- Carbon coated copper grids 200mesh were purchased from EMS

### 4.2.2 Methods:

#### (A) Expression and purification of MBP-tagged protein

For expressing MBP-Drp6 $\Delta$ GD-MD, chemically competent C41-DE3 cells were transformed with 150-200ng of pMALP2 MBP-Drp6 $\Delta$ GD-MD construct. The cells were plated on LB-agar containing 100 $\mu$ g/ml Ampicillin and grown for 14 hours at 37°C without shaking. A loop-full of colonies were scrapped from the plate and added to 400ml LB media supplemented with 100 $\mu$ g/ml ampicillin. The culture was grown to 0.2 OD<sub>600</sub> at 37°C and transferred immediately to 18°C. After 40min, expression was induced with 0.5mM IPTG for 16 hours. Cells were harvested by centrifuging the cells at 12000rpm at 4°C for 5 min.

For purifying MBP-tagged protein, the cell pellet was resuspended in 40mL of ice-cold lysis buffer (25mM HEPES, 250mM NaCl, 10% glycerol) supplemented with 1mM PMSF, 100 $\mu$ g/ml lysozyme, 150 $\mu$ L of protease inhibitor cocktail. The lysozyme treatment was carried out in 4°C with constant mixing. For lysis, the cells were transferred to a sterile 100ml glass beaker on ice-water bath and sonicated till the lysate became translucent with the following settings: 50% amplitude, Pulse 2s ON and 4s OFF. A clear lysate was obtained by centrifuging at 14000rpm for 40min, 4°C. The supernatant was collected in a 50 ml sterile

falcon tube on ice. 150µL of amylose resin was equilibrated with the lysis buffer by washing the resins with 1mL of lysis buffer thrice. The pre-equilibrated resin was added to the cleared lysate and incubated with constant mixing at 4°C for 1.5 hours. The resin was collected by centrifuging the lysate at 3500rpm at 4°C for 2min. The supernatant was discarded and the resin was transferred to a sterile 15 ml microcentrifuge tube on ice. The resin was then washed with 7 ml of lysis buffer 7 times. Elution was carried out using 20mM maltose in lysis buffer.

For dialysis, the protein was spun at 13000rpm for 10min at 4°C to remove residual resins. Protein was collected carefully through the wall of the tube to avoid taking the settled resin. Protein fractions were then pooled and the concentration was adjusted to about 120µg/ml with the lysis buffer and dialysed at 4°C with constant stirring in buffer containing 25mM HEPES pH7.5 and 250mM NaCl.

#### **(B) Size exclusion chromatography**

Protocol mentioned in 2.2.1.4 was used. Fractions were collected and analysed using western blot with anti-MBP monoclonal antibody (1:10000).

#### **(C) Transformation and expression of GFP-tagged Drp6 mutants in Tetrahymena**

The protocol mentioned in 3.2.1.3 was used.

#### **(D) Transmission electron microscopy**

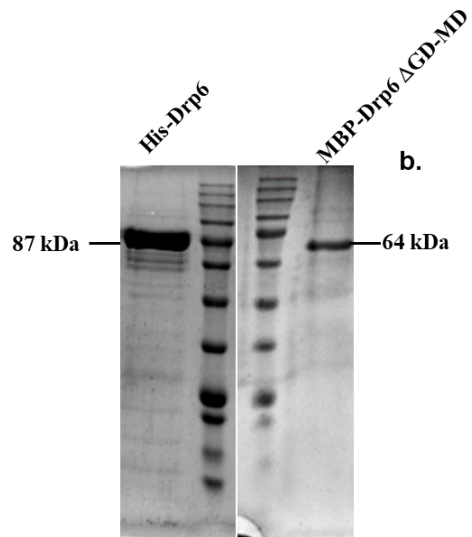
Protocol mentioned in 2.2.1.8 was used.

## **4.3 Results:**

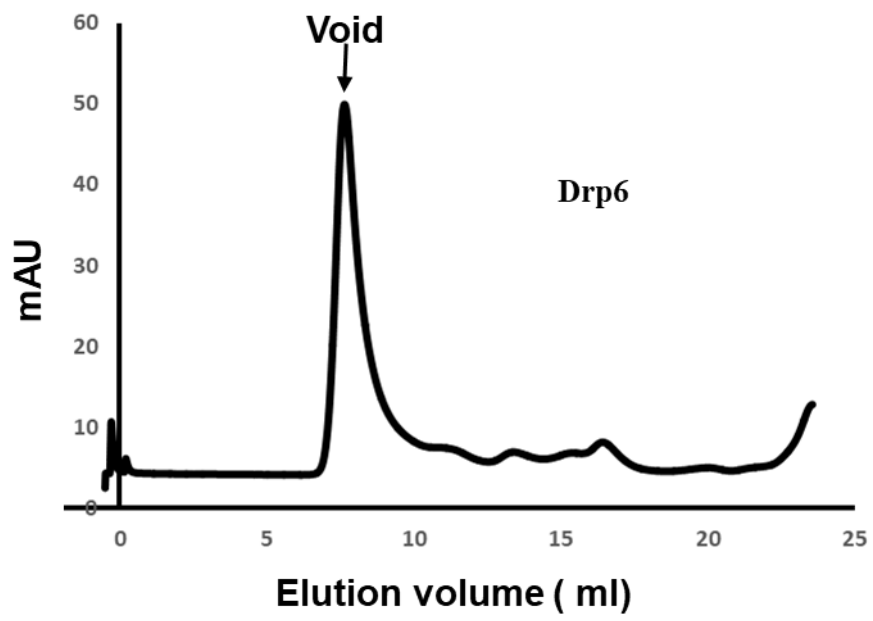
### **4.3.1 GD and MD are not essential for oligomerization**

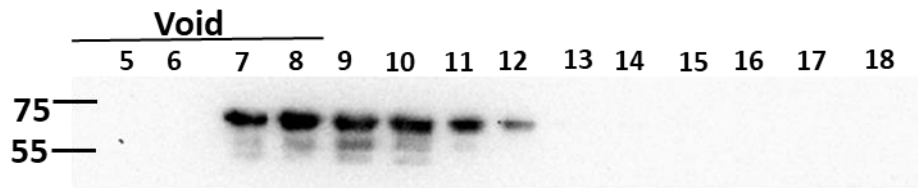
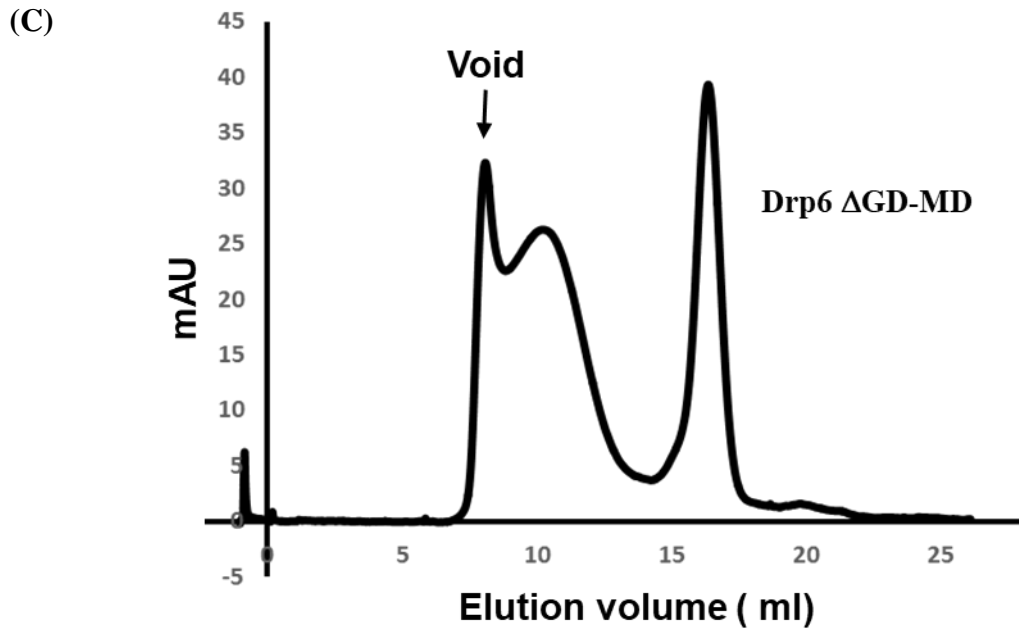
Members of dynamin family proteins self-assemble on the target membrane to perform their functions. Middle domain of all known dynamins play an essential role in their self-assembly. Drp6 similar to other family members self-assemble into rings and helical spirals (246). To investigate if the middle domain is also essential for self-assembly of Drp6, the middle domain and GTPase domain were replaced with the maltose binding protein, and expressed in bacteria. The incorporation of MBP also enabled purification of the recombinant protein (MBP-Drp6 $\Delta$ GD-MD) in soluble form (Fig. 4.3.1.1A). The oligomerization states of His-Drp6 were assessed by size exclusion chromatography and as reported earlier (246), the purified protein eluted in the void as large molecular species (Fig. 4.3.1.1B,D). Considering the exclusion limit of the column, these high molecular weight species contains at least six protomers. When the purified protein lacking GD-MD (MBP-Drp6 $\Delta$ GD-MD) was analysed under similar conditions, presence of large molecular weight species was observed eluting in the void volume (Fig. 4.3.1.1C). This result suggests that similar to wild type Drp6, the MBP- $\Delta$ GD-MD Drp6 is also able to form large oligomeric structures. In addition to the void peak there was also a peak corresponding to dimer. The presence of a less prominent dimeric peak is also observed in His-Drp6 (246). These results suggest that GTPase domain and middle domain are dispensable for oligomerization of Drp6.

(A)



(B)





(D)

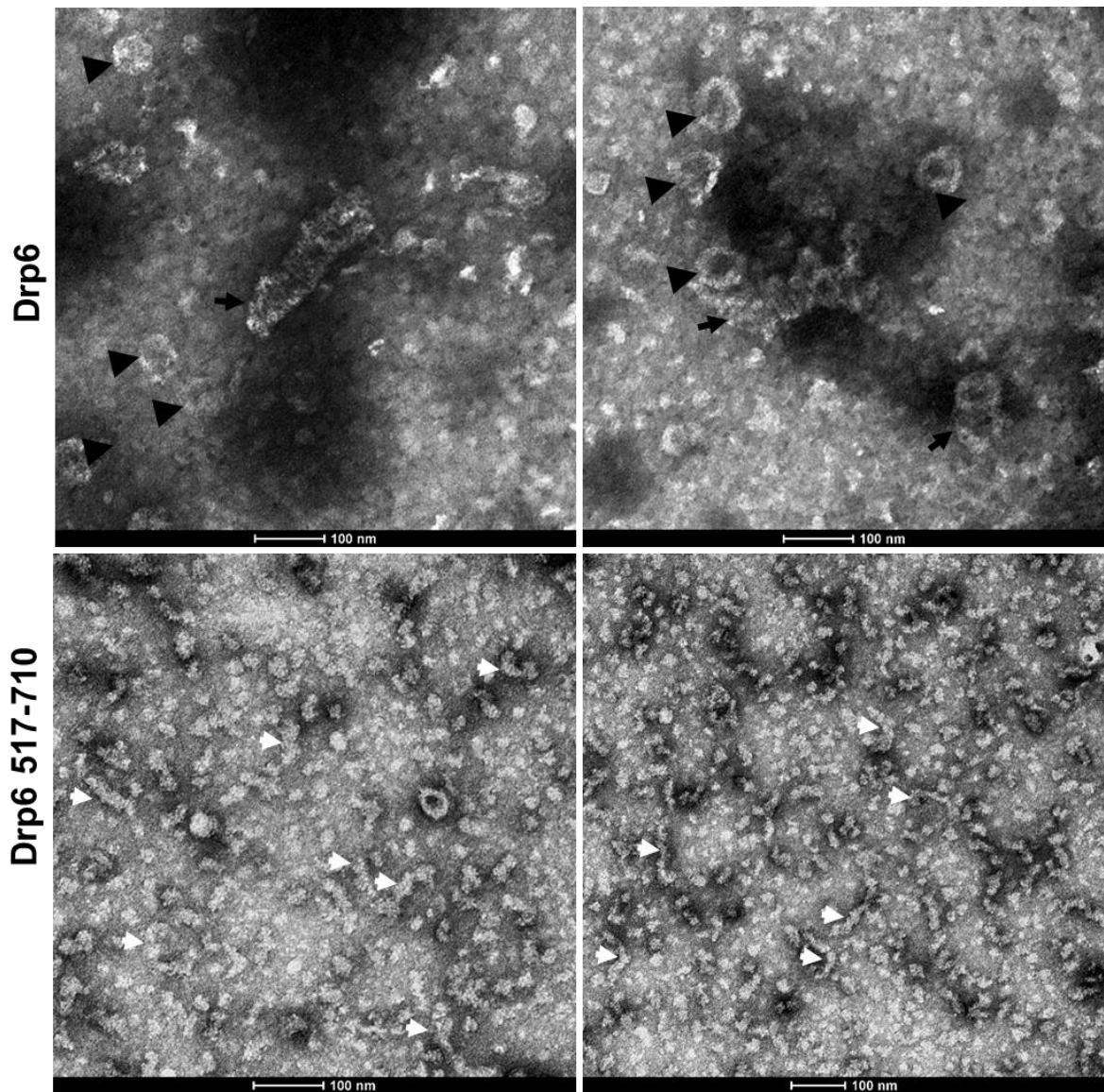
**Figure 4.3.1.1: Drp6 oligomerizes in absence of GD-MD.** (A) Coomassie stained SDS-PAGE gel showing purified His-Drp6 (left) and MBP-Drp6 $\Delta$ GD-MD (right). Molecular weights are indicated on the sides. Size exclusion chromatography of His-Drp6(B) and of Drp6 $\Delta$ GD-MD(C). (D) Western blot showing eluted fractions of Drp6 $\Delta$ GD-MD after size exclusion chromatography. Numbers indicate the elution volumes in ml. Positions of the molecular weight markers are indicated on left. A second peak around 16 ml in (C) does not contain the expected protein and may arise from some contaminating proteins from *E. coli*.

### **4.3.2 Drp6 $\Delta$ GD-MD self-assembles into helical rods**

Self-assembly to form rings and helical spiral is hall mark of all dynamin proteins, and is important for their function. Drp6 also self-assembles to form rings and helical spirals (246). To investigate if GD and MD are required for self-assembly of Drp6, the ultra-structure of MBP-Drp6 $\Delta$ GD-MD was studied by electron microscopy after negative staining. Electron microscopic analysis of Drp6 was also performed in parallel. As reported earlier, Drp6 forms both rings and helical rod/spiral structures (246). When electron micrographs of MBP-Drp6 $\Delta$ GD-MD were analysed, it was observed that it predominantly formed helical rod/spiral like structures (Fig.4.3.2.1). However, unlike wild type Drp6, the ring like structures if any were found only occasionally. These results suggest that GTPase domain and middle domain are dispensable for self-assembly. These results also suggest that GTPase domain and middle domain might play an important role in forming ring like structures.

### **4.3.3 GD and MD are important for nuclear recruitment of Drp6**

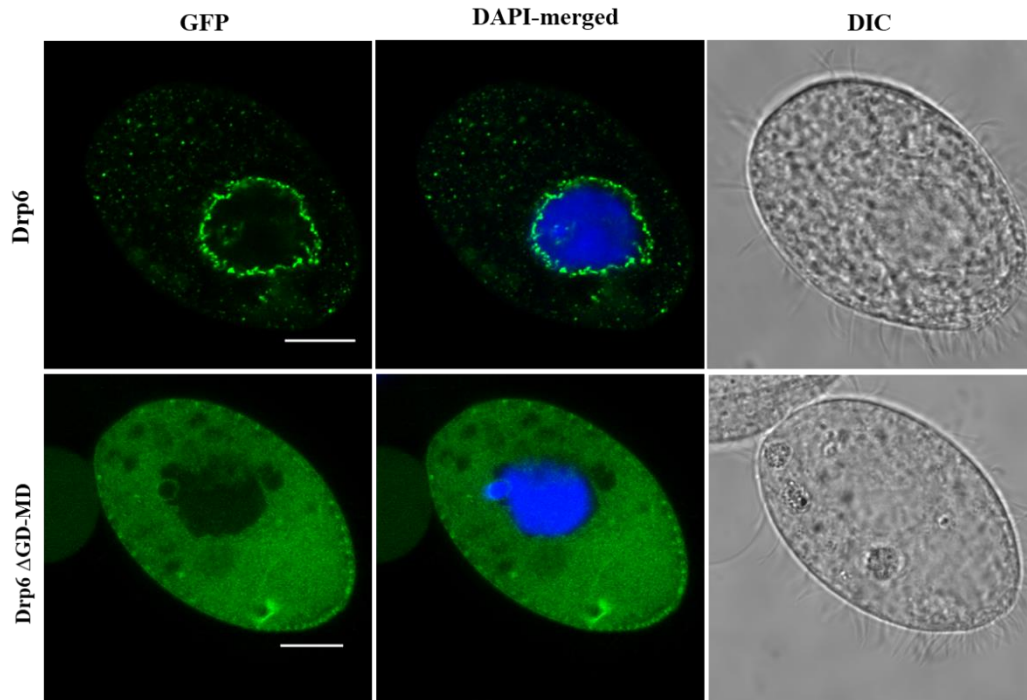
Localization to target membrane is essential for all the dynamin proteins known to function in membrane remodelling. Drp6 localizes on the nuclear envelope and is required for nuclear remodelling. Confocal images of GFP-Drp6 $\Delta$ GD-MD when analysed, does not show any detectable localization on the nuclear envelope and is almost exclusively present in the cytoplasm (Fig. 4.3.3.1) (also shown earlier in the laboratory by UP Kar). Therefore, it can be concluded that GD and MD are required for nuclear recruitment of Drp6.



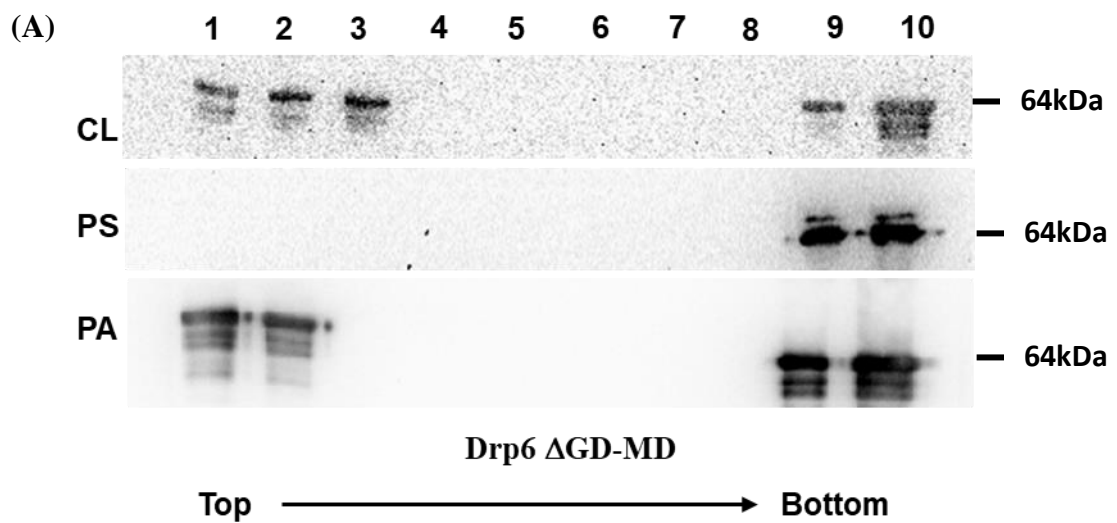
**Figure 4.3.2.1: Drp6 $\Delta$ GD-MD self-assembles to form helical rod like structures.** Electron micrograph showing self-assembled structures of purified recombinant Drp6 (top panel) and Drp6 $\Delta$ GD-MD (bottom panel). Drp6 $\Delta$ GD-MD fails to form helical spirals (arrow) or rings (arrow head) but forms helical rod like structures (white arrow).

#### **4.3.4 Loss of nuclear recruitment of Drp6 $\Delta$ GD-MD is not due to loss of cardiolipin interaction**

Proteins in dynamin family associate with lipids on the target membrane. It has been earlier shown that Drp6 interacts with three different phospholipids and interaction with cardiolipin is important for nuclear association of Drp6 (241). To evaluate if the loss of nuclear envelope localization of Drp6 $\Delta$ GD-MD is due to loss of its interaction with CL, membrane binding activity of Drp6 $\Delta$ GD-MD was assessed by liposome co-floatation assays using liposomes containing CL or PA or PS. Floatation assays were also performed with wild type Drp6 using these liposomes. As expected, wild type Drp6 interacted with all the three liposomes and appeared on the top fractions in the sucrose density gradient (Fig.4.3.4.1). While analysing the floatation assays with Drp6 $\Delta$ GD-MD, it was observed that it interacted with CL liposomes and PA liposomes but failed to interact with PS liposomes (Fig.4.3.4.1). Since *Tetrahymena* nuclear envelope lacks PS (Nozawa Y et al 1973), it can be concluded that loss of nuclear envelope localization of Drp6 $\Delta$ GD-MD is not due to defect in membrane binding. All these results indicate that GTPase domain and middle domain though is not essential for self-assembly, they are important for nuclear association, and the loss of nuclear envelope localization is not due to loss of membrane interaction.



**Figure 4.3.3.1: GFP-Drp6 $\Delta$ GD-MD fails to localize to the nuclear envelope.** Confocal images of fixed *Tetrahymena* cells expressing GFP-Drp6 (Drp6) or GFP-Drp6 $\Delta$ GD-MD (Drp6 $\Delta$ GD-MD) after DAPI staining. Bar=10 $\mu$ m



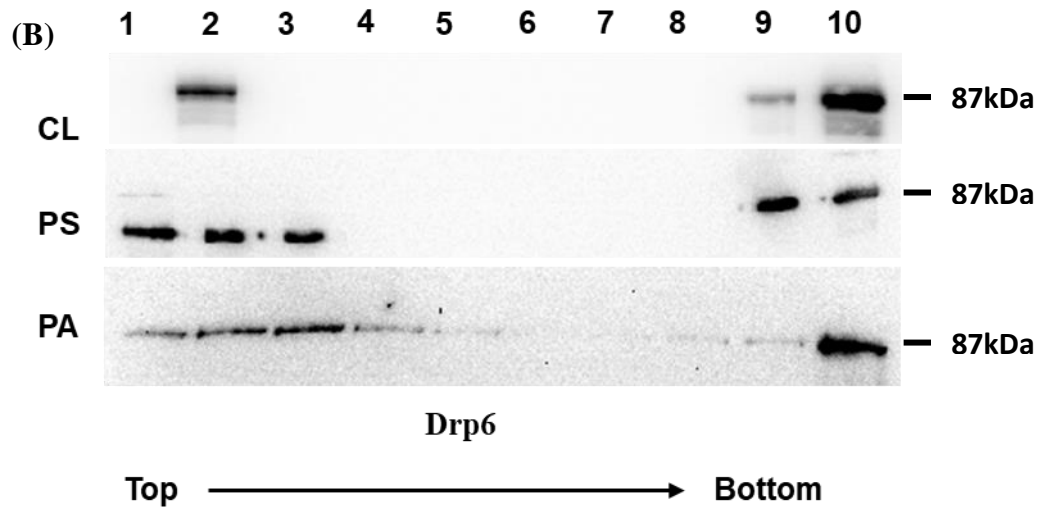


**Figure 4.3.4.1: Liposome co-floatation assay of MBP-Drp6  $\Delta$ GD-MD (A) or His-Drp6 (B) with liposomes containing PC/PE and additionally supplemented with either CL or PS or PA (indicated on the left). Western blot analysis of fractions collected from top to bottom as indicated below the figure. While anti-MBP monoclonal antibody was used in (A), anti-His monoclonal antibody was used in (B). Molecular weights are indicated alongside of the blots.**

#### 4.4 Discussion:

Members of the dynamin family proteins self-assemble on their target to perform functions. Drp6 undergoes cycles of assembly/dis-assembly on the nuclear membrane and regulates nuclear remodelling in *Tetrahymena* (230). The present study has analysed the role of the GTPase domain together with middle domain in the self-assembly of Drp6. The results show that Drp6 can self-assemble to form higher order oligomeric structure even in the absence of GTPase domain and middle domain. However, self-assembly is not sufficient to recruit

dynamamin to the nuclear membrane since the protein lacking GTPase and middle domains though formed self-assembled structure fails to associate with nuclear membrane.

The major objective of the present study was to investigate the importance of GTPase and middle domains in the self-assembly. The detailed structural studies in a number of dynamamin family proteins show presence of similar interface required for oligomerization and higher order self-assembled structure. The common properties of all the dynamamin proteins whose structures are known show participation of all the domains in the oligomerization and self-assembly. The middle domain becomes essential for self-assembly of endocytic dynamamins and also this domain plays important role in classical dynamamin Dyn1 and Dynamamin Related proteins like Drp1, Mgm1, MxA (40, 256, 262).

Unlike endocytic dynamamins, the middle domain along with GTPase domain is not essential for the formation of higher order structure of Drp6. This results implies that Drp6 may have interfaces different from endocytic dynamamin and other reported dynamamin related proteins or may have additional interfaces present in the protein lacking these two domains. In either case, these results strongly suggest that the interactions required for self-assembly are different in this group of proteins.

The localization and the function of dynamamins depend on their self-assembly on the target membrane. As for example, the mutation that affects self-assembly of dynamamin1 and dynamamin 2 also affects association with PtdIns(3,4,5)P3, PtdIns(3,4)P2, and PtdIns(4,5)P2 (50) and thereby its endocytic function. Similarly, interaction of Drp1 with cardiolipin via the B-insert region triggers its oligomerization (97). Another dynamamin related protein Mgm-1 functions in mitochondrial fusion also requires self-assembly for target membrane binding (Binding with PA, CL, and PS) and function (77). In the present study, it was evaluated if the GTPase and middle domains which are dispensable for self-assembly can associate with its target

membrane. The failure of Drp6 lacking these domains to associate with nuclear membrane suggest that self-assembly is not sufficient to bind its target membrane. It should be noted that the truncated Drp6 retains the membrane binding domain. Therefore, it appears that in addition to membrane binding domain and self-assembly property, Drp6 requires GTPase domain and middle domain for its recruitment to nuclear envelope. This is also true for other dynamins including CYTAtlastin (257) and Drp1 (60) which also need GTPase domain and middle domain for specific target membrane association. Although dimerization does not require membrane binding in case of dynamins, further assembly is dependent on its target membrane binding. Taking together, the present study reveals that Drp6 possesses interfaces for self-assembly different from other family members in which GTPase domain and middle domain are dispensable. It also suggests that membrane binding and self-assembly are not sufficient for nuclear recruitment of Drp6.

## *Chapter 5*

# *Mechanism of nuclear expansion by Drp6 and role of microtubule structure*

## 5.1 Introduction

Nuclear expansion is a universal phenomenon in all eukaryotes. Expansion of the nucleus occurs during the S-phase of cell cycle to accommodate the increasing genetic material in case of open mitosis and also post-mitosis in case of closed mitosis to equally distribute the nuclear content. In *Tetrahymena*, which undergoes closed mitosis, nuclear expansion is observed during vegetative as well as sexual phase of reproduction. Although, nuclear division during vegetative propagation involves nuclear expansion, a more pronounced effect is observed during the sexual reproduction. In particular, during MAC development stage of sexual conjugation, 2 of the 4 MICs expand 10-15 folds to form new MACs.

The nuclear membrane is a specialized extension of the ER, where several molecules can diffuse between the two compartments (170). Nuclear membrane expansion requires incorporation of new membranes to the pre-existing one. Studies have shown that control of nuclear envelope expansion is not limited by the cytosolic factors rather, it is controlled by membrane component surrounding the nucleus (263). Endoplasmic Reticulum (ER) is an endomembrane system distributed throughout the cell. It remains continuous with the nuclear membrane and hence it can be understood that nucleus is an extension of the ER. *In vitro* and *in vivo* experiments in *Xenopus* egg nuclei show that the nuclear envelope formation requires ER membranes. Specific proteins like reticulons residing in the ER which determine the ER structure are responsible for determining nuclear envelope formation as well. Proteins like Reticulon-3 and Reticulon-4 drive the formation of tubulated ER which inhibits NE formation while the other group of proteins like Climp63, p180 and kinectin drive the formation of sheet structures of ER. Inhibition of the tubulated ER enhances nuclear envelope development. These evidences show that ER is directly involved in the process of nuclear

membrane formation and expansion (264, 265). The ER which remains continuous with the nuclear envelope and surrounds the nucleus is termed as perinuclear ER (pER). The increase in the volume of nuclear envelope requires an increase in the volume of pER (263). The pER formation requires dynein mediated transport of membrane cargo to the rim of the developing pER which is essential for carrying out growth of membrane surface (266). Reconstitution experiments in mammalian nuclei using *Xenopus* egg extract show that microtubule are required for dynein to carry membrane cargo to develop the perinuclear ER membranes. Inhibition of either microtubule polymerization or dynein function leads to reduced nuclear expansion (266).

Drp6 in vegetatively growing *Tetrahymena* localizes on the nuclear envelope and associates with ER vesicles (230). During macronuclear development stage of conjugation, 2 out of 4 identical post-zygotic micronuclei expand to form new macronuclei. Drp6 exerts its functions during this macronuclear expansion stage (230). During the process of conjugation, Drp6 shows differential localization where it becomes localized in the cytoplasm during starvation and early conjugation and is recruited to the developing MAC during expansion (discussed in chapter 1). This chapter addressed the mechanism by which Drp6 brings about nuclear expansion and the role of microtubule and dynein in this process.

## 5.2 Materials and methods

### 5.2.1 Materials

- Monoclonal anti-tubulin antibody was purchased from Developmental Studies Hybridoma Bank (DSBH).
- Polyclonal anti-Drp6 antibody was custom synthesized by Imgenex
- Nocodazol, Ciliobrevin D and DMSO were purchased from Sigma Aldrich
- ER trancker green dye, DAPI and Alexa fluor-594 antibody were purchased from Invitrogen.

### 5.2.2 Methods

#### (A) Expression and purification of TAP-tagged Drp6

##### Expression of TAP-Drp6 in *Tetrahymena*:

*Tetrahymena* cells transformed with TAP-Drp6 pVGF were grown to a density of  $2.5 \times 10^5$  in 600ml SPP media containing antibiotic solution and 100  $\mu\text{g/ml}$  paromomycin sulfate in a wide bottom 3000ml Erlenmeyer flask at  $30^\circ\text{C}$ , 90rpm. The culture was induced with 2  $\mu\text{g/ml}$  cadmium for 5 hours under same growth conditions. The cells were harvested by pelleting at 1100g using sterile 250ml conical bottom centrifuge bottles. Cells were processed further for protein purification or stored at  $-80^\circ\text{C}$  for long term storage.

##### Purification of TAP-Drp6:

Expression was induced with 2 $\mu\text{g/ml}$  cadmium chloride for 5 hours at  $30^\circ\text{C}$ . Cells were collected by 1100g centrifugation for 4 min in a conical bottom centrifuge bottle. The cell pellet was resuspended in 10 ml lysis buffer (20 mM Tris-HCl (pH 8.00), 100 mM NaCl,

0.5% NP-40, 10% glycerol) supplemented with a mixture of protease inhibitor like aprotinin, pepstatin, E-64, PMSF and protease inhibitor cocktail(Roche). The lysate was cleared by ultracentrifugation at 250,000g for 1 hour using 70Ti rotor in a Beckman Coulter Optima L100K. All subsequent steps were carried out at 4°C unless mentioned otherwise. Rabbit-IgG agarose (Sigma-Aldrich) pre-equilibrated with wash buffer (20mM Tris-Cl p<sup>H</sup> 8.0, 2mM MgCl<sub>2</sub>, 0.2mM EGTA, 0.1M NaCl, 0.1% Tween20, 10% Glycerol, 1mM DTT, 0.1mM PMSF) was added to the clarified lysate and was kept for binding for 2 hours on a nutating mixer stand. Resin was collected by centrifugation at 3,000 g for 1 min and washed with 50 bed volumes of wash buffer. 2µl of TeV protease in 200 µL cleavage buffer (10 mM Tris-HCl pH 8.00, 0.1% Tween 20, 0.1 M NaCl, 1 mM DTT 0.5 mM EDTA,) was added to the resin and incubated for 1.5 hours at room temperature followed by overnight incubation at 4°C. The concentration of calcium chloride in the eluate was made to 3mM after proteolytic cleavage and mixed with 3 volumes of calmodulin binding buffer (10 mM Tris-HCl (pH 8.00), 1 mM Mg acetate, 100 mM NaCl, 2 mM CaCl<sub>2</sub>, 1 mM imidazole, , 0.1 % Tween 20, 10 mM βME). This was incubated with 100 µL of calmodulin resin (Sigma-Aldrich) at 4°C for 1 hour. The resin was recovered and washed with calmodulin binding buffer. Elution of the protein was carried out with calmodulin elution buffer (10 mM Tris-HCl (pH 8.00), and 1 mM Mg acetate, 100 mM NaCl, 1 mM imidazole, 0.1 % Tween 20, 10 mM EGTA, 10 mM βME). Eluted fractions were analysed on 10 % SDS polyacrylamide gel after silver staining.

### **(B) Microtubule destabilization using nocodazole**

To study the effect of microtubule destabilization on localization of Drp6, *Tetrahymena* cells expressing GFP-DRP6 were grown to a density of  $0.7 \times 10^5$  cells/ml and nocodazole (Sigma Aldrich) was added to 10µg/ml final concentration. For the control experiment DMSO without drug was used. The treatment was carried out for 1 hour at 30°C. GFP-Drp6 expression was

then induced with 0.5µg/ml of cadmium chloride for 4 hours. The cells were collected by centrifugation at 1100g for 2 min and fixed with 4% PFA for 20min at RT and imaged in a Zeiss LSM 780 confocal microscope.

For studying the effect on MAC expansion, the drug was added to the conjugating cells 7 hours post-mixing at same concentration as above. The cells were then collected at the end of 8 hours and fixed using 4% PFA. The cells were stained with DAPI and percent MAC development was measured after imaging.

### **(C) Dynein inhibition using Ciliobrevin D**

The procedure used for nocodazole treatment was followed to conduct the study with ciliobrevin D (Invitrogen). The concentration of ciliobrevin D used was 5µM.

### **(D) ER staining**

*Tetrahymena* cells expressing Drp6 or Drp6-K49A (induced with 1µg/ml cadmium chloride) were treated with 0.5µM of the ER tracker dye for 1 hour at 30°C. Cells were collected by centrifugation at 1100g and washed with SPP media twice to remove the excess stain. Cells were fixed using 4% PFA and imaged using Leica DMi8 confocal microscope.

### **(E) Expression of GFP-KDEL as an ER marker**

*Tetrahymena* cells expressing mCherry-Drp6 were transformed with GFP-KDEL in NCVB vector by biolistic transformation and the transformants were selected using 60µg/ml Blasticidine S hydrochloride (Sigma Aldrich) in presence of 1µg/ml cadmium chloride. The co-transformants harboring both mCherry-Drp6 and GFP-KDEL was grown in SPP without drug to a density of  $2 \times 10^5$  cells /ml and induced with 0.5µg/ml cadmium chloride for 4 hours

before imaging. For microtubule inhibition, the induced cells were treated with nocodazole (10 $\mu$ g/ml) post 3 hour of cadmium induction for 1 hour.

### 5.3 Results:

#### 5.3.1 Drp6 interacts with microtubule and dynein

Drp6 localizes to the nuclear envelope and also to ER vesicles. In live cell imaging, Drp6 also shows distribution that resembles microtubular network (Fig.5.3.1.1). The similarity of Drp6 distribution with the microtubular network strongly suggested association of Drp6 with microtubules.

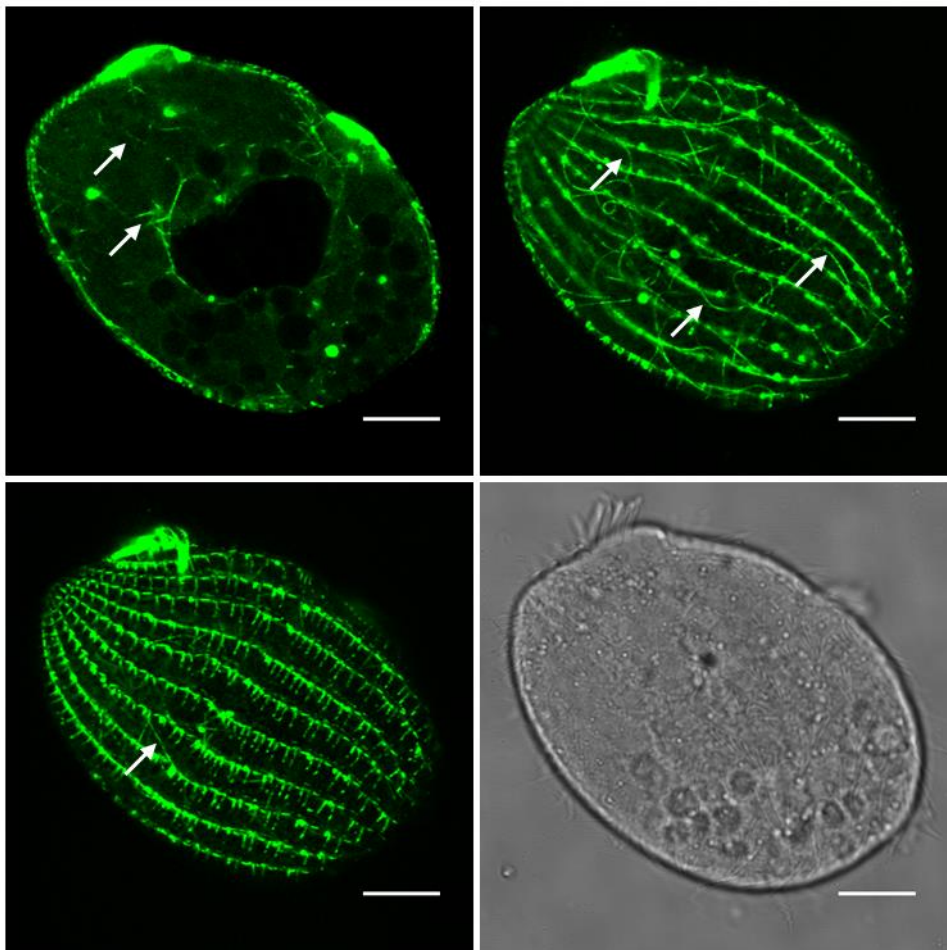


**Figure 5.3.1.1: Confocal images of a live *Tetrahymena* cell expressing GFP-Drp6.** Drp6 shows distribution that resembles microtubule network. Upper left image shows middle section, upper right (3-D projection) and lower left images show cortical region. Lower right is DIC image of the cell. Bar= 10 $\mu$ m. Arrows indicate the microtubule network-like distribution of Drp6.

To determine if Drp6 interacts with microtubule, TAP-tagged Drp6 was expressed and purified from *Tetrahymena*. Western blot analysis of the TAP-tag purified protein was performed where, anti-tubulin antibody was used to detect presence of tubulin in the purified Drp6. As shown in the Fig.5.3.1.2, the presence of tubulin in the purified Drp6 solution suggests interaction between them. To further confirm this interaction, TAP-tag purified Drp6 were subjected to Tandem-MS spectroscopic analysis. The results showed tubulin and Dynein Heavy Chain 7 (DYH7) as interacting proteins among many other proteins. These results lead to the conclusion that Drp6 can interact with the cytoskeletal elements like microtubule and dynein.

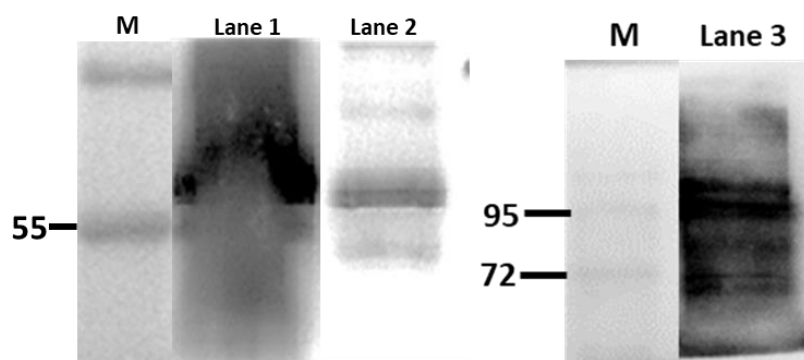


**Figure 5.3.1.2: Drp6 interacts with tubulin.** The total cell lysate (lane 1) along with purified fraction of TAP-Drp6 (lane 2) was analysed by western blotting using anti-tubulin monoclonal antibody (left panel). The right shows TAP-Drp6 protein in the purified fraction

as detected using anti-Drp6 polyclonal antibody. Molecular marker (M) weights are indicated on the left of each panel.

### **5.3.2 Interaction with microtubule and Dynein is important for nuclear envelope localization of Drp6**

To determine the role of Drp6 interaction with microtubule and dynein, GFP-Drp6 was expressed in *Tetrahymena* under conditions that destabilize microtubule (treatment with nocodazole) or that inhibit cytoplasmic dynein function (treatment with ciliobrevin D) and compared with that of untreated control cells. Localization was assessed by confocal microscopy. As expected, Drp6-GFP predominantly localized in the nuclear envelope with some cytoplasmic puncta. Both perturbation of microtubule structure and inhibition of dynein function resulted in the loss of nuclear envelope localization of Drp6 in majority of the cells. While 75% of the untreated cells had nuclear envelope localization of Drp6, only 33% of nocodazole treated cells and 42% of ciliobrevin treated cells showed nuclear envelope localization (Fig.5.3.2.1). Therefore, it can be concluded that microtubule and cytoplasmic dynein are required for nuclear association of Drp6.

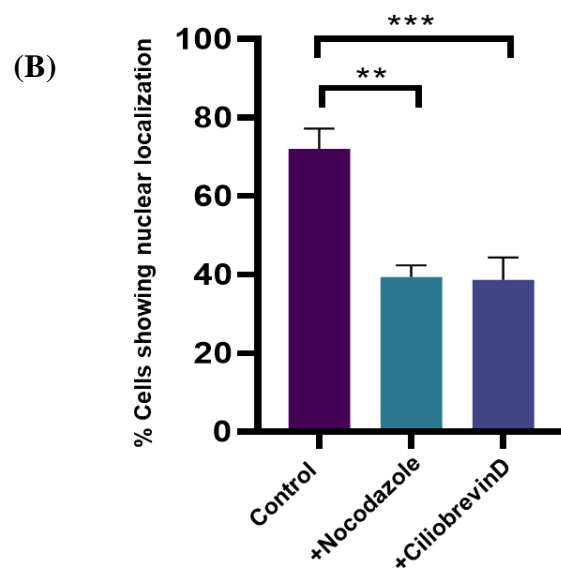
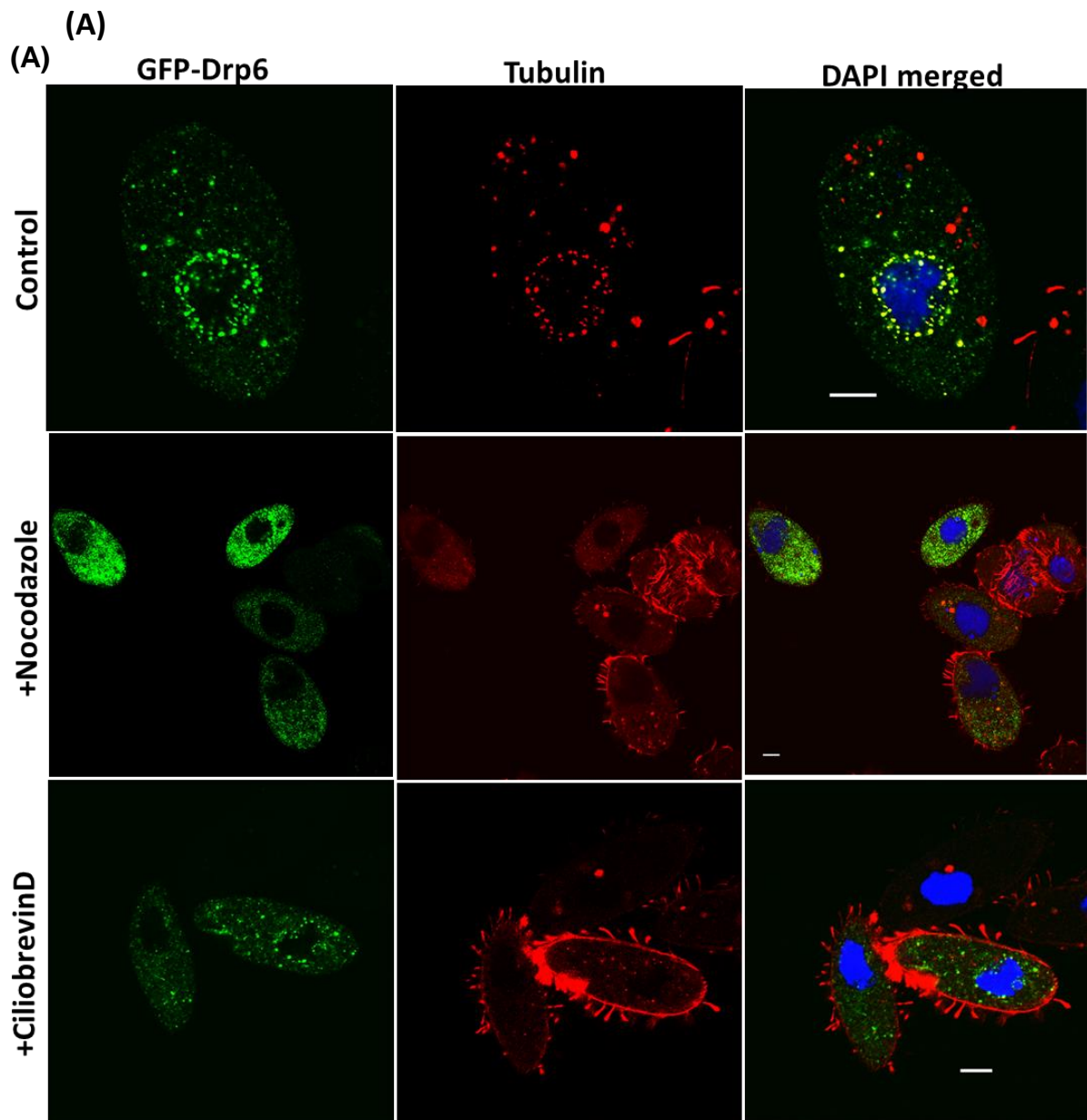
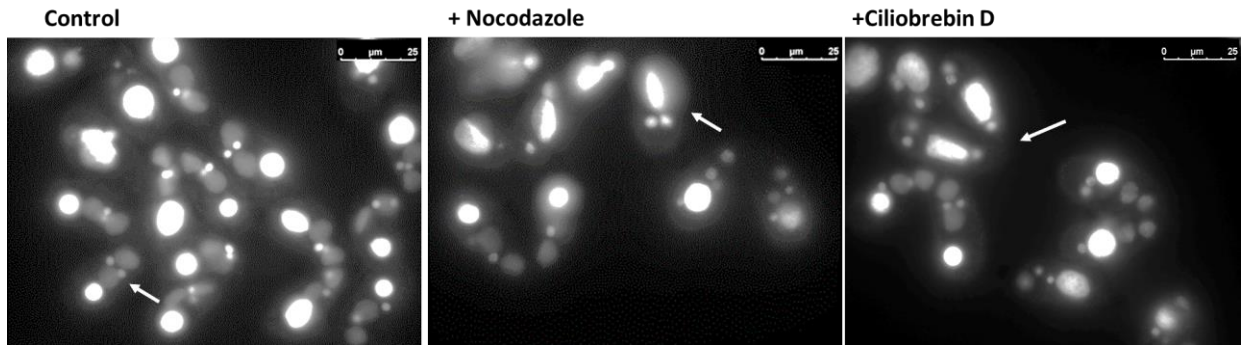


**Figure 5.3.2.1: Nuclear envelope localization of Drp6 depends on microtubule structure and dynein function.** (A) Confocal images of fixed *Tetrahymena* cells expressing GFP-Drp6 treated with nocodazole or ciliobrevin D as indicated. Control cells were treated with DMSO without any drug. Immunostaining with anti-tubulin monoclonal antibody was performed before imaging. Bar = 10µm. (B) Graph showing quantitation of cells showing nuclear envelope localization of GFP-Drp6 in absence of any drug (control) or in presence of nocodazole (+Nocodazole) or in presence of ciliobrevin D (+Ciliobrevin D) more than 300 cells at least were counted. GraphPad Prism 8.0 was used for statistical analysis. \*\* indicates P=0.0017, \*\*\* indicates P= 0.0007.

### **5.3.3 Interaction with microtubule and Dynein is required for macronuclear development**

Drp6 is involved in macronuclear expansion and its localization to nuclear envelope is dependent on microtubule structure and dynein function. To evaluate if microtubule and dynein are also important for MAC development, the conjugated pairs were either treated with nocodazole or ciliobrevin along with the control where no drug was added. Quantitation of new macronuclei development at 8h post conjugation showed that while 75% of the untreated pairs showed macronuclear expansion, around 8% of the nocodazole treated pairs exhibited MAC development. The analysis of ciliobrevin treated pairs also showed inhibition of MAC development (27% pairs had macronuclear expansion) (Fig.5.3.3.1). These results suggest that both microtubule structure and dynein function are important for MAC expansion. Since Drp6 interacts with microtubule and is also required for MAC development, it can be inferred that Drp6 is recruited to the nuclear envelope by interacting with microtubule and dynein during macronuclear expansion.

(A)



(B)

(B)

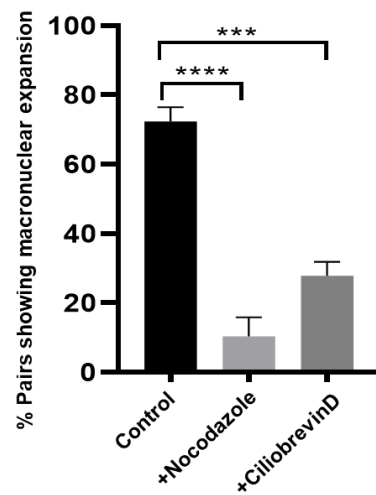


**Figure 5.3.3.1: MAC development depends on microtubule structure and dynein function.** Confocal images showing fixed and DAPI stained conjugating *Tetrahymena* cells at 8<sup>th</sup> hour post mixing in absence of any inhibitor (control) or in presence of nocodazole (+Nocodazole) or in presence ciliobrevin D (+Ciliobrevin D). Arrows indicate the expanding macronucleus (B) Graph shows quantitation of the above results, n=500. GraphPad Prism 8.0 was used for statistical analysis. \*\*\* indicates P= 0.0002, \*\*\*\* indicates P= <0.0001.

### 5.3.4 Perinuclear ER network depends on Drp6 function and microtubule structure

Developing of the perinuclear ER is essential for nuclear expansion (263) and requires addition of new membranes. However, the exact mechanism of ER network formation around the nucleus and the source of vesicles are not known in any organism. Moreover, how microtubule structure and dynein regulate perinuclear ER network and thereby nuclear expansion *in vivo* is not known. In earlier study it was shown that Drp6 regulates nuclear expansion in *Tetrahymena*. To understand the mechanism of nuclear expansion, the role of Drp6 on ER network was evaluated. For this purpose, the dominant negative allele of Drp6 (Drp6-K49A) was expressed to inhibit Drp6 function and the ER network was compared with that of wildtype cells after staining with ER tracker green. The results showed presence of extensive ER network around the nucleus in wildtype cells. However, the ER network was significantly reduced in the cells expressing Drp6-K49A (Fig. 5.3.4.1) suggesting that Drp6 is required for perinuclear ER network formation.

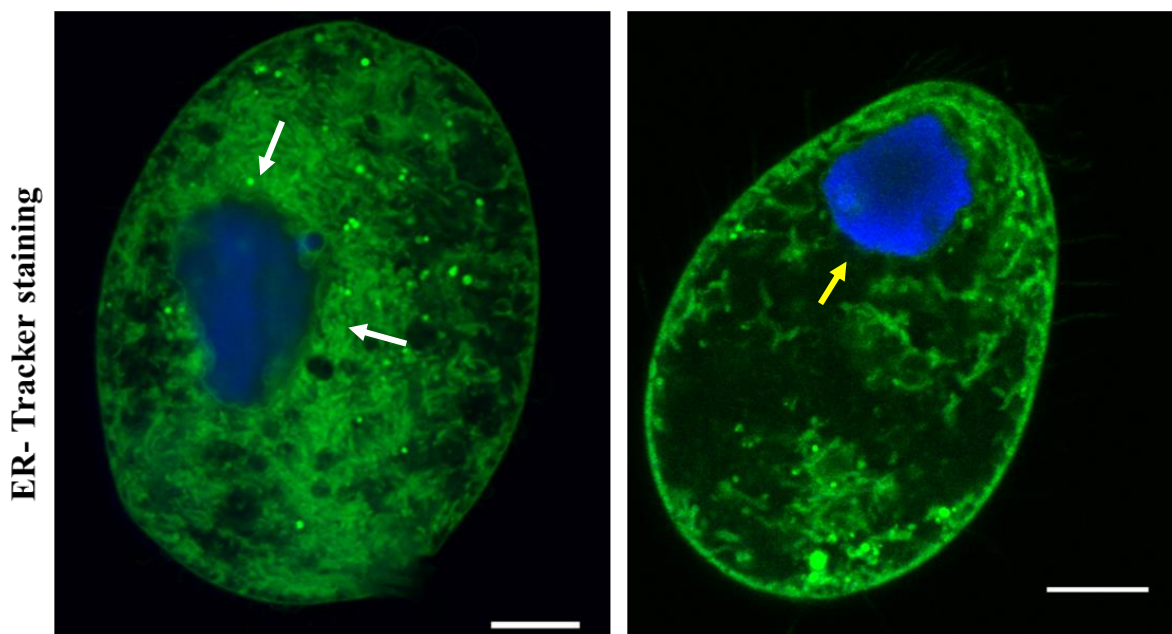
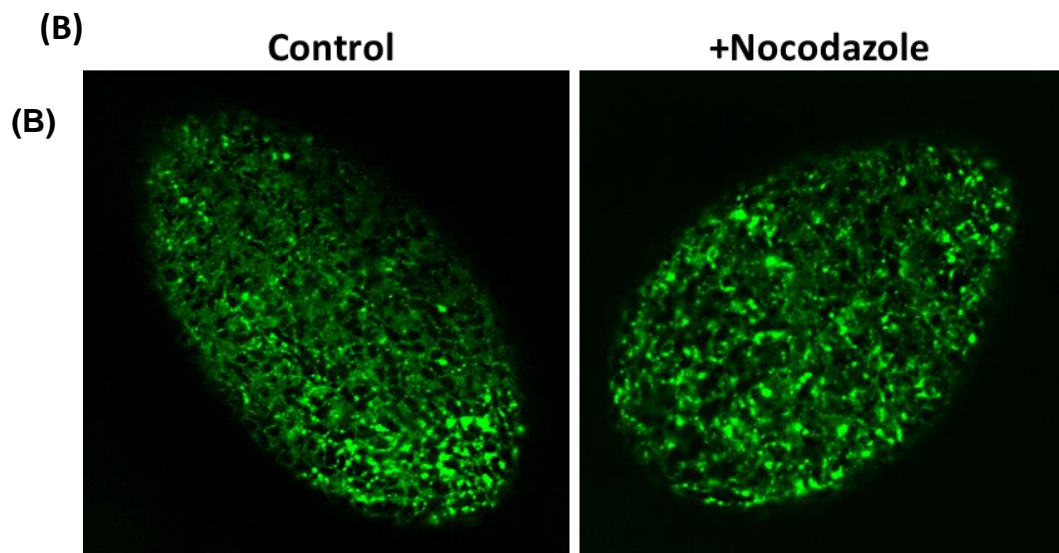
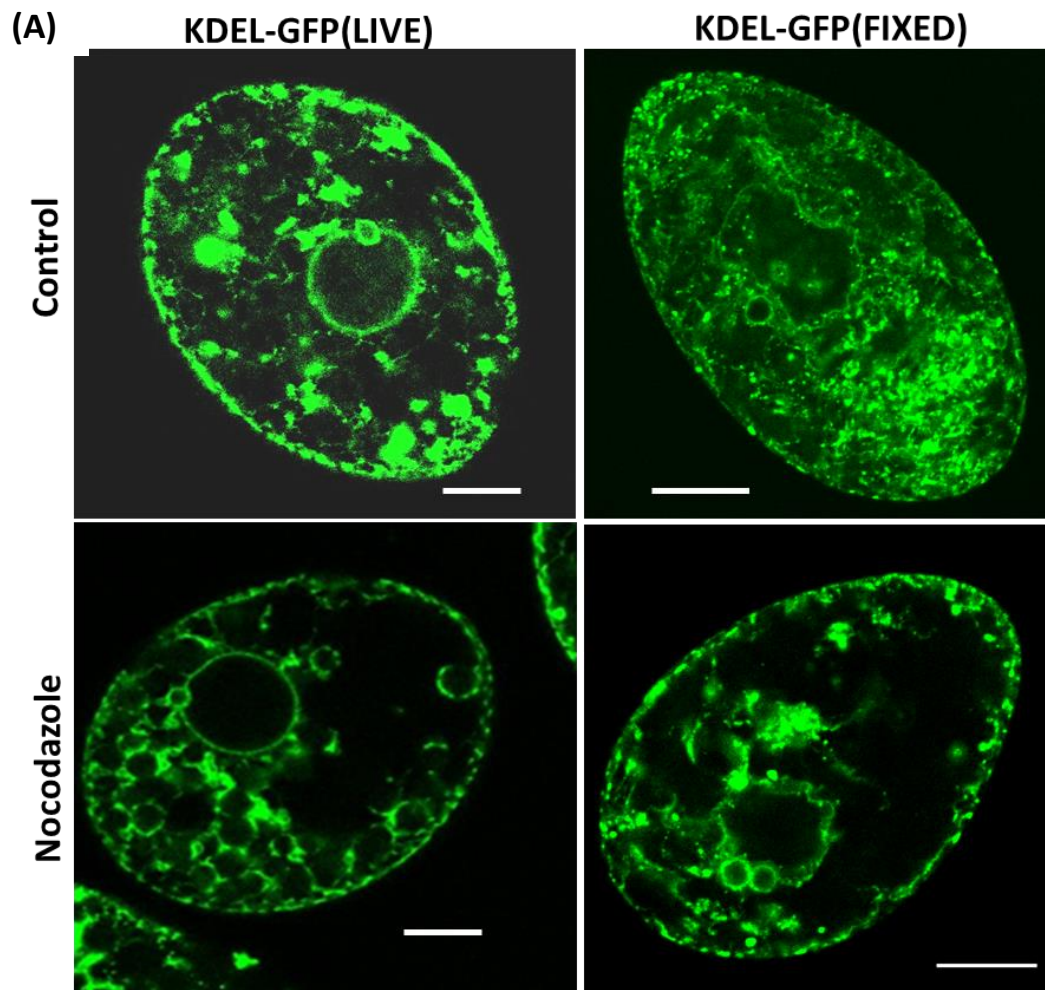


**Figure 5.3.4.1: Inhibition of Drp6 function inhibits perinuclear ER network formation.**

Confocal images of fixed wildtype *Tetrahymena* cell (left) or *Tetrahymena* cell expressing

Drp6-K49A (right) after staining with ER tracker green to label the ER and DAPI to mark the nucleus. White arrows show the Er around nucleus. Yellow arrow shows reduced ER around nucleus. Bar = 10 $\mu$ m

Nuclear expansion in mammals requires microtubule guided delivery of vesicle cargo by dynein around the expanding nucleus (266). To understand how the ER distribution around the nucleus is affected by microtubule, nocodazole treatment was performed on *Tetrahymena* cells expressing GFP-KDEL (a GFP tagged ER marker) to visualise the ER distribution. Confocal imaging showed that destabilization of microtubule structure disrupts the ER network around the nucleus (Fig.5.3.4.2A,C). This inhibition does not affect the peripheral distribution of ER (Fig.5.3.4.2B). This suggests that the ER network formation around nucleus requires microtubule network.



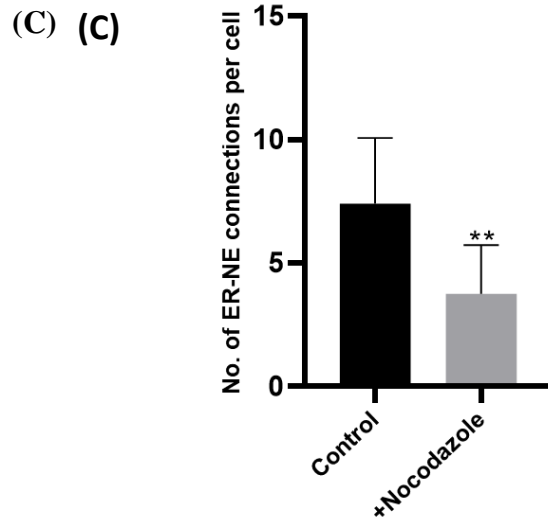


**Figure 5.3.4.2: Perturbation of microtubule structure inhibits perinuclear ER network.**

(A) Confocal images showing *Tetrahymena* cells expressing GFP-KDEL either in absence (top panel) or presence (bottom panel) of nocodazole. Distribution of peripheral ER is shown in (B) Bar = 10 $\mu$ m. (C) Graph shows quantitation of connections of ER connections with nuclear envelope either in absence (control) (n=30) or presence of nocodazole (+Nocodazole) n=40. \*\* indicates P value = 0.0017. ER-NE connections were counted manually from the middle section images of the cells.

**5.4 Discussion**

Nuclear expansion is a universal phenomenon in all eukaryotes. Studies in the mammalian nucleus have identified the role of cytoskeletal elements i.e. microtubule and dynein in this process. Nuclear envelope being a continuous extension of the ER depends on structure and volume of ER for its expansion. Drp6 which localizes on the nuclear envelope also associates with the ER vesicles in the cytoplasm (230) and live cell imaging shows that these dynamic cytoplasmic ER vesicles are capable of associating with the nuclear envelope. The findings in these study show that Drp6 interacts with microtubule and a cytoplasmic dynein. Perturbation of this interaction affects the nuclear envelope localization of Drp6 as well as the nuclear

expansion implying that translocation of Drp6 to the nuclear envelope is mediated by microtubule guided dynein. Nuclear envelope development during expansion requires increase in the membrane surface area which can be achieved by recruitment of new membrane components to the existing one. From recent studies, it is well-founded that ER contributes directly towards nuclear membrane growth however those studies do not identify any specific factor which catalyzes this process. Our studies show that ER network development around nucleus requires microtubules. The depolymerization of microtubules shows fewer connections of ER around the nucleus which means that microtubule association allows network formation by ER. A similar phenotype is observed in the ER distribution in *Tetrahymena* cell expressing a dominant negative mutant Drp6-K49A. Taken together these results suggest that Drp6 performs nuclear expansion by catalyzing microtubule guided transport of ER vesicles (membrane cargo) through dynein association. These vesicles might be essential for expanding the perinuclear ER network. Drp6 at the nuclear envelope might be responsible for establishing ER-NE membrane contact sites around the nucleus during nuclear membrane expansion.

## *Chapter 6*

# ***SUMMARY AND CONCLUSION***

## 6.1 Summary

Cell organelles undergo constant structural changes through remodeling of their membranes to carry out essential physiological processes. This is brought about by changes in their membrane curvature which is regulated by proteins. One such class of membrane remodeling proteins is known as dynamin superfamily. Dynamins are large mechanochemical GTPases which remodel their target membranes in a GTP-dependent manner (26). Based on their domain architecture, these enzymes are categorized as classical dynamins and dynamin related proteins (Drps). While the classical dynamins have a 5-domain organization, consisting of GTPase domain (GD), middle domain (MD), pleckstrin homology (PH) domain, GTPase effector domain (GED) and proline rich domain (PRD), the Drps lack the PH domain and PRD. Classical dynamins perform endocytic functions (102, 103) while the Drps are involved in maintenance of cell organelles, antiviral resistance, and cytokinesis (26). These proteins are present across the eukaryotic and prokaryotic systems, wherein, they perform a diverse array of functions. Although these proteins perform diverse functions, their underlying mechanisms are similar and is powered by self-assembly activated GTP hydrolysis (39).

*Tetrahymena thermophila*, a unicellular eukaryote, has a complex endomembrane organization which is evident from the presence of a large number of Rabs and Drps. *Tetrahymena* possesses eight Drps, of which, Drp3, 4, 5 and 6 form a separate clade indicating that these proteins evolved to perform specialized functions in *Tetrahymena* (229). Drp6, one of these specialized dynamins, has evolved to function during nuclear expansion in *Tetrahymena*. It localizes mainly on the nuclear envelope and ER derived vesicles (230). *Tetrahymena* shows nuclear dualism where a MIC is a germline nucleus and remains

transcriptionally silent in most of the cell- cycle stages and MAC is a phenotypically active somatic nucleus. Drp6 performs an essential role in nuclear differentiation (230), where micronucleus expands 10-15 times to develop into macronucleus to accommodate the increased ploidy. Drp6 shows a cell-cycle stage specific localization. This nuclear localizing dynamin starts falling off from the nucleus to become cytoplasm- localized during starvation and re-recruits to the newly developing MAC (230). The mechanism by which stage-specific localization and function of Drp6 are determined remains unknown. The study in this thesis addressed the mechanisms of Drp6 function and its nuclear recruitment. This thesis also addresses the role of post-translational modification in the regulation of its localization and function.

Generally, proteins in the dynamin family are regulated by many PTMs. These modifications allow addition of groups at particular sites on the protein which bring about changes in the biochemical properties of the protein including self-assembly, GTPase activity, localization etc. (187). Drp6 undergoes phosphorylation at 4 serine residues (S86, S248, S701, S705) and ubiquitination at 6 lysine residues. Phosphorylation at S248 reduces its GTPase activity by about 2-fold. Dynamins are self-assembly stimulated GTPases (26, 39). However, reduction in the GTPase activity of Drp6 in presence of phosphorylation does not arise from a defective self-assembly, since the size-exclusion chromatography profile of the phosphomimic (Drp6-S248D) is similar to that of unphosphorylated Drp6. Target membrane binding of dynamins require recognition of a specific lipid on the membrane. Drp6 interacts with three lipids namely PS, PA and CL (241). Of these, interaction with CL is specifically essential for its localization to nuclear envelope (241). Localization studies of the phosphomimic, S248D and phosphomutant, S248A show that presence of phosphorylation at S248 enhances the nuclear envelope localization of Drp6. The liposome co-floatation assays suggest that phosphorylation at S248 enhances the binding of Drp6 specifically towards CL containing

liposomes without affecting its affinity towards PA or PS containing liposomes. Since CL interaction of Drp6 determines its localization to nuclear envelope, enrichment of Drp6 at the nuclear envelope in presence of phosphorylation and its higher affinity to CL together imply that phosphorylation enhances localization of Drp6 at nuclear envelope by enhancing its CL binding affinity. The liposome tubulation assays revealed that similar to wildtype Drp6, Drp6-S248D also tethers CL liposomes. Apart from the tethering activity, Drp6-S248D can extensively tubulate the liposomes into network like structures having 3 or more connections. Analysis of the ultra-structure of Drp6 and Drp6-S248D shows that Drp6-S248D stabilizes ring like structures as compared to Drp6. Examination of membrane fusion function showed that Drp6 is a fusion dynamin and phosphorylation at S248 inhibits the fusion activity by inhibiting GTPase activity. The results together suggest that the enhanced binding of Drp6 to CL and extensive tubulation in presence of phosphorylation at S248 occurs by stabilizing the ring-like structures. These results also suggest that Drp6 performs nuclear expansion by membrane fusion and is regulated by phosphorylation at S248.

In addition to nuclear envelope, Drp6 also localizes to ER vesicles in the cytoplasm and to the plasma membrane. It binds to three lipids namely, PS, PA and CL (241). Drp6 requires cardiolipin binding for its localization to the nuclear envelope (241). As in case of other members of the dynamin superfamily, Drp6 also contains a lipid binding domain (DTD) which is mapped within 517-600 amino acids. This domain alone is sufficient to bind to the three above mentioned lipids but is insufficient for nuclear envelope localization (241). A specific residue I553, which resides within a hydrophobic patch (IMI) is essential for CL binding of Drp6. Mutational analysis at this position (I553M and I553A) shows that loss of CL binding of Drp6 occurs due to the absence of isoleucine at this position which emphasizes the role of isoleucine at 553<sup>rd</sup> position in recognition and binding to CL. Since the absence of isoleucine at this position did not affect binding of Drp6 to PA and PS, I553<sup>rd</sup> residue

specifically determines binding of Drp6 with CL. Analysis of the biochemical properties like self-assembly and GTPase activity of these mutants (Drp6-I553M and Drp6-I553A) shows that the mutations do not change self-assembly and GTP hydrolysis activity of Drp6. Analysis of the conformation by measuring intrinsic tryptophan fluorescence show that loss of CL binding due to loss of isoleucine is not a result of change in the Drp6 conformation. CD-spectroscopy analysis of the secondary structure of Drp6 and the mutants did not show any defect in secondary structure content and overall folding. Quenching experiments performed to analyze the local conformation changes due to mutation show quenching constants comparable to the wildtype Drp6. Since there were no significant changes observed in conformation of Drp6 due to mutation at I553, it suggests that loss of CL binding due to mutation does not arise from conformational changes in the protein. These results in turn suggest that a direct interaction with isoleucine determines CL binding specificity and nuclear association of Drp6. To understand the role of the residues in the vicinity of I553 in CL binding and nuclear targeting of Drp6, the residues E552 and M554 were mutated. These mutations did not affect the CL binding or nuclear envelope localization of Drp6. Taken together these results suggest importance of a single isoleucine in Drp6 binding specificity with CL and thereby its recruitment to the nuclear envelope.

Self-assembly of dynamins into higher-ordered structures is a pre-requisite for translocation to their target membranes. The formation of these oligomers occurs through fairly conserved interfaces across the family members. These interfaces reside mostly in the stalk domain of dynamins which is composed of the MD and GED. Although the stalk domain interactions orchestrate the tetramerization and further assembly, other domains are also required for formation of the functional structures like rings and helical spirals. In addition to these interfaces, G-domain interactions mediate dimerization. To study the dependence of Drp6 on its GD and MD for self-assembly, Drp6 $\Delta$ GD-MD was subjected to size exclusion

chromatography. The results showed that Drp6 can self-assemble into higher-ordered structures even in absence of GD and MD. Dynamins arrange themselves into rings and helical-spirals to execute their function. The study of the ultra-structure of Drp6 $\Delta$ GD-MD show that although Drp6 can form higher-order structures without GD and MD, it cannot form helical-spirals and rings. This mutant could form only short rod-like structures suggesting that formation of the functional structures required GD and MD. Localization to the nuclear envelope requires Drp6 to interact with CL (241). Since absence of GD and MD abrogates the nuclear envelope localization of Drp6, CL binding property of Drp6 $\Delta$ GD-MD was carried out to examine if the loss of nuclear envelope localization is due to defect in CL binding. Surprisingly, the Drp6 lacking GD and MD interacts with CL suggesting that CL binding though essential is not sufficient for nuclear recruitment. Since the mutant does not form rings and helical spirals but can self-assemble into rods, it can be suggested that in addition to CL binding and self-assembly, the higher order self-assembly into rings and/or helical spirals are required for nuclear association of Drp6. Since Drp6 shows localization at the plasma membrane which is enriched in PS and Drp6 $\Delta$ GD-MD fails to interact with PS, it would be interesting to investigate if interaction with PS determines recruitment to the plasma membrane.

To perform nuclear expansion function, Drp6 needs to translocate from the cytoplasm to the nuclear envelope of the developing MAC. Drp6 associates with microtubule and cytoplasmic dynein DHY7. Perturbation of microtubule structure and dynein function leads to loss of nuclear recruitment and nuclear expansion. These observations suggest that microtubule and dynein are required for localizing Drp6 to the nuclear envelope. Reconstitution experiments performed in mammalian systems reported that the process of nuclear expansion required development of the perinuclear ER (263). The accumulation of the ER network around the

developing nuclear membrane requires carrying of vesicle towards the nucleus by microtubule directed dynein (266). Our results suggest that nuclear expansion in *Tetrahymena* too requires ER accumulation around the nucleus. This process as suggested by inhibition studies, requires microtubules. De-polymerization of microtubules leads to reduced ER-NE connections. Drp6 associates with ER vesicles in the cytoplasm which moves towards and associate with the nuclear envelope (230). From the results of the present study, it can be proposed that the nuclear membrane expansion, which requires addition of new membranes to the pre-existing one, is carried out by promoting ER-NE junctions. Further, it can be suggested from the experimental evidences presented in this study that the process of nuclear expansion requires Drp6 associated ER related vesicles to be guided to NE via dynein-microtubule mediated transport.

## **6.2 Conclusion:**

In this thesis, we attempted to study the mechanism of Drp6 function and its nuclear recruitment along with regulation by post-translation modification. Based on the results, we put forward a model for the mechanism by which Drp6 translocate to the NE and mediates nuclear expansion in *Tetrahymena*. We propose that Drp6 performs nuclear expansion by membrane fusion activity. Localization of Drp6 is determined by the lipid it binds to. Binding to CL allows Drp6 to translocate to the NE. This specificity for CL is conferred by direct interaction of Drp6 with CL through a critical isoleucine residue which resides in the lipid binding domain of Drp6. Phosphorylation at S248 in the GTPase domain regulates the activity of Drp6 at NE by regulating its CL binding affinity and GTPase activity. The process of nuclear expansion requires Drp6 to carry cytoplasmic ER related vesicles towards the nucleus by its interaction with microtubule and dynein (Fig. 6.2.1). Accumulation of these vesicles around the NE might be responsible for developing the perinuclear ER connections

required for nuclear expansion. The phosphorylation enhances the membrane fusion activity of Drp6 by enhancing its binding with CL. This allows extensive tubulation of the underlying membranes.

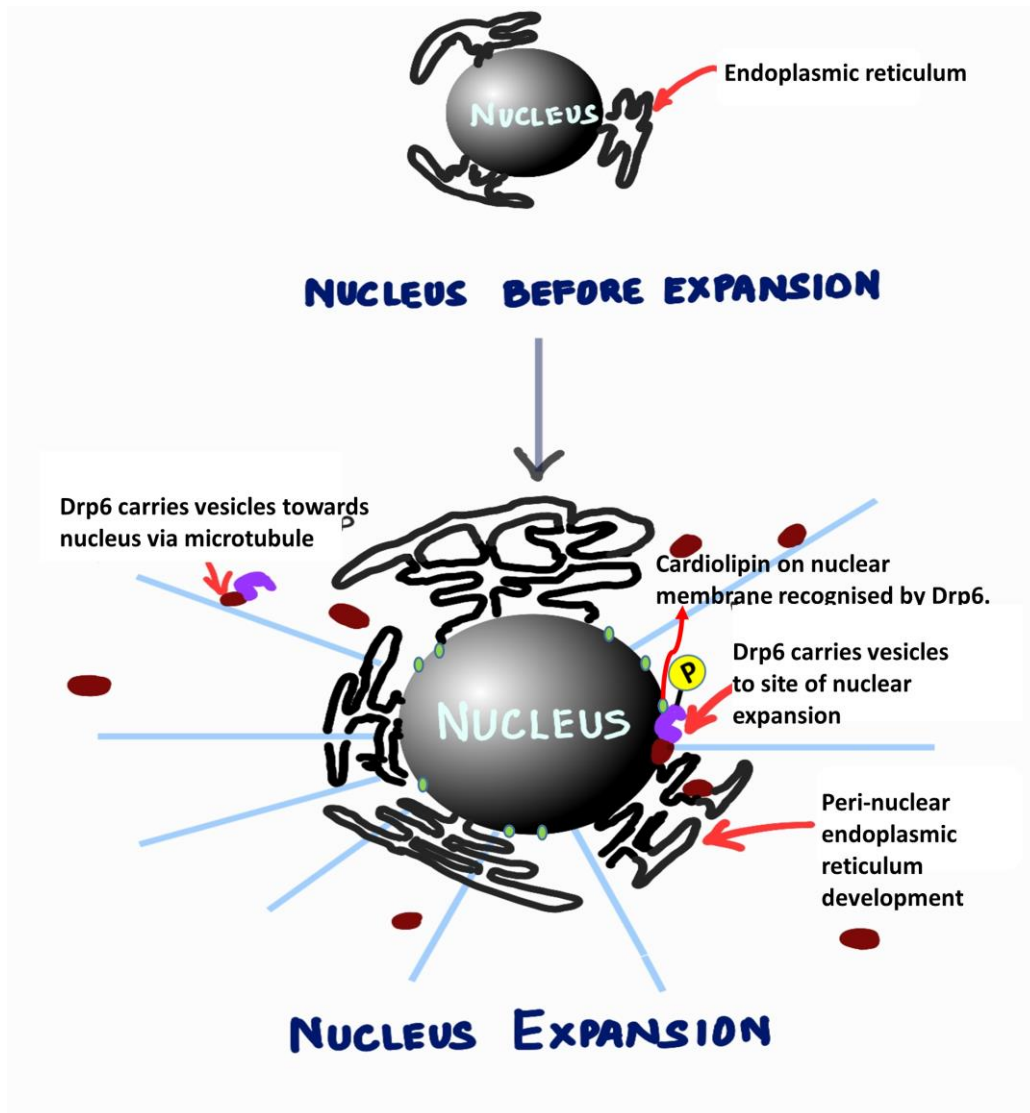


**Figure 6.2.1: Proposed model for mechanism of nuclear expansion by Drp6.** The diagram shows Drp6 (purple) might associate with the ER vesicles (brown) and transport them to the nuclear envelope through microtubule (blue) interaction to facilitate nuclear expansion. It recognizes and associates with cardiolipin (green) on the nuclear envelope to transport vesicles at the site of nuclear expansion to develop the peri-nuclear ER network (black). We propose that the phosphorylation at Ser248 (yellow) of Drp6 might be required at this stage.

As seen by liposome tubulation assay, the membranes are tubulated to form network like structures with 3 or more connections that resemble ER. This enhanced tubulation activity can be attributed to the formation of more stable ring-like structure in presence of the phosphorylation. Since this phosphorylation reduces the GTPase activity of Drp6, it is possible that the formation of stable ring-like structures requires reduced GTPase activity leading to enhanced membrane tubulation and fusion which in turn regulates nuclear expansion.



# *BIBLIOGRAPHY*

## BIBLIOGRAPHY

1. Mim C, Unger VM. Membrane curvature and its generation by BAR proteins. *Trends Biochem Sci.* 2012;37(12):526-33.
2. Ferguson SM, De Camilli P. Dynamin, a membrane-remodelling GTPase. *Nat Rev Mol Cell Biol.* 2012;13(2):75-88.
3. Stachowiak JC, Schmid EM, Ryan CJ, Ann HS, Sasaki DY, Sherman MB, et al. Membrane bending by protein-protein crowding. *Nat Cell Biol.* 2012;14(9):944-9.
4. Campelo F, McMahon HT, Kozlov MM. The hydrophobic insertion mechanism of membrane curvature generation by proteins. *Biophys J.* 2008;95(5):2325-39.
5. McMahon HT, Boucrot E. Membrane curvature at a glance. *J Cell Sci.* 2015;128(6):1065-70.
6. Drin G, Bigay J, Antony B. [Regulation of vesicular transport by membrane curvature]. *Med Sci (Paris).* 2009;25(5):483-8.
7. Rao Y, Haucke V. Membrane shaping by the Bin/amphiphysin/Rvs (BAR) domain protein superfamily. *Cell Mol Life Sci.* 2011;68(24):3983-93.
8. Cooke IR, Deserno M. Coupling between lipid shape and membrane curvature. *Biophys J.* 2006;91(2):487-95.
9. van Meer G, Voelker DR, Feigenson GW. Membrane lipids: where they are and how they behave. *Nat Rev Mol Cell Biol.* 2008;9(2):112-24.
10. Lewis RN, McElhaney RN. The physicochemical properties of cardiolipin bilayers and cardiolipin-containing lipid membranes. *Biochim Biophys Acta.* 2009;1788(10):2069-79.
11. Renner LD, Weibel DB. Cardiolipin microdomains localize to negatively curved regions of *Escherichia coli* membranes. *Proc Natl Acad Sci U S A.* 2011;108(15):6264-9.

12. Prinz WA, Hinshaw JE. Membrane-bending proteins. *Crit Rev Biochem Mol Biol.* 2009;44(5):278-91.
13. Simunovic M, Voth GA, Callan-Jones A, Bassereau P. When Physics Takes Over: BAR Proteins and Membrane Curvature. *Trends Cell Biol.* 2015;25(12):780-92.
14. Mettlen M, Chen PH, Srinivasan S, Danuser G, Schmid SL. Regulation of Clathrin-Mediated Endocytosis. *Annu Rev Biochem.* 2018;87:871-96.
15. Morlot S, Roux A. Mechanics of dynamin-mediated membrane fission. *Annu Rev Biophys.* 2013;42:629-49.
16. Kamerkar SC, Kraus F, Sharpe AJ, Pucadyil TJ, Ryan MT. Dynamin-related protein 1 has membrane constricting and severing abilities sufficient for mitochondrial and peroxisomal fission. *Nat Commun.* 2018;9(1):5239.
17. Lee MW, Lee EY, Lai GH, Kennedy NW, Posey AE, Xian W, et al. Molecular Motor Dnm1 Synergistically Induces Membrane Curvature To Facilitate Mitochondrial Fission. *ACS Cent Sci.* 2017;3(11):1156-67.
18. Rosendale M, Van TNN, Grillo-Bosch D, Sposini S, Claverie L, Gauthereau I, et al. Functional recruitment of dynamin requires multimeric interactions for efficient endocytosis. *Nat Commun.* 2019;10(1):4462.
19. Liu YW, Mattila JP, Schmid SL. Dynamin-catalyzed membrane fission requires coordinated GTP hydrolysis. *PLoS One.* 2013;8(1):e55691.
20. van der Blik AM, Meyerowitz EM. Dynamin-like protein encoded by the *Drosophila* shibire gene associated with vesicular traffic. *Nature.* 1991;351(6325):411-4.
21. Grigliatti TA, Hall L, Rosenbluth R, Suzuki DT. Temperature-sensitive mutations in *Drosophila melanogaster*. XIV. A selection of immobile adults. *Mol Gen Genet.* 1973;120(2):107-14.

22. Suzuki DT, Grigliatti T, Williamson R. Temperature-sensitive mutations in *Drosophila melanogaster*. VII. A mutation (para-ts) causing reversible adult paralysis. *Proc Natl Acad Sci U S A*. 1971;68(5):890-3.
23. Shpetner HS, Vallee RB. Identification of dynamin, a novel mechanochemical enzyme that mediates interactions between microtubules. *Cell*. 1989;59(3):421-32.
24. Shpetner HS, Vallee RB. Dynamin is a GTPase stimulated to high levels of activity by microtubules. *Nature*. 1992;355(6362):733-5.
25. Takahashi K, Miyoshi H, Otomo M, Osada K, Yamaguchi N, Nakashima H. Suppression of dynamin GTPase activity by sertraline leads to inhibition of dynamin-dependent endocytosis. *Biochem Biophys Res Commun*. 2010;391(1):382-7.
26. Praefcke GJ, McMahon HT. The dynamin superfamily: universal membrane tubulation and fission molecules? *Nat Rev Mol Cell Biol*. 2004;5(2):133-47.
27. Hinshaw JE. Dynamin and its role in membrane fission. *Annu Rev Cell Dev Biol*. 2000;16:483-519.
28. Heymann JA, Hinshaw JE. Dynamins at a glance. *J Cell Sci*. 2009;122(Pt 19):3427-31.
29. Cao H, Garcia F, McNiven MA. Differential distribution of dynamin isoforms in mammalian cells. *Mol Biol Cell*. 1998;9(9):2595-609.
30. Nakata T, Takemura R, Hirokawa N. A novel member of the dynamin family of GTP-binding proteins is expressed specifically in the testis. *J Cell Sci*. 1993;105 ( Pt 1):1-5.
31. Sontag JM, Fykse EM, Ushkaryov Y, Liu JP, Robinson PJ, Sudhof TC. Differential expression and regulation of multiple dynamins. *J Biol Chem*. 1994;269(6):4547-54.
32. Gray NW, Fourgeaud L, Huang B, Chen J, Cao H, Oswald BJ, et al. Dynamin 3 is a component of the postsynapse, where it interacts with mGluR5 and Homer. *Curr Biol*. 2003;13(6):510-5.

33. Clark SG, Shurland DL, Meyerowitz EM, Bargmann CI, van der Bliek AM. A dynamin GTPase mutation causes a rapid and reversible temperature-inducible locomotion defect in *C. elegans*. *Proc Natl Acad Sci U S A*. 1997;94(19):10438-43.
34. Niemann HH, Knetsch ML, Scherer A, Manstein DJ, Kull FJ. Crystal structure of a dynamin GTPase domain in both nucleotide-free and GDP-bound forms. *EMBO J*. 2001;20(21):5813-21.
35. Reubold TF, Eschenburg S, Becker A, Leonard M, Schmid SL, Vallee RB, et al. Crystal structure of the GTPase domain of rat dynamin 1. *Proc Natl Acad Sci U S A*. 2005;102(37):13093-8.
36. Faelber K, Posor Y, Gao S, Held M, Roske Y, Schulze D, et al. Crystal structure of nucleotide-free dynamin. *Nature*. 2011;477(7366):556-60.
37. Ford MG, Jenni S, Nunnari J. The crystal structure of dynamin. *Nature*. 2011;477(7366):561-6.
38. Chappie JS, Acharya S, Leonard M, Schmid SL, Dyda F. G domain dimerization controls dynamin's assembly-stimulated GTPase activity. *Nature*. 2010;465(7297):435-40.
39. Antony B, Burd C, De Camilli P, Chen E, Daumke O, Faelber K, et al. Membrane fission by dynamin: what we know and what we need to know. *EMBO J*. 2016;35(21):2270-84.
40. Gao S, von der Malsburg A, Paeschke S, Behlke J, Haller O, Kochs G, et al. Structural basis of oligomerization in the stalk region of dynamin-like MxA. *Nature*. 2010;465(7297):502-6.
41. Chappie JS, Acharya S, Liu YW, Leonard M, Pucadyil TJ, Schmid SL. An intramolecular signaling element that modulates dynamin function in vitro and in vivo. *Mol Biol Cell*. 2009;20(15):3561-71.

42. Ramachandran R, Surka M, Chappie JS, Fowler DM, Foss TR, Song BD, et al. The dynamin middle domain is critical for tetramerization and higher-order self-assembly. *EMBO J*. 2007;26(2):559-66.
43. Warnock DE, Hinshaw JE, Schmid SL. Dynamin self-assembly stimulates its GTPase activity. *J Biol Chem*. 1996;271(37):22310-4.
44. Tuma PL, Collins CA. Activation of dynamin GTPase is a result of positive cooperativity. *J Biol Chem*. 1994;269(49):30842-7.
45. Smirnova E, Shurland DL, Newman-Smith ED, Pishvae B, van der Blik AM. A model for dynamin self-assembly based on binding between three different protein domains. *J Biol Chem*. 1999;274(21):14942-7.
46. Okamoto PM, Tripet B, Litowski J, Hodges RS, Vallee RB. Multiple distinct coiled-coils are involved in dynamin self-assembly. *J Biol Chem*. 1999;274(15):10277-86.
47. Lemmon MA. Pleckstrin homology (PH) domains and phosphoinositides. *Biochem Soc Symp*. 2007(74):81-93.
48. Musacchio A, Gibson T, Rice P, Thompson J, Saraste M. The PH domain: a common piece in the structural patchwork of signalling proteins. *Trends Biochem Sci*. 1993;18(9):343-8.
49. Saraste M, Hyvonen M. Pleckstrin homology domains: a fact file. *Curr Opin Struct Biol*. 1995;5(3):403-8.
50. Klein DE, Lee A, Frank DW, Marks MS, Lemmon MA. The pleckstrin homology domains of dynamin isoforms require oligomerization for high affinity phosphoinositide binding. *J Biol Chem*. 1998;273(42):27725-33.
51. Achiriloaie M, Barylko B, Albanesi JP. Essential role of the dynamin pleckstrin homology domain in receptor-mediated endocytosis. *Mol Cell Biol*. 1999;19(2):1410-5.

52. Scaife RM, Margolis RL. The role of the PH domain and SH3 binding domains in dynamin function. *Cell Signal*. 1997;9(6):395-401.
53. Cho W, Stahelin RV. Membrane-protein interactions in cell signaling and membrane trafficking. *Annu Rev Biophys Biomol Struct*. 2005;34:119-51.
54. Lemmon MA. Membrane recognition by phospholipid-binding domains. *Nat Rev Mol Cell Biol*. 2008;9(2):99-111.
55. Lee A, Frank DW, Marks MS, Lemmon MA. Dominant-negative inhibition of receptor-mediated endocytosis by a dynamin-1 mutant with a defective pleckstrin homology domain. *Curr Biol*. 1999;9(5):261-4.
56. Brereton E, Fassi E, Araujo GC, Dodd J, Telegrafi A, Pathak SJ, et al. Mutations in the PH Domain of DNMI are associated with a nonepileptic phenotype characterized by developmental delay and neurobehavioral abnormalities. *Mol Genet Genomic Med*. 2018;6(2):294-300.
57. Vallis Y, Wigge P, Marks B, Evans PR, McMahon HT. Importance of the pleckstrin homology domain of dynamin in clathrin-mediated endocytosis. *Curr Biol*. 1999;9(5):257-60.
58. Mehrotra N, Nichols J, Ramachandran R. Alternate pleckstrin homology domain orientations regulate dynamin-catalyzed membrane fission. *Mol Biol Cell*. 2014;25(6):879-90.
59. Ramachandran R, Pucadyil TJ, Liu YW, Acharya S, Leonard M, Lukiyanchuk V, et al. Membrane insertion of the pleckstrin homology domain variable loop 1 is critical for dynamin-catalyzed vesicle scission. *Mol Biol Cell*. 2009;20(22):4630-9.
60. Lu B, Kennedy B, Clinton RW, Wang EJ, McHugh D, Stepanyants N, et al. Steric interference from intrinsically disordered regions controls dynamin-related protein 1 self-assembly during mitochondrial fission. *Sci Rep*. 2018;8(1):10879.

61. Muhlberg AB, Warnock DE, Schmid SL. Domain structure and intramolecular regulation of dynamin GTPase. *EMBO J.* 1997;16(22):6676-83.
62. Lupas A, Van Dyke M, Stock J. Predicting coiled coils from protein sequences. *Science.* 1991;252(5009):1162-4.
63. Luo L, Xue J, Kwan A, Gamsjaeger R, Wielens J, von Kleist L, et al. The Binding of Syndapin SH3 Domain to Dynamin Proline-rich Domain Involves Short and Long Distance Elements. *J Biol Chem.* 2016;291(18):9411-24.
64. Owen DJ, Wigge P, Vallis Y, Moore JD, Evans PR, McMahon HT. Crystal structure of the amphiphysin-2 SH3 domain and its role in the prevention of dynamin ring formation. *EMBO J.* 1998;17(18):5273-85.
65. Barylko B, Binns D, Lin KM, Atkinson MA, Jameson DM, Yin HL, et al. Synergistic activation of dynamin GTPase by Grb2 and phosphoinositides. *J Biol Chem.* 1998;273(6):3791-7.
66. Yoon SY, Jeong MJ, Yoo J, Lee KI, Kwon BM, Lim DS, et al. Grb2 dominantly associates with dynamin II in human hepatocellular carcinoma HepG2 cells. *J Cell Biochem.* 2001;84(1):150-5.
67. Scaife R, Gout I, Waterfield MD, Margolis RL. Growth factor-induced binding of dynamin to signal transduction proteins involves sorting to distinct and separate proline-rich dynamin sequences. *EMBO J.* 1994;13(11):2574-82.
68. Szaszak M, Gaborik Z, Turu G, McPherson PS, Clark AJ, Catt KJ, et al. Role of the proline-rich domain of dynamin-2 and its interactions with Src homology 3 domains during endocytosis of the AT1 angiotensin receptor. *J Biol Chem.* 2002;277(24):21650-6.
69. Barylko B, Wang L, Binns DD, Ross JA, Tassin TC, Collins KA, et al. The proline/arginine-rich domain is a major determinant of dynamin self-activation. *Biochemistry.* 2010;49(50):10592-4.

70. Montessuit S, Somasekharan SP, Terrones O, Lucken-Ardjomande S, Herzig S, Schwarzenbacher R, et al. Membrane remodeling induced by the dynamin-related protein Drp1 stimulates Bax oligomerization. *Cell*. 2010;142(6):889-901.
71. Stowell MH, Marks B, Wigge P, McMahon HT. Nucleotide-dependent conformational changes in dynamin: evidence for a mechanochemical molecular spring. *Nat Cell Biol*. 1999;1(1):27-32.
72. Basu K, Lajoie D, Aumentado-Armstrong T, Chen J, Koning RI, Bossy B, et al. Molecular mechanism of DRP1 assembly studied in vitro by cryo-electron microscopy. *PLoS One*. 2017;12(6):e0179397.
73. von der Malsburg A, Abutbul-Ionita I, Haller O, Kochs G, Danino D. Stalk domain of the dynamin-like MxA GTPase protein mediates membrane binding and liposome tubulation via the unstructured L4 loop. *J Biol Chem*. 2011;286(43):37858-65.
74. Daumke O, Gao S, von der Malsburg A, Haller O, Kochs G. Structure of the MxA stalk elucidates the assembly of ring-like units of an antiviral module. *Small GTPases*. 2010;1(1):62-4.
75. Vopel T, Syguda A, Britzen-Laurent N, Kunzelmann S, Ludemann MB, Dovengerds C, et al. Mechanism of GTPase-activity-induced self-assembly of human guanylate binding protein 1. *J Mol Biol*. 2010;400(1):63-70.
76. Chang CR, Manlandro CM, Arnoult D, Stadler J, Posey AE, Hill RB, et al. A lethal de novo mutation in the middle domain of the dynamin-related GTPase Drp1 impairs higher order assembly and mitochondrial division. *J Biol Chem*. 2010;285(42):32494-503.
77. Meglei G, McQuibban GA. The dynamin-related protein Mgm1p assembles into oligomers and hydrolyzes GTP to function in mitochondrial membrane fusion. *Biochemistry*. 2009;48(8):1774-84.

78. Byrnes LJ, Singh A, Szeto K, Benveniste NM, O'Donnell JP, Zipfel WR, et al. Structural basis for conformational switching and GTP loading of the large G protein atlastin. *EMBO J*. 2013;32(3):369-84.
79. Mishra R, Smaczynska-de R, II, Goldberg MW, Ayscough KR. Expression of Vps1 I649K a self-assembly defective yeast dynamin, leads to formation of extended endocytic invaginations. *Commun Integr Biol*. 2011;4(1):115-7.
80. Zimmerberg J, Kozlov MM. How proteins produce cellular membrane curvature. *Nat Rev Mol Cell Biol*. 2006;7(1):9-19.
81. Roux A, Uyhazi K, Frost A, De Camilli P. GTP-dependent twisting of dynamin implicates constriction and tension in membrane fission. *Nature*. 2006;441(7092):528-31.
82. Song BD, Leonard M, Schmid SL. Dynamin GTPase domain mutants that differentially affect GTP binding, GTP hydrolysis, and clathrin-mediated endocytosis. *J Biol Chem*. 2004;279(39):40431-6.
83. Jeong MJ, Yoo J, Lee SS, Lee KI, Cho A, Kwon BM, et al. Increased GTP-binding to dynamin II does not stimulate receptor-mediated endocytosis. *Biochem Biophys Res Commun*. 2001;283(1):136-42.
84. Binns DD, Barylko B, Grichine N, Atkinson MA, Helms MK, Jameson DM, et al. Correlation between self-association modes and GTPase activation of dynamin. *J Protein Chem*. 1999;18(3):277-90.
85. Varne A, Muthukumaraswamy K, Jatiani SS, Mittal R. Conformational analysis of the GTP-binding protein MxA using limited proteolysis. *FEBS Lett*. 2002;516(1-3):129-32.
86. Ghosh A, Praefcke GJ, Renault L, Wittinghofer A, Herrmann C. How guanylate-binding proteins achieve assembly-stimulated processive cleavage of GTP to GMP. *Nature*. 2006;440(7080):101-4.

87. Rennie ML, McKelvie SA, Bulloch EM, Kingston RL. Transient dimerization of human MxA promotes GTP hydrolysis, resulting in a mechanical power stroke. *Structure*. 2014;22(10):1433-45.
88. Richter MF, Schwemmle M, Herrmann C, Wittinghofer A, Staeheli P. Interferon-induced MxA protein. GTP binding and GTP hydrolysis properties. *J Biol Chem*. 1995;270(22):13512-7.
89. Damke H, Binns DD, Ueda H, Schmid SL, Baba T. Dynamin GTPase domain mutants block endocytic vesicle formation at morphologically distinct stages. *Mol Biol Cell*. 2001;12(9):2578-89.
90. Damke H, Baba T, Warnock DE, Schmid SL. Induction of mutant dynamin specifically blocks endocytic coated vesicle formation. *J Cell Biol*. 1994;127(4):915-34.
91. Ugarte-Urbe B, Muller HM, Otsuki M, Nickel W, Garcia-Saez AJ. Dynamin-related protein 1 (Drp1) promotes structural intermediates of membrane division. *J Biol Chem*. 2014;289(44):30645-56.
92. Ban T, Ishihara T, Kohno H, Saita S, Ichimura A, Maenaka K, et al. Molecular basis of selective mitochondrial fusion by heterotypic action between OPA1 and cardiolipin. *Nat Cell Biol*. 2017;19(7):856-63.
93. Bethoney KA, King MC, Hinshaw JE, Ostap EM, Lemmon MA. A possible effector role for the pleckstrin homology (PH) domain of dynamin. *Proc Natl Acad Sci U S A*. 2009;106(32):13359-64.
94. Kenniston JA, Lemmon MA. Dynamin GTPase regulation is altered by PH domain mutations found in centronuclear myopathy patients. *EMBO J*. 2010;29(18):3054-67.
95. Liu YW, Neumann S, Ramachandran R, Ferguson SM, Pucadyil TJ, Schmid SL. Differential curvature sensing and generating activities of dynamin isoforms provide

opportunities for tissue-specific regulation. *Proc Natl Acad Sci U S A*. 2011;108(26):E234-42.

96. Ramachandran R, Schmid SL. Real-time detection reveals that effectors couple dynamin's GTP-dependent conformational changes to the membrane. *EMBO J*. 2008;27(1):27-37.

97. Bustillo-Zabalbeitia I, Montessuit S, Raemy E, Basanez G, Terrones O, Martinou JC. Specific interaction with cardiolipin triggers functional activation of Dynamin-Related Protein 1. *PLoS One*. 2014;9(7):e102738.

98. Rebecchi MJ, Scarlata S. Pleckstrin homology domains: a common fold with diverse functions. *Annu Rev Biophys Biomol Struct*. 1998;27:503-28.

99. Lemmon MA, Ferguson KM. Signal-dependent membrane targeting by pleckstrin homology (PH) domains. *Biochem J*. 2000;350 Pt 1:1-18.

100. Bramkamp M. Bacterial dynamin-like proteins reveal mechanism for membrane fusion. *Nat Commun*. 2018;9(1):3993.

101. Cao YL, Meng S, Chen Y, Feng JX, Gu DD, Yu B, et al. MFN1 structures reveal nucleotide-triggered dimerization critical for mitochondrial fusion. *Nature*. 2017;542(7641):372-6.

102. Altschuler Y, Barbas SM, Terlecky LJ, Tang K, Hardy S, Mostov KE, et al. Redundant and distinct functions for dynamin-1 and dynamin-2 isoforms. *J Cell Biol*. 1998;143(7):1871-81.

103. Wu Y, O'Toole ET, Girard M, Ritter B, Messa M, Liu X, et al. A dynamin 1-, dynamin 3- and clathrin-independent pathway of synaptic vesicle recycling mediated by bulk endocytosis. *Elife*. 2014;3:e01621.

104. Danino D, Moon KH, Hinshaw JE. Rapid constriction of lipid bilayers by the mechanochemical enzyme dynamin. *J Struct Biol*. 2004;147(3):259-67.

105. Sweitzer SM, Hinshaw JE. Dynamin undergoes a GTP-dependent conformational change causing vesiculation. *Cell*. 1998;93(6):1021-9.
106. Sundborger AC, Fang S, Heymann JA, Ray P, Chappie JS, Hinshaw JE. A dynamin mutant defines a superconstricted pre-fission state. *Cell Rep*. 2014;8(3):734-42.
107. Jones SM, Howell KE, Henley JR, Cao H, McNiven MA. Role of dynamin in the formation of transport vesicles from the trans-Golgi network. *Science*. 1998;279(5350):573-7.
108. Yu X, Cai M. The yeast dynamin-related GTPase Vps1p functions in the organization of the actin cytoskeleton via interaction with Sla1p. *J Cell Sci*. 2004;117(Pt 17):3839-53.
109. Gammie AE, Kurihara LJ, Vallee RB, Rose MD. DNM1, a dynamin-related gene, participates in endosomal trafficking in yeast. *J Cell Biol*. 1995;130(3):553-66.
110. Hoepfner D, van den Berg M, Philippsen P, Tabak HF, Hettema EH. A role for Vps1p, actin, and the Myo2p motor in peroxisome abundance and inheritance in *Saccharomyces cerevisiae*. *J Cell Biol*. 2001;155(6):979-90.
111. Kuravi K, Nagotu S, Krikken AM, Sjollem K, Deckers M, Erdmann R, et al. Dynamin-related proteins Vps1p and Dnm1p control peroxisome abundance in *Saccharomyces cerevisiae*. *J Cell Sci*. 2006;119(Pt 19):3994-4001.
112. Nothwehr SF, Conibear E, Stevens TH. Golgi and vacuolar membrane proteins reach the vacuole in vps1 mutant yeast cells via the plasma membrane. *J Cell Biol*. 1995;129(1):35-46.
113. Peters C, Baars TL, Buhler S, Mayer A. Mutual control of membrane fission and fusion proteins. *Cell*. 2004;119(5):667-78.
114. Vater CA, Raymond CK, Ekena K, Howald-Stevenson I, Stevens TH. The VPS1 protein, a homolog of dynamin required for vacuolar protein sorting in *Saccharomyces*

cerevisiae, is a GTPase with two functionally separable domains. *J Cell Biol.* 1992;119(4):773-86.

115. Hong Z, Bednarek SY, Blumwald E, Hwang I, Jurgens G, Menzel D, et al. A unified nomenclature for Arabidopsis dynamin-related large GTPases based on homology and possible functions. *Plant Mol Biol.* 2003;53(3):261-5.

116. Taylor NG. A role for Arabidopsis dynamin related proteins DRP2A/B in endocytosis; DRP2 function is essential for plant growth. *Plant Mol Biol.* 2011;76(1-2):117-29.

117. Huang J, Fujimoto M, Fujiwara M, Fukao Y, Arimura S, Tsutsumi N. Arabidopsis dynamin-related proteins, DRP2A and DRP2B, function coordinately in post-Golgi trafficking. *Biochem Biophys Res Commun.* 2015;456(1):238-44.

118. Zhao G, Cao K, Xu C, Sun A, Lu W, Zheng Y, et al. Crosstalk between Mitochondrial Fission and Oxidative Stress in Paraquat-Induced Apoptosis in Mouse Alveolar Type II Cells. *Int J Biol Sci.* 2017;13(7):888-900.

119. Burman JL, Pickles S, Wang C, Sekine S, Vargas JNS, Zhang Z, et al. Mitochondrial fission facilitates the selective mitophagy of protein aggregates. *J Cell Biol.* 2017;216(10):3231-47.

120. Vidoni S, Zanna C, Rugolo M, Sarzi E, Lenaers G. Why mitochondria must fuse to maintain their genome integrity. *Antioxid Redox Signal.* 2013;19(4):379-88.

121. Jones BA, Fangman WL. Mitochondrial DNA maintenance in yeast requires a protein containing a region related to the GTP-binding domain of dynamin. *Genes Dev.* 1992;6(3):380-9.

122. Wong ED, Wagner JA, Gorsich SW, McCaffery JM, Shaw JM, Nunnari J. The dynamin-related GTPase, Mgm1p, is an intermembrane space protein required for maintenance of fusion competent mitochondria. *J Cell Biol.* 2000;151(2):341-52.

123. Alexander C, Votruba M, Pesch UE, Thiselton DL, Mayer S, Moore A, et al. OPA1, encoding a dynamin-related GTPase, is mutated in autosomal dominant optic atrophy linked to chromosome 3q28. *Nat Genet.* 2000;26(2):211-5.
124. Delettre C, Lenaers G, Griffoin JM, Gigarel N, Lorenzo C, Belenguer P, et al. Nuclear gene OPA1, encoding a mitochondrial dynamin-related protein, is mutated in dominant optic atrophy. *Nat Genet.* 2000;26(2):207-10.
125. Hales KG, Fuller MT. Developmentally regulated mitochondrial fusion mediated by a conserved, novel, predicted GTPase. *Cell.* 1997;90(1):121-9.
126. Hermann GJ, Thatcher JW, Mills JP, Hales KG, Fuller MT, Nunnari J, et al. Mitochondrial fusion in yeast requires the transmembrane GTPase Fzo1p. *J Cell Biol.* 1998;143(2):359-73.
127. Rapaport D, Brunner M, Neupert W, Westermann B. Fzo1p is a mitochondrial outer membrane protein essential for the biogenesis of functional mitochondria in *Saccharomyces cerevisiae*. *J Biol Chem.* 1998;273(32):20150-5.
128. Santel A, Fuller MT. Control of mitochondrial morphology by a human mitofusin. *J Cell Sci.* 2001;114(Pt 5):867-74.
129. Chen H, Detmer SA, Ewald AJ, Griffin EE, Fraser SE, Chan DC. Mitofusins Mfn1 and Mfn2 coordinately regulate mitochondrial fusion and are essential for embryonic development. *J Cell Biol.* 2003;160(2):189-200.
130. Otsuga D, Keegan BR, Brisch E, Thatcher JW, Hermann GJ, Bleazard W, et al. The dynamin-related GTPase, Dnm1p, controls mitochondrial morphology in yeast. *J Cell Biol.* 1998;143(2):333-49.
131. Bleazard W, McCaffery JM, King EJ, Bale S, Mozdy A, Tieu Q, et al. The dynamin-related GTPase Dnm1 regulates mitochondrial fission in yeast. *Nat Cell Biol.* 1999;1(5):298-304.

132. Smirnova E, Griparic L, Shurland DL, van der Bliek AM. Dynamin-related protein Drp1 is required for mitochondrial division in mammalian cells. *Mol Biol Cell*. 2001;12(8):2245-56.
133. Imoto M, Tachibana I, Urrutia R. Identification and functional characterization of a novel human protein highly related to the yeast dynamin-like GTPase Vps1p. *J Cell Sci*. 1998;111 ( Pt 10):1341-9.
134. Kamimoto T, Nagai Y, Onogi H, Muro Y, Wakabayashi T, Hagiwara M. Dymple, a novel dynamin-like high molecular weight GTPase lacking a proline-rich carboxyl-terminal domain in mammalian cells. *J Biol Chem*. 1998;273(2):1044-51.
135. Shin HW, Shinotsuka C, Torii S, Murakami K, Nakayama K. Identification and subcellular localization of a novel mammalian dynamin-related protein homologous to yeast Vps1p and Dnm1p. *J Biochem*. 1997;122(3):525-30.
136. Yoon Y, Pitts KR, Dahan S, McNiven MA. A novel dynamin-like protein associates with cytoplasmic vesicles and tubules of the endoplasmic reticulum in mammalian cells. *J Cell Biol*. 1998;140(4):779-93.
137. Ban T, Kohno H, Ishihara T, Ishihara N. Relationship between OPA1 and cardiolipin in mitochondrial inner-membrane fusion. *Biochim Biophys Acta Bioenerg*. 2018;1859(9):951-7.
138. DeVay RM, Dominguez-Ramirez L, Lackner LL, Hoppins S, Stahlberg H, Nunnari J. Coassembly of Mgm1 isoforms requires cardiolipin and mediates mitochondrial inner membrane fusion. *J Cell Biol*. 2009;186(6):793-803.
139. Hoppins S, Lackner L, Nunnari J. The machines that divide and fuse mitochondria. *Annu Rev Biochem*. 2007;76:751-80.

140. Ingerman E, Perkins EM, Marino M, Mears JA, McCaffery JM, Hinshaw JE, et al. Dnm1 forms spirals that are structurally tailored to fit mitochondria. *J Cell Biol.* 2005;170(7):1021-7.
141. Mears JA, Lackner LL, Fang S, Ingerman E, Nunnari J, Hinshaw JE. Conformational changes in Dnm1 support a contractile mechanism for mitochondrial fission. *Nat Struct Mol Biol.* 2011;18(1):20-6.
142. Koshihara T, Detmer SA, Kaiser JT, Chen H, McCaffery JM, Chan DC. Structural basis of mitochondrial tethering by mitofusin complexes. *Science.* 2004;305(5685):858-62.
143. Haller O, Acklin M, Staeheli P. Influenza virus resistance of wild mice: wild-type and mutant Mx alleles occur at comparable frequencies. *J Interferon Res.* 1987;7(5):647-56.
144. Reeves RH, O'Hara BF, Pavan WJ, Gearhart JD, Haller O. Genetic mapping of the Mx influenza virus resistance gene within the region of mouse chromosome 16 that is homologous to human chromosome 21. *J Virol.* 1988;62(11):4372-5.
145. Staeheli P, Grob R, Meier E, Sutcliffe JG, Haller O. Influenza virus-susceptible mice carry Mx genes with a large deletion or a nonsense mutation. *Mol Cell Biol.* 1988;8(10):4518-23.
146. Staeheli P, Pravtcheva D, Lundin LG, Acklin M, Ruddle F, Lindenmann J, et al. Interferon-regulated influenza virus resistance gene Mx is localized on mouse chromosome 16. *J Virol.* 1986;58(3):967-9.
147. Staeheli P, Sutcliffe JG. Identification of a second interferon-regulated murine Mx gene. *Mol Cell Biol.* 1988;8(10):4524-8.
148. Zurcher T, Pavlovic J, Staeheli P. Nuclear localization of mouse Mx1 protein is necessary for inhibition of influenza virus. *J Virol.* 1992;66(8):5059-66.
149. Spitaels J, Van Hoecke L, Roose K, Kochs G, Saelens X. Mx1 in Hematopoietic Cells Protects against Thogoto Virus Infection. *J Virol.* 2019;93(15).

150. Verhelst J, Parthoens E, Schepens B, Fiers W, Saelens X. Interferon-inducible protein Mx1 inhibits influenza virus by interfering with functional viral ribonucleoprotein complex assembly. *J Virol.* 2012;86(24):13445-55.
151. Jin HK, Takada A, Kon Y, Haller O, Watanabe T. Identification of the murine Mx2 gene: interferon-induced expression of the Mx2 protein from the feral mouse gene confers resistance to vesicular stomatitis virus. *J Virol.* 1999;73(6):4925-30.
152. Sandrock M, Frese M, Haller O, Kochs G. Interferon-induced rat Mx proteins confer resistance to Rift Valley fever virus and other arthropod-borne viruses. *J Interferon Cytokine Res.* 2001;21(9):663-8.
153. Haller O, Kochs G. Human MxA protein: an interferon-induced dynamin-like GTPase with broad antiviral activity. *J Interferon Cytokine Res.* 2011;31(1):79-87.
154. Pletneva LM, Haller O, Porter DD, Prince GA, Blanco JC. Interferon-inducible Mx gene expression in cotton rats: cloning, characterization, and expression during influenza viral infection. *J Interferon Cytokine Res.* 2006;26(12):914-21.
155. Holzinger D, Jorns C, Stertz S, Boisson-Dupuis S, Thimme R, Weidmann M, et al. Induction of MxA gene expression by influenza A virus requires type I or type III interferon signaling. *J Virol.* 2007;81(14):7776-85.
156. Aebi M, Fah J, Hurt N, Samuel CE, Thomis D, Bazzigher L, et al. cDNA structures and regulation of two interferon-induced human Mx proteins. *Mol Cell Biol.* 1989;9(11):5062-72.
157. Liu Z, Pan Q, Ding S, Qian J, Xu F, Zhou J, et al. The interferon-inducible MxB protein inhibits HIV-1 infection. *Cell Host Microbe.* 2013;14(4):398-410.
158. Yi DR, An N, Liu ZL, Xu FW, Raniga K, Li QJ, et al. Human MxB Inhibits the Replication of Hepatitis C Virus. *J Virol.* 2019;93(1).

159. Matzinger SR, Carroll TD, Dutra JC, Ma ZM, Miller CJ. Myxovirus resistance gene A (MxA) expression suppresses influenza A virus replication in alpha interferon-treated primate cells. *J Virol.* 2013;87(2):1150-8.
160. Kochs G, Haller O. GTP-bound human MxA protein interacts with the nucleocapsids of Thogoto virus (Orthomyxoviridae). *J Biol Chem.* 1999;274(7):4370-6.
161. Mitchell PS, Patzina C, Emerman M, Haller O, Malik HS, Kochs G. Evolution-guided identification of antiviral specificity determinants in the broadly acting interferon-induced innate immunity factor MxA. *Cell Host Microbe.* 2012;12(4):598-604.
162. Melen K, Keskinen P, Ronni T, Sareneva T, Lounatmaa K, Julkunen I. Human MxB protein, an interferon-alpha-inducible GTPase, contains a nuclear targeting signal and is localized in the heterochromatin region beneath the nuclear envelope. *J Biol Chem.* 1996;271(38):23478-86.
163. King MC, Raposo G, Lemmon MA. Inhibition of nuclear import and cell-cycle progression by mutated forms of the dynamin-like GTPase MxB. *Proc Natl Acad Sci U S A.* 2004;101(24):8957-62.
164. Verhelst J, Hulpiau P, Saelens X. Mx proteins: antiviral gatekeepers that restrain the uninvited. *Microbiol Mol Biol Rev.* 2013;77(4):551-66.
165. Haller O, Kochs G, Weber F. The interferon response circuit: induction and suppression by pathogenic viruses. *Virology.* 2006;344(1):119-30.
166. Kane M, Yadav SS, Bitzegeio J, Kutluay SB, Zang T, Wilson SJ, et al. MX2 is an interferon-induced inhibitor of HIV-1 infection. *Nature.* 2013;502(7472):563-6.
167. Cramer M, Bauer M, Caduff N, Walker R, Steiner F, Franzoso FD, et al. MxB is an interferon-induced restriction factor of human herpesviruses. *Nat Commun.* 2018;9(1):1980.
168. Staeheli P, Haller O. Human MX2/MxB: a Potent Interferon-Induced Postentry Inhibitor of Herpesviruses and HIV-1. *J Virol.* 2018;92(24).

169. Voeltz GK, Rolls MM, Rapoport TA. Structural organization of the endoplasmic reticulum. *EMBO Rep.* 2002;3(10):944-50.
170. Baumann O, Walz B. Endoplasmic reticulum of animal cells and its organization into structural and functional domains. *Int Rev Cytol.* 2001;205:149-214.
171. Hu J, Shibata Y, Zhu PP, Voss C, Rismanchi N, Prinz WA, et al. A class of dynamin-like GTPases involved in the generation of the tubular ER network. *Cell.* 2009;138(3):549-61.
172. Orso G, Pendin D, Liu S, Toso J, Moss TJ, Faust JE, et al. Homotypic fusion of ER membranes requires the dynamin-like GTPase atlastin. *Nature.* 2009;460(7258):978-83.
173. Summerville JB, Faust JF, Fan E, Pendin D, Daga A, Formella J, et al. The effects of ER morphology on synaptic structure and function in *Drosophila melanogaster*. *J Cell Sci.* 2016;129(8):1635-48.
174. Moss TJ, Andrezza C, Verma A, Daga A, McNew JA. Membrane fusion by the GTPase atlastin requires a conserved C-terminal cytoplasmic tail and dimerization through the middle domain. *Proc Natl Acad Sci U S A.* 2011;108(27):11133-8.
175. Sauter SM, Engel W, Neumann LM, Kunze J, Neesen J. Novel mutations in the Atlastin gene (SPG3A) in families with autosomal dominant hereditary spastic paraplegia and evidence for late onset forms of HSP linked to the SPG3A locus. *Hum Mutat.* 2004;23(1):98.
176. Behrendt L, Kurth I, Kaether C. A disease causing ATLASTIN 3 mutation affects multiple endoplasmic reticulum-related pathways. *Cell Mol Life Sci.* 2019;76(7):1433-45.
177. Thompson HM, Skop AR, Euteneuer U, Meyer BJ, McNiven MA. The large GTPase dynamin associates with the spindle midzone and is required for cytokinesis. *Curr Biol.* 2002;12(24):2111-7.

178. Wienke DC, Knetsch ML, Neuhaus EM, Reedy MC, Manstein DJ. Disruption of a dynamin homologue affects endocytosis, organelle morphology, and cytokinesis in *Dictyostelium discoideum*. *Mol Biol Cell*. 1999;10(1):225-43.
179. Feng B, Schwarz H, Jesuthasan S. Furrow-specific endocytosis during cytokinesis of zebrafish blastomeres. *Exp Cell Res*. 2002;279(1):14-20.
180. Pelissier A, Chauvin JP, Lecuit T. Trafficking through Rab11 endosomes is required for cellularization during *Drosophila* embryogenesis. *Curr Biol*. 2003;13(21):1848-57.
181. David C, McPherson PS, Mundigl O, de Camilli P. A role of amphiphysin in synaptic vesicle endocytosis suggested by its binding to dynamin in nerve terminals. *Proc Natl Acad Sci U S A*. 1996;93(1):331-5.
182. Galas MC, Chasserot-Golaz S, Dirrig-Grosch S, Bader MF. Presence of dynamin--syntaxin complexes associated with secretory granules in adrenal chromaffin cells. *J Neurochem*. 2000;75(4):1511-9.
183. Gu X, Verma DP. Phragmoplastin, a dynamin-like protein associated with cell plate formation in plants. *EMBO J*. 1996;15(4):695-704.
184. Verma DP. Cytokinesis and Building of the Cell Plate in Plants. *Annu Rev Plant Physiol Plant Mol Biol*. 2001;52:751-84.
185. Hong Z, Geisler-Lee CJ, Zhang Z, Verma DP. Phragmoplastin dynamics: multiple forms, microtubule association and their roles in cell plate formation in plants. *Plant Mol Biol*. 2003;53(3):297-312.
186. Kang BH, Busse JS, Bednarek SY. Members of the *Arabidopsis* dynamin-like gene family, ADL1, are essential for plant cytokinesis and polarized cell growth. *Plant Cell*. 2003;15(4):899-913.
187. Kar UP, Dey H, Rahaman A. Regulation of dynamin family proteins by post-translational modifications. *J Biosci*. 2017;42(2):333-44.

188. Shajahan AN, Timblin BK, Sandoval R, Tiruppathi C, Malik AB, Minshall RD. Role of Src-induced dynamin-2 phosphorylation in caveolae-mediated endocytosis in endothelial cells. *J Biol Chem.* 2004;279(19):20392-400.
189. Anggono V, Smillie KJ, Graham ME, Valova VA, Cousin MA, Robinson PJ. Syndapin I is the phosphorylation-regulated dynamin I partner in synaptic vesicle endocytosis. *Nat Neurosci.* 2006;9(6):752-60.
190. Tan TC, Valova VA, Malladi CS, Graham ME, Berven LA, Jupp OJ, et al. Cdk5 is essential for synaptic vesicle endocytosis. *Nat Cell Biol.* 2003;5(8):701-10.
191. Chan DC. Mitochondrial fusion and fission in mammals. *Annu Rev Cell Dev Biol.* 2006;22:79-99.
192. Davies VJ, Hollins AJ, Piechota MJ, Yip W, Davies JR, White KE, et al. Opa1 deficiency in a mouse model of autosomal dominant optic atrophy impairs mitochondrial morphology, optic nerve structure and visual function. *Hum Mol Genet.* 2007;16(11):1307-18.
193. Knott AB, Bossy-Wetzel E. Impairing the mitochondrial fission and fusion balance: a new mechanism of neurodegeneration. *Ann N Y Acad Sci.* 2008;1147:283-92.
194. Liesa M, Palacin M, Zorzano A. Mitochondrial dynamics in mammalian health and disease. *Physiol Rev.* 2009;89(3):799-845.
195. Taguchi N, Ishihara N, Jofuku A, Oka T, Mihara K. Mitotic phosphorylation of dynamin-related GTPase Drp1 participates in mitochondrial fission. *J Biol Chem.* 2007;282(15):11521-9.
196. Cereghetti GM, Stangherlin A, Martins de Brito O, Chang CR, Blackstone C, Bernardi P, et al. Dephosphorylation by calcineurin regulates translocation of Drp1 to mitochondria. *Proc Natl Acad Sci U S A.* 2008;105(41):15803-8.

197. Strack S, Wilson TJ, Cribbs JT. Cyclin-dependent kinases regulate splice-specific targeting of dynamin-related protein 1 to microtubules. *J Cell Biol.* 2013;201(7):1037-51.
198. Pyakurel A, Savoia C, Hess D, Scorrano L. Extracellular regulated kinase phosphorylates mitofusin 1 to control mitochondrial morphology and apoptosis. *Mol Cell.* 2015;58(2):244-54.
199. Leboucher GP, Tsai YC, Yang M, Shaw KC, Zhou M, Veenstra TD, et al. Stress-induced phosphorylation and proteasomal degradation of mitofusin 2 facilitates mitochondrial fragmentation and apoptosis. *Mol Cell.* 2012;47(4):547-57.
200. Komander D, Rape M. The ubiquitin code. *Annu Rev Biochem.* 2012;81:203-29.
201. Karbowski M, Neutzner A, Youle RJ. The mitochondrial E3 ubiquitin ligase MARCH5 is required for Drp1 dependent mitochondrial division. *J Cell Biol.* 2007;178(1):71-84.
202. Tang J, Hu Z, Tan J, Yang S, Zeng L. Parkin Protects against Oxygen-Glucose Deprivation/Reperfusion Insult by Promoting Drp1 Degradation. *Oxid Med Cell Longev.* 2016;2016:8474303.
203. Park YY, Cho H. Mitofusin 1 is degraded at G2/M phase through ubiquitylation by MARCH5. *Cell Div.* 2012;7(1):25.
204. Kim HJ, Nagano Y, Choi SJ, Park SY, Kim H, Yao TP, et al. HDAC6 maintains mitochondrial connectivity under hypoxic stress by suppressing MARCH5/MITOL dependent MFN2 degradation. *Biochem Biophys Res Commun.* 2015;464(4):1235-40.
205. Sugiura A, Nagashima S, Tokuyama T, Amo T, Matsuki Y, Ishido S, et al. MITOL regulates endoplasmic reticulum-mitochondria contacts via Mitofusin2. *Mol Cell.* 2013;51(1):20-34.
206. de Brito OM, Scorrano L. Mitofusin 2 tethers endoplasmic reticulum to mitochondria. *Nature.* 2008;456(7222):605-10.

207. Anton F, Dittmar G, Langer T, Escobar-Henriques M. Two deubiquitylases act on mitofusin and regulate mitochondrial fusion along independent pathways. *Mol Cell*. 2013;49(3):487-98.
208. Zunino R, Schauss A, Rippstein P, Andrade-Navarro M, McBride HM. The SUMO protease SENP5 is required to maintain mitochondrial morphology and function. *J Cell Sci*. 2007;120(Pt 7):1178-88.
209. Figueroa-Romero C, Iniguez-Lluhi JA, Stadler J, Chang CR, Arnoult D, Keller PJ, et al. SUMOylation of the mitochondrial fission protein Drp1 occurs at multiple nonconsensus sites within the B domain and is linked to its activity cycle. *FASEB J*. 2009;23(11):3917-27.
210. Harder Z, Zunino R, McBride H. Sumo1 conjugates mitochondrial substrates and participates in mitochondrial fission. *Curr Biol*. 2004;14(4):340-5.
211. Guo C, Hildick KL, Luo J, Dearden L, Wilkinson KA, Henley JM. SENP3-mediated deSUMOylation of dynamin-related protein 1 promotes cell death following ischaemia. *EMBO J*. 2013;32(11):1514-28.
212. Gould N, Doulias PT, Tenopoulou M, Raju K, Ischiropoulos H. Regulation of protein function and signaling by reversible cysteine S-nitrosylation. *J Biol Chem*. 2013;288(37):26473-9.
213. Wang G, Moniri NH, Ozawa K, Stamler JS, Daaka Y. Nitric oxide regulates endocytosis by S-nitrosylation of dynamin. *Proc Natl Acad Sci U S A*. 2006;103(5):1295-300.
214. Wang Z, Kim JI, Frilot N, Daaka Y. Dynamin2 S-nitrosylation regulates adenovirus type 5 infection of epithelial cells. *J Gen Virol*. 2012;93(Pt 10):2109-17.
215. Nakamura T, Cieplak P, Cho DH, Godzik A, Lipton SA. S-nitrosylation of Drp1 links excessive mitochondrial fission to neuronal injury in neurodegeneration. *Mitochondrion*. 2010;10(5):573-8.

216. Wada J, Nakatsuka A. Mitochondrial Dynamics and Mitochondrial Dysfunction in Diabetes. *Acta Med Okayama*. 2016;70(3):151-8.
217. Cho DH, Nakamura T, Fang J, Cieplak P, Godzik A, Gu Z, et al. S-nitrosylation of Drp1 mediates beta-amyloid-related mitochondrial fission and neuronal injury. *Science*. 2009;324(5923):102-5.
218. Haun F, Nakamura T, Shiu AD, Cho DH, Tsunemi T, Holland EA, et al. S-nitrosylation of dynamin-related protein 1 mediates mutant huntingtin-induced mitochondrial fragmentation and neuronal injury in Huntington's disease. *Antioxid Redox Signal*. 2013;19(11):1173-84.
219. Yang XJ, Seto E. Lysine acetylation: codified crosstalk with other posttranslational modifications. *Mol Cell*. 2008;31(4):449-61.
220. Glozak MA, Sengupta N, Zhang X, Seto E. Acetylation and deacetylation of non-histone proteins. *Gene*. 2005;363:15-23.
221. Xiong Y, Guan KL. Mechanistic insights into the regulation of metabolic enzymes by acetylation. *J Cell Biol*. 2012;198(2):155-64.
222. Jing E, Emanuelli B, Hirschey MD, Boucher J, Lee KY, Lombard D, et al. Sirtuin-3 (Sirt3) regulates skeletal muscle metabolism and insulin signaling via altered mitochondrial oxidation and reactive oxygen species production. *Proc Natl Acad Sci U S A*. 2011;108(35):14608-13.
223. Samant SA, Zhang HJ, Hong Z, Pillai VB, Sundaresan NR, Wolfgeher D, et al. SIRT3 deacetylates and activates OPA1 to regulate mitochondrial dynamics during stress. *Mol Cell Biol*. 2014;34(5):807-19.
224. Moens PB, Rapport E. Spindles, spindle plaques, and meiosis in the yeast *Saccharomyces cerevisiae* (Hansen). *J Cell Biol*. 1971;50(2):344-61.

225. Sazer S, Lynch M, Needleman D. Deciphering the evolutionary history of open and closed mitosis. *Curr Biol.* 2014;24(22):R1099-103.
226. Orias E, Flacks M. Macronuclear genetics of *Tetrahymena*. I. Random distribution of macronuclear gene copies in *T. pyriformis*, syngen 1. *Genetics.* 1975;79(2):187-206.
227. Doerder FP, Debault LE. Cytofluorimetric analysis of nuclear DNA during meiosis, fertilization and macronuclear development in the ciliate *Tetrahymena pyriformis*, syngen 1. *J Cell Sci.* 1975;17(3):471-93.
228. Eisen JA, Coyne RS, Wu M, Wu D, Thiagarajan M, Wortman JR, et al. Macronuclear genome sequence of the ciliate *Tetrahymena thermophila*, a model eukaryote. *PLoS Biol.* 2006;4(9):e286.
229. Elde NC, Morgan G, Winey M, Sperling L, Turkewitz AP. Elucidation of clathrin-mediated endocytosis in *tetrahymena* reveals an evolutionarily convergent recruitment of dynamin. *PLoS Genet.* 2005;1(5):e52.
230. Rahaman A, Elde NC, Turkewitz AP. A dynamin-related protein required for nuclear remodeling in *Tetrahymena*. *Curr Biol.* 2008;18(16):1227-33.
231. Ahn S, Kim J, Lucaveche CL, Reedy MC, Luttrell LM, Lefkowitz RJ, et al. Src-dependent tyrosine phosphorylation regulates dynamin self-assembly and ligand-induced endocytosis of the epidermal growth factor receptor. *J Biol Chem.* 2002;277(29):26642-51.
232. Armbruster M, Messa M, Ferguson SM, De Camilli P, Ryan TA. Dynamin phosphorylation controls optimization of endocytosis for brief action potential bursts. *Elife.* 2013;2:e00845.
233. Ekena K, Vater CA, Raymond CK, Stevens TH. The VPS1 protein is a dynamin-like GTPase required for sorting proteins to the yeast vacuole. *Ciba Found Symp.* 1993;176:198-211; discussion -4.

234. Nannapaneni S, Wang D, Jain S, Schroeder B, Highfill C, Reustle L, et al. The yeast dynamin-like protein Vps1:vps1 mutations perturb the internalization and the motility of endocytic vesicles and endosomes via disorganization of the actin cytoskeleton. *Eur J Cell Biol.* 2010;89(7):499-508.
235. Smaczynska-de R, II, Marklew CJ, Allwood EG, Palmer SE, Booth WI, Mishra R, et al. Phosphorylation Regulates the Endocytic Function of the Yeast Dynamin-Related Protein Vps1. *Mol Cell Biol.* 2015;36(5):742-55.
236. Han XJ, Lu YF, Li SA, Kaitsuka T, Sato Y, Tomizawa K, et al. CaM kinase I alpha-induced phosphorylation of Drp1 regulates mitochondrial morphology. *J Cell Biol.* 2008;182(3):573-85.
237. Yu T, Jhun BS, Yoon Y. High-glucose stimulation increases reactive oxygen species production through the calcium and mitogen-activated protein kinase-mediated activation of mitochondrial fission. *Antioxid Redox Signal.* 2011;14(3):425-37.
238. Jahani-Asl A, Huang E, Irrcher I, Rashidian J, Ishihara N, Lagace DC, et al. CDK5 phosphorylates DRP1 and drives mitochondrial defects in NMDA-induced neuronal death. *Hum Mol Genet.* 2015;24(16):4573-83.
239. Cho B, Cho HM, Kim HJ, Jeong J, Park SK, Hwang EM, et al. CDK5-dependent inhibitory phosphorylation of Drp1 during neuronal maturation. *Exp Mol Med.* 2014;46:e105.
240. Chang CR, Blackstone C. Cyclic AMP-dependent protein kinase phosphorylation of Drp1 regulates its GTPase activity and mitochondrial morphology. *J Biol Chem.* 2007;282(30):21583-7.
241. Kar UP, Dey H, Rahaman A. Cardiolipin targets a dynamin-related protein to the nuclear membrane. *Elife.* 2021;10.

242. Ramachandran R, Schmid SL. The dynamin superfamily. *Curr Biol.* 2018;28(8):R411-R6.
243. Smaczynska-de R, II, Marklew CJ, Palmer SE, Allwood EG, Ayscough KR. Mutation of key lysine residues in the Insert B region of the yeast dynamin Vps1 disrupts lipid binding and causes defects in endocytosis. *PLoS One.* 2019;14(4):e0215102.
244. Suetsugu S, Kurisu S, Takenawa T. Dynamic shaping of cellular membranes by phospholipids and membrane-deforming proteins. *Physiol Rev.* 2014;94(4):1219-48.
245. Cole ES, Cassidy-Hanley D, Hemish J, Tuan J, Bruns PJ. A mutational analysis of conjugation in *Tetrahymena thermophila*. 1. Phenotypes affecting early development: meiosis to nuclear selection. *Dev Biol.* 1997;189(2):215-32.
246. Kar UP, Dey H, Rahaman A. *Tetrahymena* dynamin-related protein 6 self-assembles independent of membrane association. *J Biosci.* 2018;43(1):139-48.
247. Pillai AN, Shukla S, Gautam S, Rahaman A. Small phosphatidate phosphatase (TtPAH2) of *Tetrahymena* complements respiratory function and not membrane biogenesis function of yeast PAH1. *J Biosci.* 2017;42(4):613-21.
248. Pillai AN, Shukla S, Rahaman A. An evolutionarily conserved phosphatidate phosphatase maintains lipid droplet number and endoplasmic reticulum morphology but not nuclear morphology. *Biol Open.* 2017;6(11):1629-43.
249. Zegarlinka J, Piascik M, Sikorski AF, Czogalla A. Phosphatidic acid - a simple phospholipid with multiple faces. *Acta Biochim Pol.* 2018;65(2):163-71.
250. Kay JG, Koivusalo M, Ma X, Wohland T, Grinstein S. Phosphatidylserine dynamics in cellular membranes. *Mol Biol Cell.* 2012;23(11):2198-212.
251. Salim K, Bottomley MJ, Querfurth E, Zvelebil MJ, Gout I, Scaife R, et al. Distinct specificity in the recognition of phosphoinositides by the pleckstrin homology domains of dynamin and Bruton's tyrosine kinase. *EMBO J.* 1996;15(22):6241-50.

252. Rujiviphat J, Meglei G, Rubinstein JL, McQuibban GA. Phospholipid association is essential for dynamin-related protein Mgm1 to function in mitochondrial membrane fusion. *J Biol Chem.* 2009;284(42):28682-6.
253. Wang M, Guo X, Yang X, Zhang B, Ren J, Liu A, et al. Mycobacterial dynamin-like protein IniA mediates membrane fission. *Nat Commun.* 2019;10(1):3906.
254. Planas-Iglesias J, Dwarakanath H, Mohammadyani D, Yanamala N, Kagan VE, Klein-Seetharaman J. Cardiolipin Interactions with Proteins. *Biophys J.* 2015;109(6):1282-94.
255. Song BD, Yarar D, Schmid SL. An assembly-incompetent mutant establishes a requirement for dynamin self-assembly in clathrin-mediated endocytosis in vivo. *Mol Biol Cell.* 2004;15(5):2243-52.
256. Frohlich C, Grabiger S, Schwefel D, Faelber K, Rosenbaum E, Mears J, et al. Structural insights into oligomerization and mitochondrial remodelling of dynamin 1-like protein. *EMBO J.* 2013;32(9):1280-92.
257. Bian X, Klemm RW, Liu TY, Zhang M, Sun S, Sui X, et al. Structures of the atlastin GTPase provide insight into homotypic fusion of endoplasmic reticulum membranes. *Proc Natl Acad Sci U S A.* 2011;108(10):3976-81.
258. Chappie JS, Dyda F. Building a fission machine--structural insights into dynamin assembly and activation. *J Cell Sci.* 2013;126(Pt 13):2773-84.
259. Yu C, Zhao J, Yan L, Qi Y, Guo X, Lou Z, et al. Structural insights into G domain dimerization and pathogenic mutation of OPA1. *J Cell Biol.* 2020;219(7).
260. Chugh J, Chatterjee A, Kumar A, Mishra RK, Mittal R, Hosur RV. Structural characterization of the large soluble oligomers of the GTPase effector domain of dynamin. *FEBS J.* 2006;273(2):388-97.

261. Chugh J, Sharma S, Kumar D, Misra JR, Hosur RV. Effect of a single point mutation on the stability, residual structure and dynamics in the denatured state of GED: relevance to self-assembly. *Biophys Chem.* 2008;137(1):13-8.
262. Sever S, Muhlberg AB, Schmid SL. Impairment of dynamin's GAP domain stimulates receptor-mediated endocytosis. *Nature.* 1999;398(6727):481-6.
263. Mukherjee RN, Salle J, Dmitrieff S, Nelson KM, Oakey J, Minc N, et al. The Perinuclear ER Scales Nuclear Size Independently of Cell Size in Early Embryos. *Dev Cell.* 2020;54(3):395-409 e7.
264. Anderson DJ, Hetzer MW. Shaping the endoplasmic reticulum into the nuclear envelope. *J Cell Sci.* 2008;121(Pt 2):137-42.
265. Theerthagiri G, Eisenhardt N, Schwarz H, Antonin W. The nucleoporin Nup188 controls passage of membrane proteins across the nuclear pore complex. *J Cell Biol.* 2010;189(7):1129-42.
266. Hara Y, Merten CA. Dynein-Based Accumulation of Membranes Regulates Nuclear Expansion in *Xenopus laevis* Egg Extracts. *Dev Cell.* 2015;33(5):562-75.

